Evaluation of Stability Boundaries in Power Systems

Katelynn A. Vance

Dissertation submitted to the faculty of Virginia Polytechnic Institute and State University in partial fulfillment of the requirements for the degree of

Doctor of Philosophy

In

Electrical Engineering

James S. Thorp, Chair

Virgilio A. Centeno

Arun G. Phadke

Alfred L. Wicks

Madhav V. Marathe

March 10, 2017

Blacksburg, Virginia

Keywords: Small signal stability, Inter-area oscillations, Lyapunov, Synchrophasor Applications

Evaluation of Stability Boundaries in Power Systems

Katelynn A. Vance

ABSTRACT

Power systems are extremely non-linear systems which require substantial modeling and control efforts to run continuously. The movement of the power system in parameter and state space is often not well understood, thus making it difficult or impossible to determine whether the system is nearing instability. This dissertation demonstrates several ways in which the power system stability boundary can be calculated. The power system movements evaluated here address the effects of inter-area oscillations on the system which occur in the seconds to minutes time period.

The first uses gain scheduling techniques through creation of a set of linear parameter varying (LPV) systems for many operating points of the non-linear system. In the case presented, load and line reactance are used as parameters. The scheduling variables are the power flows in tie lines of the system due to the useful information they provide about the power system state in addition to being available for measurement. A linear controller is developed for the LPV model using $\boldsymbol{H_2/H_\infty}$ with pole placement objectives. When the control is applied to the non-linear system, the proposed algorithm predicts the response of the non-linear system to the control by determining if the current system state is located within the domain of attraction of the equilibrium. If the stability domain contains a convex combination of the two points, the control will aid the system in moving towards the equilibrium.

The second contribution of this thesis is through the development and implementation of a pseudo non-linear evaluation of a power system as it moves through state space. A system linearization occurs first to compute a multi-objective state space controller. For each contingency definition, many variations of the power system example are created and assigned to the particular contingency class. The powerflow variations and contingency controls are combined to run sets of time series analysis in which the Lyapunov function is tracked over three time steps. This data is utilized for a classification analysis which identifies and classifies the data by the contingency type. The goal is that whenever a new event occurs on the system, real time data can be fed into the trained tree to provide a control for application to increase system damping.

Evaluation of Stability Boundaries in Power Systems

Katelynn A. Vance

GENERAL AUDIENCE ABSTRACT

The goal of the utility, reliability coordinators, academics, and regulators is to keep the lights on. The contributions presented in this dissertation aims to provide a methodology and algorithm with which that goal can be met. Although the power system requires the balancing of many different components, it can be boiled down to ensuring equilibrium between load served and generation provided. Because the utility goal is to keep the lights on – and thus not change the load of the customers by turning their lights off, the utility only has control over the generation side of this equation. A see-saw can be used to imagine this balance, but it will also require a feedback loop to ensure that generation will increase or decrease as the load changes.

Another way to visualize the power system is to imagine a marble at the bottom of a bowl. If the marble is perturbed too much, it will fly out of the bowl and become what is called unstable. However, if the marble is nudged lightly, it will return back to its resting place at the bottom of the ball – which could be considered a stable equilibrium. A possible control for this type of system would tilt the bowl with a feedback signal based on the location or speed of the marble as it moved around the inside of the bowl. By providing a feedback control, the strength with which the marble can be hit can increase beyond if the bowl were to remain stagnant. However, if the marble is hit very hard, it will not matter if there is feedback control, the marble will veer out of the bowl into instability. This example serves as an analogy for the power system where the current operating point of the power system is the marble and the stable areas of operation are represented by the bowl. The feedback control for the work explored here utilizes information about the generator states to feedback to HVDC lines to strengthen the system. The power system modeling and control design involved in this dissertation aims to determine how much the power system can be perturbed before reaching the edge of the "bowl."

Acknowledgements

There is a madness and beauty to the intensity of a graduate education that I could have never conceived of prior to having completed the experience. While I am technically the one to be "crossing the finish line," I absolutely know that I would have never overcome the intellectual, physical, and emotional hurdles throughout this process without the patience, encouragement, and guidance of a special few.

I am eternally grateful to my advisor, Dr. James S. Thorp for his aid throughout these years. He is an inspiring man to work under for so many reasons – not the least of which is his desire to continually find new and challenging problems in need of exploration. Not only has he spent many hours talking about research and writing out equations with me on his white pads of paper, but also has helped me prepare for and navigate what lies ahead in both professional and personal realms by sharing stories and lessons learned.

I also really want to thank Dr. Virgilio Centeno for his help and support throughout these years. I have had the opportunity to learn from you both in the classroom and as an advisor in ways that have helped me become a professional and well rounded engineer. I am also very grateful for the helping hand and constructive feedback from Dr. Arun Phadke, Dr. Alfred Wicks, Dr. Madhav Marathe, and Dr. Jaime De La Ree. It has been an unbelievable privilege to work and learn from all of you.

The community fostered through the Power Lab at Virginia Tech was extremely beneficial. Having a group of cohorts with which we could do homework, commiserate over exams,

celebrate journal or conference acceptances, and collaborate on new ideas was invaluable. In particular, I'd like to thank Anamitra Pal for his honest and helpful advice.

Furthermore, I must thank my family, Leonard, Toni, and Tyler Vance and my grandmother, Ida Testa, for their unending and unwavering love and assistance. Each of them, and especially my little brother, has contributed immensely to my success in this degree. Finally, I extend my sincerest gratitude to my soon-to-be husband, Marcus Thoreson. I am so thankful that you have not only been a pillar to which I could ground myself in trying times, but also a partner in crime for our career, travel, and bunny adventures.

Table of Contents

List of Figures

List of Tables

Chapter 1. Introduction

What was the longest period of time you have gone without electricity in the last several years? Most likely, it probably was not very long – but the whole time you were without, it seemed like a long nightmare. And so, to begin, I will call attention to the fact that you are most likely reading an electronic copy of this document. This means that electricity is available to you currently, or it was available to charge your mobile device for long enough to allow you to read this. In North America, reliable and consistent electricity has become so common that it is often taken for granted. Routine activities can no longer occur without the use of electricity.

This introduction will first explore some of the history and background of the power industry. The object is provision of a foundation for understanding why research and development must play a vital role in continual modernization of the power grid. The second component introduces control systems theories and processes which are integral to understanding the analyses conducted here. In the most basic terms, this thesis has sought to find ways to utilize control theory to parameterize and study power systems.

1.1 **The Electrification of the Power Grid**

First, it is necessary to understand the complexity of a power system. The National Academy of Engineering calls electrification the greatest engineering feat of the 20^{th} century [1]. The transmission and distribution systems are the backbone of the power grid. Unfortunately, the current infrastructure is essentially the same as the grid in the 1960's. The 2003 blackout drew much attention to this reality, and subsequently investments in research and development in power systems have grown significantly since.

Despite having been stagnant for many years, the current power system in North America is extremely multifaceted – and is only gaining in complexity. Due to advances in FACTs technologies and HVDC lines, increased government subsidies for renewable resource integration, the retirement of coal plants, and the never ending battle cry "not in my backyard," utilities desperately need new and innovative ideas for reliably providing power for their consumers. Additionally, these changes are happening at a pace which has not been seen before in the industry.

There have been many major blackouts around the world in the last 50 years. Most of these blackouts stemmed from a series of unfortunate events – not one singular event. These events could include the removal of a transmission line for maintenance on a hot day which causes unintended overloads of the lines still in use causing them to be removed from the transmission system. If there is any break in the communication about the state of the power system during events like these, power system operators will not have time to react properly before more lines are tripped and the system begins to separate and drop load and generation. Utilizing current technology being implemented into the smart grid, catastrophes like these can be avoided.

The new power grid aims to use the latest technologies to increase reliability and sustainability. It involves the integration of new communication technology which is necessary to use the wide area measurements (WAMs) of the system for real time monitoring and control analysis. Renewable generation is necessary for the sustainability of the power system; and reliably integrating it will also require knowledge of the system gained from using WAMs. Due to the reliance on communication technologies, cyber security has become an unexpected component of the smart grid [2]. Finally, economic planning is another facet of the smart grid – creating a balance between reliability, sustainability, and cost effectiveness.

The North American Reliability Corporation (NERC), formed in 2006 by the Federal Energy Regulatory Agency, is the national, non-profit Electric Regulatory Organization with the mission to "ensure the reliability of the North American bulk power system." NERC issues mandatory power Standards for a region covering the US, most of Canada, and Baja California Norte, Mexico. Figure 1.1 shows the nine Regional Entities that ensure power system owners, operators, and users comply with NERC standards. NERC follows their mission by creating and enforcing standards [3, 4].

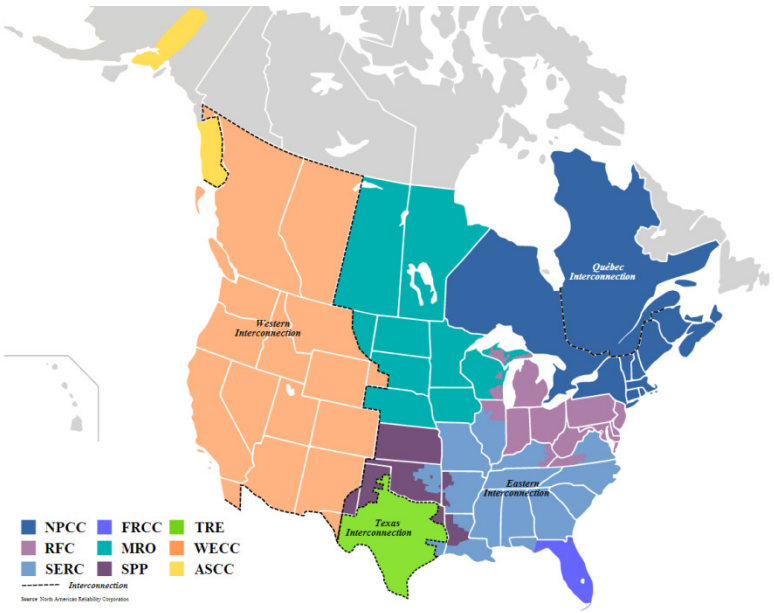

Figure 1.1 - Regional Entity Boundaries

The Department of Energy has created a working group to help guarantee the success of the smart grid. Although developed by the DOE, the key tenets of its approach apply to all power systems around the world. The grid is a complex system that does not have one single correct setting. The Grid Tech Team (GTT) assembled by the DOE in 2011 advocates for modernizing the grid by creating a dialogue between the consumers and power companies. It also aims to maximize the impact of new technologies on the system by minding the economic markets, public policy, regulations, and standards. Additionally, regional engagements are needed to evaluate geographic differences and sensitivities associated with implementing smart grid technology at regional, state, and local levels.

The Federal Energy Regulatory Commission, FERC, is the primary federal regulator of the transmission of electricity. FERC regulates interstate transmission, as well as rates for interstate sales of electricity. States regulate intrastate power generation and transmission. Of relevance for this thesis is the role FERC plays in ensuring the stability of the grid. Working in collaboration with NERC, FERC issues the federal regulations governing grid reliability. NERC is the FERC certified electric reliability organization that writes the grid reliability

standards. NERC reliability standards are then essentially converted into federal laws through FERC orders and regulations.

1.1.1 Global Scale Applicability

Electricity has been changing the world since the late 1800's. Developments in both the United States and Europe led to the creation of an AC power grid. Initially, these systems were individual and local; however, it became clear that connecting them would decrease small local blackouts. Interconnection is desirable because physics dictates that if a direct pathway between the load and generation is no longer available, power will flow in a different path to reach the load. A load is the consumption of energy caused by powering anything requiring electricity. As the United States and European power grids grew, Asia, South America, and Africa followed. However, there are 1.3 billion people in the world living without electricity as of 2009 [5]. All regions where power is either not available or available on a schedule are trying to quickly build and/or strengthen their grid. The push towards global electrification requires unique and innovative solutions to find energy resources that do not harm the environment, decrease the strain on the transmission systems, and keep the economic costs down.

Due to the interconnection of the small power grids, there have been many major blackouts around the world in the last 50 years. Decreasing the number of small blackouts comes at the cost of potentially huge blackouts of the interconnected system. Most of these blackouts stemmed from a series of unfortunate events – not one singular event. For example, these events could include the removal of a transmission line for maintenance on a hot day which causes unintended overloads and sagging of the lines still in use causing them to be removed from the transmission system. If there is any break in the communication about the state of the power system during events like these, power system operators will not have time to react properly before more lines are tripped and the system begins to separate and drop load and generation. The Northeastern Blackout of 2003 and the 2012 Indian Blackout are examples of how blackouts cascaded and, in the case of the Indian Blackout, persisted for several days. A consulting company estimated that the economic cost of the 2003 outage was between $7-10 billion dollars for the national economy [6]. By applying current technology that is now being implemented into the smart grid, the impact, frequency and size of catastrophes like these can be significantly reduced.

1.2 **Systems & Controls**

Even when they were not formally recognized as such, humans have been using controls to predict and modify their surroundings since the early roman aqueducts which prevented flooding through the use of valves. One of the most significant initial control systems, the fly ball governor, was initially designed by Robert Hook and Christian Huygens, but later adapted by James Watt in 1769 as a way to regulate engine speed in steam engines. His technology proliferated throughout the industrial revolution and by 1868, there were around 75,000 governors in use [7]! In the years to follow, mathematicians tackled the challenge of defining the mathematical equations which govern control systems. Up until the 1950s, these classical approaches only addressed scalar inputs and outputs of linear time-invariant systems. In the 1950s, mathematicians and engineers alike, began developing ways to evaluate multivariable, time varying systems, and nonlinear systems. Further information on these developments can be found in [8, 9].

Starting broadly again, to exert control over an object, one must influence its behavior to achieve the desired goal. In very rough terms, control theory can be broken into two lines of work. The first line of work assumes that someone or something wants to optimize the behavior of a particular object in addition to requiring that the given object has a proper model. An example of this is how physics and engineering specifications can be used to calculate the trajectory of an airplane such that the amount of fuel consumption is reduced. The second line of work evaluates the constraints that model or environmental uncertainty exerts on the object of interest. In order to determine these effects, feedback must be used because one wants to correct for deviations in the desired behaviors. For example, when there are errors in a predetermined flight plan, feedback control can be used to keep the craft on the approximate course. In general, the differences between these are of little consequence when designing control systems because their processes overlap in many ways [7].

This object over which the user would like to exert control is the system in question. A system is intended to define how a machine changes over time in accordance with its physical characteristics. All of the information needed to know the future evolution of the system is contained in the state, x. This is assuming that there are no external forces [10]. The state space

representation of a system can be described by the state variables. The state equations relate the current and output system states to its current input and previous states.

$$\dot{x}(t) = Ax(t) + Bu(t) \tag{1.1}$$

$$y(t) = Cx(t) + Du(t)$$

where

- $A \in \boldsymbol{R}^{n\times n}$ is the state matrix. It is square and has the dimension equal to the number of states.
- $B \in \boldsymbol{R}^{n\times p}$ is the input matrix. It gives the proportion of the individual inputs that are applied to each state equation.
- $C \in \boldsymbol{R}^{p\times n}$ is the output matrix.
- $D \in \boldsymbol{R}^{p\times p}$ is the feed forward matrix.
- $x(t)$ is the state vector.
- $u(t)$ is the input vector.
- $y(t)$ is the output vector.

Think of the integer, p, as the number of independent measurements that are taken each instant. Normally, the minimum number of state variables necessary to represent a given system is n or the number of defining differential equations for the system.

1.3 **Translating the Power System into a Control System**

Power system stability is a multifaceted topic which can be approached in many different ways. However, before evaluating power system stability, it would be useful to understand both mathematically and in plain words what a system is. This section will be used to break down the meaning of the power system state and how it is currently calculated.

Utility control centers began popping up in the 1960's in order to provide operators with a central place to collect measurements and data to determine the system state. Currently, bulk electric system (BES) is operated using an energy management system (EMS). The EMS receives telemetry data consisting of complex voltages from all of the nodes across the network. This is considered to be the power system state [11]. These measurements combined with the system topology and constant line impedances allow for the calculation of the line flows in the

network through large load flow calculations. This was not sufficient for providing operators with the information needed to run the grid reliably. Static state estimation which was introduced in the 1960's utilized measurements of the system voltages, current injections, and real and reactive power flow to create an over determined system [12, 13, 14]. These unsynchronized measurements which are scanned in a 1-10s time period provide an input to a non-linear State Estimator which solves over several iterations. The output of this calculation is the minimal solution of the state estimator – or in more simple terms, the power system state.

Although this design process has worked well over the years, vast improvements became more feasible with the insurgence of computer and microprocessor technologies. The concept of the power system state is based in measurement, making better measurement techniques and

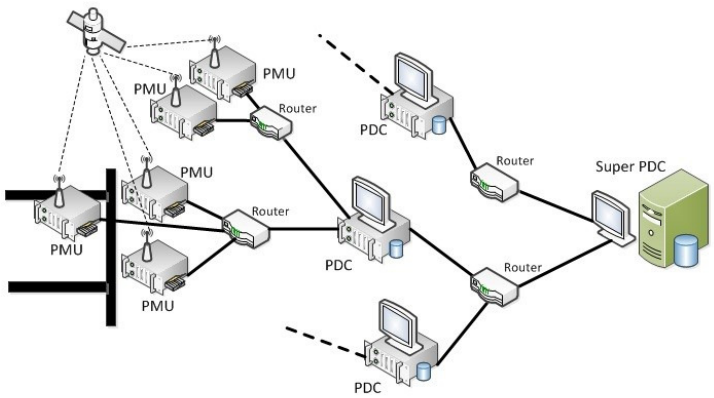

Figure 1.2 - PMU-PDC Data Transfer

methodologies the next logical step in power system understanding. After working on protection algorithms which would better use the digital relaying [15], James Thorp and Arun Phadke recognized that time synchronized measurements were now possible due to the advent of GPS technologies [16, 17]. Time synchronized measurements opened a new world of possibilities for the understanding of power systems because the calculation of the phase angles does not require computationally intensive non-linear state estimation anymore. The computation is simplified to a linear calculation which will always have a solution. These time-stamped signals measure voltage and current magnitudes and phase angles with respect to a reference point in the power system. Additionally, these measurements can be taken up to 60 times per second enabling the capture of previously unstudied dynamic behaviors and can be applied in a plethora of

applications [18, 19, 20, 21, 22]. There is much research as well into the particular locations in a power system where these units should be placed for maximum observability [23, 24, 25, 26]. Wide Area Measurements (WAMs) is the term for this new technology and the technology which captures this information is a Phasor Measurement Unit (PMU). An intuitive way to think of a PMU is to imagine many cameras dispersed throughout the grid taking snapshots of voltages at exactly the same time. A linear state estimator can then stitch these synchrophasor snapshots together – similar to a panorama.

Although synchrophasor technology is a vast improvement on traditional state estimation, it is still necessary to ensure that the incoming data is accurate [27, 28]. Previously, when data quality was poor, it would be apparent because the state estimator would stop solving. With the linear state estimator, there will always be a solution so data conditioning becomes that much more significant.

This is an enormous technological innovation in the field of power systems because this information provides the actual system state at a given instant rather than just a periodic estimation. Traditional state estimation scanned the power system over a longer period of time which means that it did not accurately represent quickly occurring activities and could have many errors. Figure 1.2 provides a view of how PMU data is gathered and compiled through Phasor Data Concentrators (PDCs).

For the time being, synchrophasor data is not replacing traditional SCADA data, but instead work alongside it as a complement. It should be noted that the technology for both positive sequence and three phase phasor only state estimation is available [29]. The conservative nature of the power industry is such that change is made extremely slowly, so new technologies must run in parallel with current ones until a comfort level is developed with them. Even though they are not being utilized for state estimation, the applications of synchrophasor data far exceed those of traditional SCADA data due to the synchronicity of the data points. Power system modeling provides a good example for the application of synchrophasor data. Because of the speed of the data capture, it is easier to model how the system actually responds to stressed conditions and dynamic events.

This high level overview was meant to demonstrate that the translation of the power system into a more robust and useful control problem is in large part possible because of the deployment of PMUs across the power system. More information on this translation will be provided in Chapter 3.

1.4 **Power System Stability**

As this thesis works to explore the stability of the power system, thus, a well-defined understanding of power system stability is necessary. Most recently, system stability was defined by [30]:

"Power system stability is the ability of an electric power system, for a given initial operating condition, to regain a state of operating equilibrium after being subjected to a physical disturbance, with most system variables bounded so that practically the entire system remains intact."

There are several ways to classify power system stability. These classifications aid in the analysis of stability problems, identification of factors which contribute to instability, and ways to improve stable operations. The classifications are based on the physical nature of the instability which occurred, the size of the disturbance studied, and the devices and time span of the instability.

There are several sets of modeling requirements for the study of each type of stability. For transient stability, the time period is in the order of a few seconds. The initial operating conditions of the system need to be known in the form of the network, load levels, voltages, and power flow conditions. Additionally, generator rotor dynamics, exciters systems, AVRs, PSSs, governors, SVCs, HVDC lines, and protective relaying on transmission lines all need to be modeled correctly. The loads should include voltage dependent characteristics as well [31]. A power swing is a fluctuation in power flow that happens when generator rotor angles increase or decrease relative to each other as they respond to system disturbances. Disturbances include, but are not limited to, faults, changes in load, line switching, and generation loss. When a power system is stable, any of these sorts of events should be able to occur without generators oscillating against one another or in conjunction as a set, but instead, should respond such that the system can move toward a new equilibrium state. When there is an unstable swing an out-of-

step condition may arise in which generator poles slip and stability cannot be regained. A situation like this currently would require manual intervention which may not come quickly enough to save equipment from damage or prevent a blackout. However, synchrophasor technology, which measures the angles in reference to a single point, can detect these swings without knowledge of the topology or network model. Unfortunately, without proper control in place, there would need to be significant control room procedures which would need to be implemented to address these issues in an appropriate manner.

The post-event system condition is dependent on the initial system operating condition as well as the nature of the disturbance. This means that power system stability is a property of the system motion around an equilibrium set. Equilibrium sets are composed of opposing forces that are instantaneously equal for an equilibrium point as well as forces over a cycle. For small cyclical variations from small continuous fluctuations in loads or period attractors, the system is still considered inside the equilibrium set.

1.5 **Gain Scheduling & Adaptive Control Applications**

Gain scheduling control has been increasingly developed over the last 20 years as a way to improve the performance of nonlinear systems with varying parameters and/or uncertainties [32, 33]. According to a survey paper [32], gain scheduling can be conceptualized in many ways. Examples given in [32] state that gain scheduling can be thought of as switching various gains or controllers at preset times or based on the current system's operating conditions. The underlying basis of gain scheduling problems is that a linear control is designed and applied to a nonlinear system [32]. The heuristic approach to gain scheduling that uses extensive testing and relies on the linearization being close to the non-linear model has been practiced for many years in jet engines, submarines, etc. However, there has been little theory developed to guarantee the performance of the control when applied to the actual non-linear system [34]. In this work, multiple controllers are developed for several predetermined operating points of an example power system. The operating points for which controllers are designed are contingencies in the power system, for example, a line outage or a load increase.

The time at which the controls change is determined by scheduling variables. For power systems, it is natural to make these variables PMU measurements because they provide real time information about the power system's operating condition at that instant. Specifically, the

scheduling variables are power flows across tie lines in the system. The tie line flow provides useful information about the system. For example, the flows indicate when lines are out, variations in generation and load occur, or other system parameters change. After all of the operating points have been determined and a control has been found for each of them, it is necessary to determine which point provides the best control for the current system condition.

The methodology developed provides a unique and simple way of determining whether the linearization technique provides suitable gain scheduling control. Although it does not prove sufficiency, it is a considerable improvement to the notion of assuming that it works because the linearization is similar to the non-linear system. Additionally, it is extremely easy to scale to large power systems where there are many power flows because two points in scheduling variable space can always be connected with a line. However, for further work and to actually provide sufficiency, the quadratic Lyapunov function would need to be calculated numerically to find the exact stability domain of the non-linear system.

1.6 **Pseudo-Non Linear Control using Lyapunov Functions**

Although linear estimations of non-linear systems provide some level of insight, it is desirable to model some of the truly non-linear behavior of a power system. For large power systems, this is extremely difficult due to how non-linear it is by nature. The linearization of the power system model provides a state space realization which can be used to design a controller using the state feedback of the generator angles and speeds. This state feedback control was developed using a multi-objective H_2/H_∞ problem with pole placement. Continuing with the traditional linear control theory, it is possible to determine a Lyapunov function for the closed loop state space realization. Chapter 3 will provide more rigorous proofs and information regarding this theory.

The initial set-up of this study begins much like other linear analysis. Once the controller is applied to the power system during a transient simulation of the contingencies with which it was designed, these same state feedback signals are used to track the Lyapunov function which was developed earlier. In order to determine which gain should be applied at any given operating point, many permutations of the contingency operating points must be created. These steady state variations in the contingency cases provide a blanket set of operating points to which any of the contingencies can be applied.

After all of the power flow files have been created using DSATools PSAT program, a transient simulation is performed with the predetermined contingency set using their program, TSAT [35]. The control designed for the applied contingency is included so that the optimal response from the system is derived. The dynamic data files for the HVDC lines and SVCs include the control feedback designed in Matlab [36]. When all of the transient simulations for the permutations of controls, contingencies, and steady state operating points are completed, the state and derivative state data can be multiplied with the Lypaunov matrix found previously to find a pseudo-non-linear Lyapunov function. The many calculated functions provide the measurement set to be analyzed through data mining. Due to its popularity for power systems use, Decision Trees were an obvious way to implement this calculation. The output of the decision trees is the desired control necessary for a given system based on the state measurements.

A decision tree functions much like an actual tree in that all of the data which stems out in the branches is initially contained within the trunk, or root node. The information is extracted in the form of "branches" that manifest to the user as a set of if-else statements. As one follows the path of the if-else statements, the final end point of the branch provides the classification. When a set of sample data is entered at the root of the classification tree, the information travels down the branches until it is classified by the tree when it reaches the terminal node. The classification and regression tree (CART) [37] analysis is performed with a non-parametric decision tree learning technique. It is particularly applicable in power systems due to the complex non-linear system dynamics [38, 39].

The traditional CART methodology organizes data into arrays where the events/outcomes form the rows and the columns are the measurements in time. One decision tree is created for each contingency. For many power systems applications utilizing synchrophasor data, this traditional approach neglects to address the real and imaginary components of a phasor. Reference [40] provides a new and inventive way of ensuring that the decision tree uses all of the relevant data to obtain the most optimal result.

After the decision trees have been created, the splitting values needed to determine the class of test data are provided to the dynamic data files for the HVDC lines and SVCs. The next component is the testing of this process by computing the Lyapunov function in the dynamic

files and ensuring that the correct control is applied. Chapter 6 will provide the results found for the Four Machine and 127 Bus System [41, 42]**.**

1.7 **Motivation and Objective**

The main motivation for this work is to explore the applications of control theory in power systems. Because it is necessary and important to understand in detail how the power system operates and changes during various conditions, fully understanding how it can fit into different types of control system frameworks can provide valuable insights. Additionally, by extending this work to include a non-linear application of Lyapunov theory to power systems in a larger test system, this work has provided a new approach to power system stability which will actually account for the dynamic nature of the system. Furthermore, it is useful to ensure that even with a linearization of a power system, valuable results can be found by extending the results back into the non-linear system.

The algorithm proposed in Chapter 5 will provide a service in which real time data is collected through WAMs and fed into the classification algorithm. Once processed, the control designed for a system of with similar outages and topology will be provided for application to the HVDC line control. This work provides the framework for being able to follow the chart shown in Figure 1.3 for any contingency in the system.

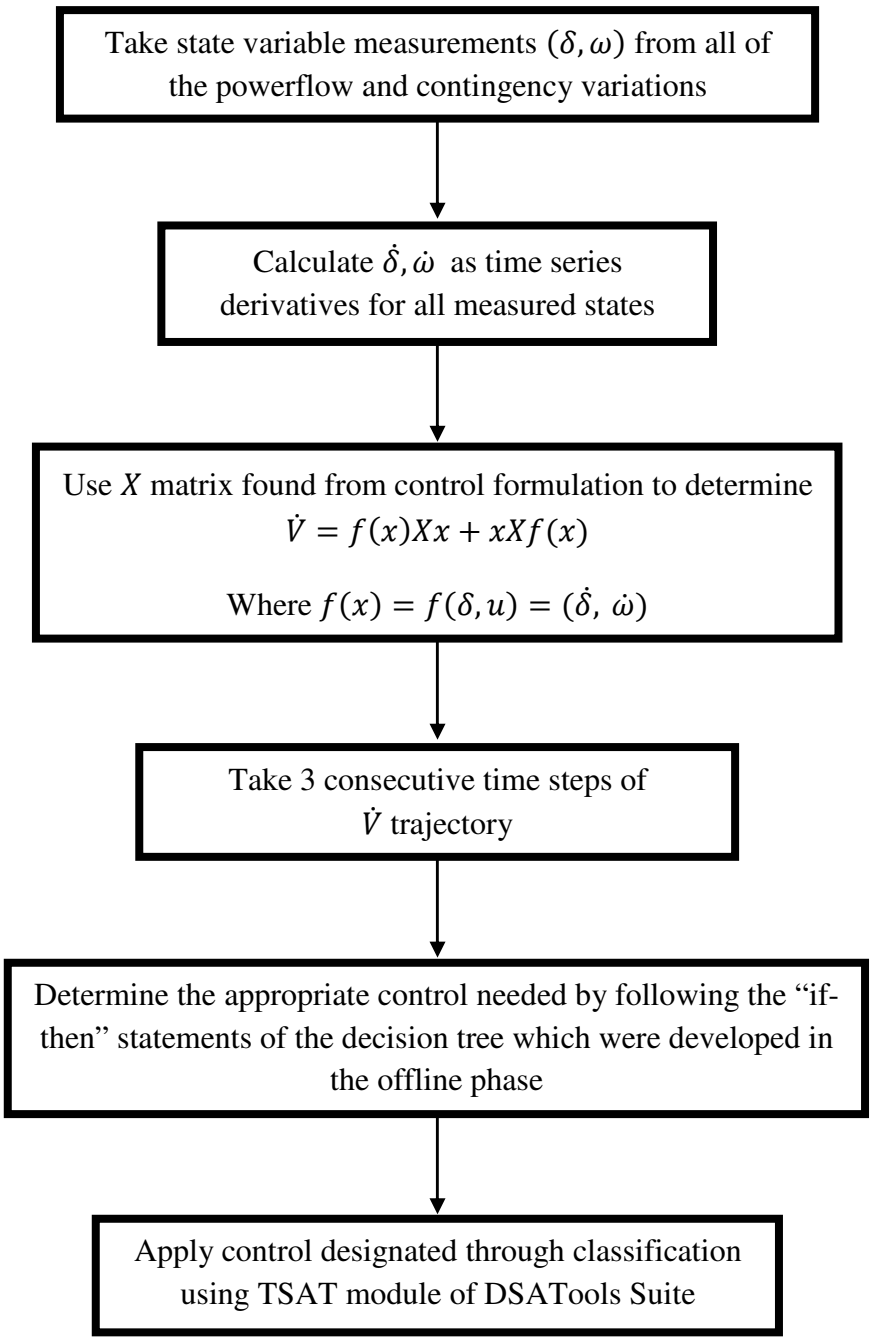

Figure 1.3 – Flowchart for Incoming Data

1.8 **Overview**

Chapter 1: Introduction

The introduction provides some background knowledge of power systems and the application of control theory to them. There is a brief discussion of some of the historically relevant moments

in each industry as well. It further outlines some of the different control applications employed and provides a basic overview of why it is desirable to evaluate power systems in the context of a control problem.

Chapter 2: Power System Stability & Solutions

In order to set the foundation for the rest of the work, this chapter will outline power system stability. Additionally, there will be fundamental information provided regarding the calculations necessary for the stability theory presented later.

Chapter 3: Gain Scheduling & Adaptive Control

Using the definitions and fundamentals laid out in [32], this chapter evaluates the applications of gain scheduling to power systems. Power flow measurements are utilized as scheduling variables and stability bounds are constructed through this parameterization. An example is shown utilizing the 4 machine system.

Chapter 4: Pseudo-Non-Linear Lyapunov Control Applications

This chapter will explore the theory and application of direct Lyapunov methods to power systems. The controls implemented were developed with linear models, but this is a novel methodology that combines the linear approximation with the transient simulations to predict the current system conditions and which controller needs to be applied.

Chapter 5: Problem Formulation and Testing

Finally, by applying the theory laid out in Chapter 4, we will now delve into the results and details of the implementation of this problem. The example systems were the 4 machine system as well as the simplified 127 Bus WECC model. Both models utilized HVDC lines and FACTs devices with state space control feedback. The controls were designed through Matlab [36] and then modeled using Powertech's DSATools Suite [35].

Chapter 6: Conclusions and Future Work

In addition to reviewing the results, this chapter serves as a jumping board for utility scale application. It also provides information on how regulation and policy will dictate the significance of centralized control in the power system operation.

Chapter 2. Power System Stability Overview

The following table provides a historical background and motivation for why small signal control problems are significant for the power grid as a whole. The slower moving oscillation events listed here would have benefited from the types of linear and non-linear techniques developed in this work.

Early 1960's	Oscillations were observed when the Detroit Edison (DE), Ontario Hydro (OH) and Hydro-Québec (HQ) systems were inter-connected
1969	Oscillations observed under several operating conditions in the Finland-Sweden (and Norway)-Denmark interconnected system
1971 and 1972	Over 70 incidents of unstable inter-area oscillations occurred in the Mid-Continent Area Power Pool (MAAP) system in North America
1971-1974	0.19-0.36 Hz oscillations observed in the UCTE/CENTREL interconnection in Europe [48]
1975	Unstable oscillations of 0.6 Hz were encountered on the interconnected power system of New South Wales and Victoria
1982 and 1983	State Energy Commission of Western Australia (SECWA) experienced lightly damped system oscillations in the frequency range of 0.2-0.3 Hz
1984	0.15-0.25 Hz oscillations observed in Brazil [49]
1985	0.6 Hz oscillations observed in the Hydro-Québec system [50]
1996	Pacific AC Inter-tie (PACI) in WECC experienced unstable low frequency inter-area oscillations following the outage of four 400 kV lines
2003	Blackout in eastern Canada and US coincided with 0.4-Hz oscillations [51]
2012	A number of inter-area oscillations were observed between the upper Midwest

	and the New England/New Brunswick areas in the 0.25 Hz family

In order to understand how these types of power system events can be mitigated, it is necessary to have an understanding of dynamic control systems. In the process of translating a power system into a dynamic control system, there are three very basic steps which need to be accomplished. First, a set of differential and algebraic equations which describes the physical system need to be developed. Next, the constant and variable values of the system need to be determined. This is to provide the detailed condition of the physical system at some instant in time. Finally, the differential equations are integrated with the values determined in step two as the initial conditions. In addition to these variables, it is possible to include inputs to the system that follow logic developed outside of the simulation itself.

Thus, the quantities in a dynamic simulation can be classified as one of the following:

- Constants: Values which do not vary during the period of simulation
- State Variables: Quantities that vary and are defined at each instantaneous step through differential equations
- Algebraic Variables: The values of algebraic variables can be found when the values of the state variables, constants, and input variables are known.
- Input Variables: Values that can be determined at any instant through logic outside of the simulation

The first set of differential equations includes the generators, motors, controls, and other dynamic devices. The second set of equations includes the algebraic network equations and information about the transmission network and the internal static behavior of passive devices such as static loads, phase shifters, and shunt capacitors [43]. Together these equations form the continuous time model.

2.1 **Continuous Time Model**

The study of power system dynamics begins with the translation of the physical components into a continuous time model. This dynamic behavior is governed by two sets of non-linear Equations, (2.1) and (2.2):

$$\dot{x} = f(x, u) \tag{2.1}$$

$$y = h(x, u) \tag{2.2}$$

The first set of differential equations includes the generators, motors, controls, and other dynamic devices.

By imposing the condition that the state equations provide equilibrium for the system at zero, it is possible to compute the steady state system conditions for pre- or post-fault states. This can be represented with Equation (2.3), where x_{eq} is an equilibrium state which corresponds to a constant input of u_{eq}.

$$f(x_{eq}, u_{eq}) = 0 \tag{2.3}$$

Also, y_{eq} will be the corresponding constant output:

$$y_{eq} = h(x_{eq}, u_{eq}) \tag{2.4}$$

The security assessment which takes place when evaluating power systems is two-fold. The static component of the assessment determines if the properties of the post fault equilibrium state are acceptable. This is accomplished by ensuring that equilibrium is locally stable and the steady-state voltage magnitudes and currents satisfy their operating constraints. The assessment's dynamic component determines whether the system would actually be able to reach the post-fault operating condition.

Even though the physical specifications of a generator do not influence its steady state system response outside of their expected MW outputs, they do affect its dynamic response significantly [30]. Steam and combustion turbines, hydro turbines, diesel engines, and wind turbines all contain prime movers do not have prime movers in the classical sense, but their effect on dynamics can be explored more thoroughly in [44]**.** In general, steam and combustion turbines have high speed cylindrical rotors with two or four rotors. Salient pole rotors with multiple poles are utilized for hydro turbine generators.

For the purposes of evaluating the power system model, it is helpful to begin with the development of equations from a single machine infinite bus (SMIB) model using a classical generator. Using a classical synchronous involves the following simplifying assumptions.

- The mechanical input power is constant

- The generator is represented by a constant EMF behind the direct axis transient reactance, X_d'.
- The voltage angle behind the transient reactance represents the mechanical rotor angle.

Figure 2.1 is a very basic representation of the mechanical power used to turn the shaft to produce electrical power from the generator.

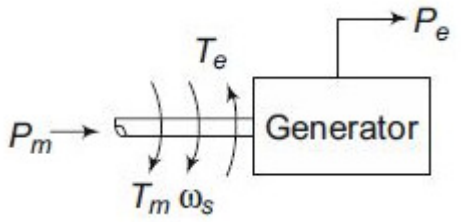

Figure 2.1 – Synchronous Machine Diagram

When exploring power systems, it is useful to go back to the very fundamentals. Although Wikipedia may not be a scholarly source, it often has elegant definitions of basic concepts. Thus, according to Wikipedia [45]: "Inertia is the resistance of any physical object to any change in its state of motion (this includes changes to its speed, direction or state of rest)." For a generator that is online and connected to the transmission network, its inertia is the mechanical energy that is stored in the rotating components which include the turbine, generator, shaft, and exciter. However, note that if the exciter is driven by a different prime mover, it would not contribute to the unit's inertia. When there is a disturbance that acts on the rotor, the net torque being applied will cause acceleration or deceleration based on Equation (2.5).

$$T = T_m - T_e \tag{2.5}$$

where

$$T_a = accelerating\ torque\ in\ N \cdot m$$
$$T_m = mechanical\ torque\ in\ N \cdot m$$
$$T_e = electromagnetic\ torque\ in\ N \cdot m$$

The values of T_m and T_e are positive for a generator and negative for a motor in Equation (2.5). The generator inertia determines the mechanical and electrical response of the machine to

disturbances. The combined moment of inertia of the generator and the turbine, J $(kg \cdot m^2)$ is the parameter which quantifies the mechanical resistance of the generator to changes in its state of rotation. This value is related to the rotating speed and total mass of the components. Equation (2.6) shows that

$$J\frac{d\omega_m}{dt} = T_a = T_m - T_e \tag{2.6}$$

where

$$J = combined\ moment\ inertia\ of\ generator\ and\ turbine, kg \cdot m^2$$
$$\omega_m = angular\ velocity\ of\ the\ rotor, mech.rad/s$$
$$t = time, s$$

The inertia constant, H $(MW - seconds/MVA)$, is defined as the total rotational energy stored by the rotating components divided by the MVA rating on the nameplate.

$$H = \frac{stored\ energy\ at\ rated\ speed\ in\ MW * s}{MVA\ Rating} \tag{2.7}$$

The equation of motion can be normalized in terms of the per unit inertia constant, H, as seen in Equation (2.8). The value ω_{0m} denotes the rated speed in mechanical radians per second as shown in Equation (2.9). This allows the inertial constant to be normalized based on the prime mover, not on the MVA rating of the unit.

$$H = \frac{1}{2}\frac{J\omega_{0m}^2}{VA_{base}} \tag{2.8}$$

$$\omega_{0m} = rated\ angular\ velocity\ in\ \frac{mechanical\ radians}{s} = 2 * \pi * \frac{RPM}{60} \tag{2.9}$$

The moment of inertia, J, in terms of H, is defined in Equation (2.10)

$$J = \frac{2H}{\omega_{0m}^2}VA_{base} \tag{2.10}$$

The swing equation (2.11) is then defined by substituting (2.10) into (2.6). By rearranging (2.11), it is possible to find (2.12).

$$\frac{2H}{\omega_{0m}^2}VA_{base} = \frac{d\omega_m}{dt} = T_m - T_e \tag{2.11}$$

$$2H\frac{d}{dt}\left(\frac{\omega_m}{\omega_{0m}}\right)=\frac{T_m-T_e}{VA_{base}/\omega_{0m}}=\frac{T_m-T_e}{T_{base}} \tag{2.12}$$

Thus, the per unit equation of motion is as follows in (2.13):

$$2H\frac{d\bar{\omega}_r}{dt}=\bar{T}_m-\bar{T}_e \tag{2.13}$$

Where $\bar{\omega}_r$ (rad/s) is calculated in Equation (2.14) as the rotor angular velocity, using ω_0 as its rated value, and p_f as the number of field poles.

$$\bar{\omega}_r=\frac{\omega_m}{\omega_{0m}}=\frac{\frac{\omega_r}{P_f}}{\frac{\omega_0}{P_f}}=\frac{\omega_r}{\omega_0} \tag{2.14}$$

Furthermore, assume that δ is the angular position of the rotor in electrical radians with respect to a synchronously rotating reference, where δ_0 is the value of δ at time $t=0$.

$$\delta=\omega_r t-\omega_0 t+\delta_0 \tag{2.15}$$

Equations (2.16) and (2.17) are the result of taking the derivative of Equation (2.15) with respect to time.

$$\frac{d\delta}{dt}=\omega_r-\omega_0=\Delta\omega_r \tag{2.16}$$

$$\frac{d^2\delta}{dt^2}=\frac{d\omega_r}{dt}=\frac{d(\Delta\omega_r)}{dt} \tag{2.17}$$

$$=\omega_0\frac{d\bar{\omega}_r}{dt}=\omega_0\frac{d(\Delta\bar{\omega}_r)}{dt}$$

By substituting $\frac{d\bar{\omega}_r}{dt}$ into Equation (2.13), the result is

$$\frac{2H}{\omega_0}\frac{d^2\delta}{dt^2}=\bar{T}_m-\bar{T}_e \tag{2.18}$$

This does not account for the damping torque, which is not included in the calculation of T_e. This addition is made by including a term that is proportional to the speed deviation in order to account for damping.

$$\frac{2H}{\omega_0}\frac{d^2\delta}{dt^2}=\bar{T}_m-\bar{T}_e-K_D\Delta\bar{\omega}_r \tag{2.19}$$

From Equation (2.16), it can be seen that: $\Delta\bar{\omega}_r=\frac{\Delta\omega_r}{\omega_0}=\frac{1}{\omega_0}\frac{d\delta}{dt}$.

Equation (2.19) provides the final equation of motion for a synchronous generator. It is commonly referred to as the swing equation because it provides insight into how the rotor angle,δ, will swing during a system disturbance. The second order differential equation in (2.19) can also be represented as a set of two first order differential equations shown in Equations (2.20) and (2.21). A block diagram of the SMIB model shown in Figure 2.2 provides a quick visualization. It is assumed that the following values are in per unit, angle δ is in electrical radians, and ω_0 is equal to $2\pi f$.

$$\frac{d\Delta\omega_r}{dt} = \frac{1}{2H}(T_m - T_e - K_D\Delta\omega_r) \tag{2.20}$$

$$\frac{d\delta}{dt} = \omega_0\Delta\omega_r \tag{2.21}$$

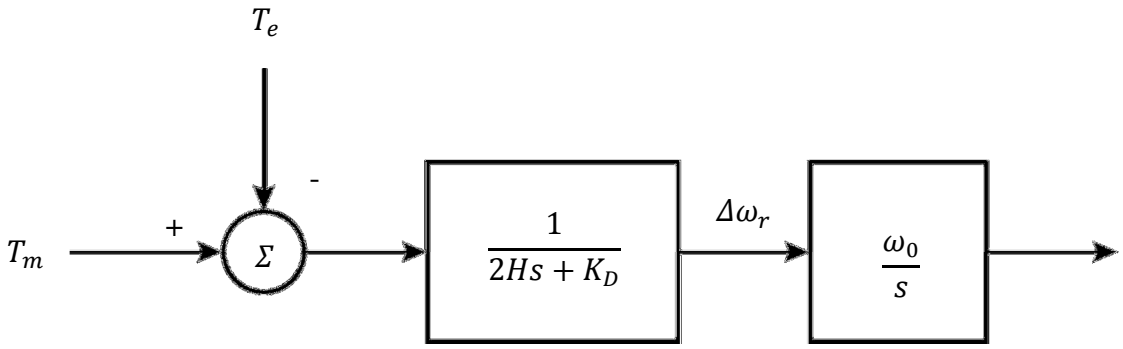

Figure 2.2 - Block Diagram of Swing Equations

2.2 **Large-Disturbance or Transient Stability**

When evaluating large disturbances like short circuit faults, the change in the generator speed or angle could be high and will not behave linearly. These studies are called transient stability studies. The transient stability of an SMIB system can be analyzed using the equal area criterion. This criterion can be determined through the swing equation, starting with Equation (2.22).

$$\frac{d^2\delta}{dt^2} = \frac{\pi f_i}{H}(P_m - P_{max}sin\delta) \tag{2.22}$$

Next, multiply both sides of Equation (2.22) by $2\frac{d\delta}{dt}$ to find Equation (2.23):

$$2\frac{d\delta}{dt}\frac{d^2\delta}{dt^2} = \frac{\pi f}{H}(P_m - P_{max}sin\delta)\left(2\frac{d\delta}{dt}\right) \tag{2.23}$$

The Equation (2.23) can be further simplified by recognizing that $\frac{d}{dt}\left[\frac{d\delta}{dt}\right]^2 = 2\frac{d\delta}{dt}\frac{d^2\delta}{dt^2}$ in Equation (2.24).

$$\frac{d}{dt}\left[\frac{d\delta}{dt}\right]^2 = \frac{\pi f_2}{H}(P_m - P_{max}sin\delta)\frac{d\delta}{dt} \tag{2.24}$$

$$d\left[\frac{d\delta}{dt}\right]^2 = \frac{\pi f_s}{H}(P_m - P_{max}sin\delta)d\delta$$

Next, it is necessary to integrate both sides and take the square root to find Equation (2.25)

$$\frac{d\delta}{dt} = \sqrt{\frac{\pi f_s}{H}\int_{\delta_o}^{\delta}(P_m - P_{max}sin\delta)d\delta} \tag{2.25}$$

In a stable system, the rotor angle δ must settle to the steady state value eventually. This means that Equation (2.25) equals zero because the rate of change of angle with respect to time should be zero in steady state as is shown in Equation (2.26).

$$\frac{d\delta}{dt} = 0 \Rightarrow \int_{\delta_0}^{\delta}(P_m - P_{max}sin\delta)d\delta = 0 \tag{2.26}$$

The swing equation and a preliminary understanding of the dynamics of the generators feeding power to the transmission network provide some insight into the physical forces at play when discussing power system stability.

2.3 **Linearization of the Continuous Time (CT) Model**

Despite all of the nonlinearities described above, to proceed, there needs to be some discussion of how and why linearizing a system is beneficial for understanding it – as well as the limits of studying a linear system. Linearization is useful because there are many more established ways of understanding linear systems. The superposition principle still holds, a unique equilibrium or continuum of equilibria is provided, and there are easy tests for controllability and observability of the system in question. Because of this, engineers can gain some amount of insight and understanding into the nonlinear system. In short, a linearized model is a good place to start, but it is necessary to be cognizant of its short comings.

Linearization is just an approximation of the neighborhood around an operating point. Because of this, it can only provide "local" behavior for the real nonlinear system. This means that no

information is gathered about the other regions in which the non-linear system could be operating. Additionally, the linear models often ignore more complicated system dynamics which can be "essential nonlinear phenomena" to understanding the system [46]. There is no prediction of non-local or global behavior.

2.3.1 Linearization to State Space Form

The following section will involve taking the equations in (2.1) and (2.2) and transforming them into linear equations. This process begins by supposing that $\left(x^*(t), u^*(t)\right)$ is a trajectory corresponding to the output, $y^*(t)$ as seen in Equations (2.27) and (2.28).

$$\dot{x^*} = f(x^*, u^*, t), \qquad x^*(t_0) = x_0 \tag{2.27}$$

$$y^* = h(x^*, u^*, t) \tag{2.28}$$

By taking a multivariable Taylor series expansion in Equations (2.29) and (2.30):

$$\dot{x} = f(x^*, u^*, t) + \left.\frac{\partial f}{\partial x}\right|^* (x - x^*) + \left.\frac{\partial f}{\partial u}\right|^* (u - u^*) + Rem_f(x, u, t) \tag{2.29}$$

$$y = h(x^*, u^*, t) + \left.\frac{\partial h}{\partial x}\right|^* (x - x^*) + \left.\frac{\partial h}{\partial u}\right|^* (u - u^*) + Rem_h(x, u, t) \tag{2.30}$$

The remainder terms of Equations (2.29) and (2.30) decrease faster than linearly because as $(x, u) \to (x^*, u^*)$:

$$\lim_{(x,u)\to(x^*,u^*)} \frac{Rem_{\{f,h\}}(x, u, t)}{\| (x, u) - (x^*, u^*) \|} = 0 \tag{2.31}$$

By defining perturbation variables as:

$$\tilde{x} = x - x^* \tag{2.32}$$

$$\tilde{u} = u - u^* \tag{2.33}$$

$$\tilde{y} = y - y^* \tag{2.34}$$

The limit that $(x, u) \to (x^*, u^*)$ provides the linearized model such that:

$$\dot{\tilde{x}} = A(t)\tilde{x} + B(t)\tilde{u}, \quad \tilde{x}(0) = x_0 - x^*(0) \tag{2.35}$$

$$\tilde{y} = C(t)\tilde{x} + D(t)\tilde{u} \tag{2.36}$$

Where the state matrices are defined as:

$$A(t) = \frac{\partial f}{\partial x}\Big|^{*} \tag{2.37}$$

$$B(t) = \frac{\partial f}{\partial u}\Big|^{*} \tag{2.38}$$

$$C(t) = \frac{\partial h}{\partial x}\Big|^{*} \tag{2.39}$$

$$D(t) = \frac{\partial h}{\partial u}\Big|^{*} \tag{2.40}$$

In the event that $x^{*}$is constant, the state matrices become time invariant as well such that $A(t) = A$. This says that near x^{*}, the function can be approximated by a linear function plus a co-term or that $x(t) \equiv x^{e}$ and $f(x^{e}) = 0$. For a system of equations this can be written out in Equation (2.41).

$$\begin{aligned} f_1(x_1^e, x_2^e, \dots, x_n^e) &= 0 \\ f_2(x_1^e, x_2^e, \dots, x_n^e) &= 0 \\ &\vdots \\ f_n(x_1^e, x_2^e, \dots, x_n^e) &= 0 \end{aligned} \tag{2.41}$$

This can be displayed similar to the above as:

$$\dot{x} = Ax + Bu \tag{2.42}$$

$$y = Cx + Du \tag{2.43}$$

Such that at time, t, the n-vector x(t) is the state vector, the m-vector *u(t)* is the input vector, and the p-vector *y(t)* is the output vector. The $n \times n$ matrix A is sometimes called the system matrix. Respectively, the matrices $B, C,$ and D have the dimensions $n \times m, p \times n, and\ p \times m$. This system can be described in scalar terms through:

$$\begin{aligned} \dot{x}_1 &= a_{11}x_1 + \cdots + a_{1n}x_n + b_{11}u_1 + \cdots + b_{1m}u_m \\ &\vdots \\ \dot{x}_n &= a_{n1}x_1 + \cdots + a_{nn}x_n + b_{n1}u_1 + \cdots + b_{nm}u_m \end{aligned} \tag{2.44}$$

And

$$y_1 = c_{11}x_1 + \cdots + c_{1n}x_n + d_{11}u_1 + \cdots + d_{1m}u_m$$

$$\vdots \tag{2.45}$$

$$y_n = c_{p1}x_1 + \cdots + c_{pn}x_n + d_{p1}u_1 + \cdots + d_{pm}u_m$$

The transfer function representation of these matrices is shown in Equation (2.46).

$$T(s) = C(sI - A)^{-1} + D \tag{2.46}$$

2.3.2 Eigenvalue Analysis

Whether real parts of all eigenvalues in a system are negative is important. When they are, transients in a linear dynamic system decay over time. A stable system is one in which all transients decay. An unstable system is one in which one or more transients grow.

Unstable power systems do not operate. But power systems are nonlinear. A linearized model may have a complex eigenvalue with a positive real component. When this happens, system oscillations of constant amplitude can occur, subject to limitation by the system's nonlinearity. The system, though compromised, can remain in operation for at least a while. However, a growing oscillation can result in system collapse and failure. The system is threatened in either case.

At a basic level, the first step made towards controlling the system needs to be evaluating the role each generator plays in each mode. The first step is looking at the solution to the state equation. This is evaluated with Equation (2.47).

$$x = \sum_{i=1}^{n} u_i \, z_i \tag{2.47}$$

where

- u_i is the ith right eigenvector of A
- z_i is the ith mode

One way to evaluate the roles of the generators is through modal analysis. When a state vector of a particular mode has a large entry corresponding its right eigenvector, it should be evaluated [18, 47]. This eigenvector is commonly referred to as the mode shape. Another way of stating

this is that a mode's right eigenvector provides the relative amplitude of the mode which is observed through the dynamic system states [47]. The largest amplitude of oscillation for a particular mode corresponds to the state with the largest eigenvector magnitude. When an eigenvector coefficient is zero for a certain state, the measurements of that state cannot see that mode [47]. The mode shapes can determine coherent machine groups in multi-machine systems [18]. The ith eigenvalue, ith left eigenvector, and system input define the ith mode as a scalar function of time. Each mode satisfies the linear differential equation in Equation (2.48).

$$\frac{dz_i}{dt} = \lambda_i z_i + v_i B u \tag{2.48}$$

where

- λ_i is the ith eigenvalue of A
- v_i is the ith left eigenvector of A

The eigenvalue of the A matrix can be found by solving Equation (2.49).

$$\det(A - \lambda I) = 0 \tag{2.49}$$

Additionally, the ith right eigenvector satisfies Equation (2.50).

$$A u_i = \lambda_i u_i \tag{2.50}$$

The ith left eigenvector satisfies Equation (2.51).

$$v_i A = \lambda_i v_i \tag{2.51}$$

The eigenvalue of a mode can be represented by Equation (2.52).

$$\lambda = -\zeta\omega_n \pm j\omega_d = -\sigma \pm j\omega_d \tag{2.52}$$

where

- ζ is the damping ratio
- $\omega_n = |\lambda|$ is the undamped natural frequency and is an indication of rise time
- ω_d is the damped natural frequency
- σ is the real part of the pole

The damping ratio and frequency of oscillation in Hertz can be provided by Equations (2.53) and (2.54).

$$\zeta = \frac{\sigma}{\omega_n} \tag{2.53}$$

$$f = \frac{\omega}{2\pi} \tag{2.54}$$

When the damping ratio is positive, there is positive damping. It should be noted that oscillations in power systems do not normally require heavy damping, but that with the added system stresses of today's system, it is desirable to have more than 5% damping [47]**.**

The eigenvalues calculated from the linearized system are extremely useful for understanding the modes of different generators and how they interact with each other. In future chapters, these values are utilized for determining the efficacy of the control.

The generic linearization techniques provide a useful way to distill information from the nonlinear power systems equations for further analysis and insight.

Chapter 3. Linearized Gain Scheduling Techniques

Technological advancements in the field of power systems provide the opportunity to explore new and interesting problems. The advent of Phasor Measurement Units (PMUs) allows for synchronized time-tagged Wide Area Measurements (WAMs) that provide a real-time snapshot of the power system. This information can be utilized for many applications [18, 19, 20, 21]. This chapter focuses mainly on applications related to the control and small signal stability analysis of power systems.

The movement from optimality to robustness in control design has enabled the evolution of new areas of control theory [51]. The application of optimal control theory to real world problems is difficult in practice and does not always provide a useful result [30]. As most systems are inherently non-linear, it is desirable to determine a way to linearize them so that a controller can be more easily developed [51]. Specifically, the application of control theory to power systems raises the question of how to create a robust controller for a highly non-linear system. It is desirable to design one robust controller for a given problem under variable operating conditions. However, finding a controller that is robust and capable of this variation may yield conservative results or an infeasible controller [51, 52, 53, 54]. A way to circumvent this problem is to use gain scheduling control techniques. These techniques provide flexibility by scheduling controllers that are based on the linearized operating points of the system, which are developed from the non-linear system.

Gain scheduling control has been increasingly developed over the last 20 years as a way to improve the performance of nonlinear systems with varying parameters and/or uncertainties [55]

[56]. According to one survey paper [56], gain scheduling can be conceptualized in many ways. Examples given in [56] argue that gain scheduling could be thought of as switching between various gains or controllers, either at preset times or based on the current system's operating conditions. The underlying basis of problems with gain scheduling is that a linear control is designed and applied to a nonlinear system [56]. The heuristic approach to gain scheduling uses extensive testing and relies on the linearization being close to the non-linear model. This approach has been practiced for many years in jet engines, submarines, etc. However, there has been little theory developed to guarantee the performance of the control when applied to the actual non-linear system [34]. Here, multiple controllers are developed for several predetermined operating points of an exemplary power system. The operating points for which controllers are designed are contingencies in the power system, *e.g*. a line outage or a load increase.

The time at which the controls change is determined by scheduling variables. For power systems, it is natural to make these variables PMU measurements because they provide real time information about the power system's operating condition at that instant. Specifically, the scheduling variables are power flows across tie lines in the system. The tie line flow provides useful information about the system. For example, the flows indicate when lines are out, variations in generation and load occur, or other system parameters change.

After all of the operating points have been determined and a control has been found for each of them, it is necessary to determine which point provides the best control for the current system condition.

This chapter is organized as follows: Section3.1 provides the mathematical background associated with gain scheduling controllers. Section 3.2 explains how controllers designed through gain scheduling are applied in state feedback. Section 3.3 presents the results of these controllers as applied to an example system. Section 3.4 summarizes the findings of the work done in this research area.

3.1 **Necessary Mathematical Concepts**

The following mathematical definitions are necessary for understanding the power systems applications presented in the remainder of Chapter 3.

3.1.1 Linear Time-Invariant Parameter Dependent Systems

Linear time-invariant parameter-dependent (LTIPD) systems are defined in Equation (3.1).

$$\dot{x} = A(\rho)x \tag{3.1}$$

$$A(\rho) = A_0 + \rho A_g$$

For a multi-parameter dependent system, the LTIPD will be defined as in Equation (3.2).

$$\dot{x} = \left(A_0 + \sum_{i=1}^{m} \rho_i A_i \right) x \tag{3.2}$$

The map v from the set of nxn real Hurwitz matrices $\mathcal{A}\ onto\ \mathbb{R}$ is a semi-guardian map, assuming that it is continuous, non-zero, and that $A \in \partial\,\mathcal{A} \Rightarrow v(A) = 0$. To determine the stability of the two-parameter quadratically–dependent matrix over the domain $(r_1, r_2) \in [0,1]x[0,1]$, Equation (3.3) must be examined.

$$A(\rho_1, \rho_2) = \left(\sum_{i_1, i_2, =0}^{i_1+i_2=m} \rho_1^{i_1} \rho_2^{i_2} A_{i_1, i_2} \right) \tag{3.3}$$

The notation that will be utilized throughout this chapter is provided in Table 3.1.

Table 3.1 - Notation for Chapter 3 Reference

$\otimes \oplus$	Kronecker product and sum
$\star$	Bialternate product
$\lambda_i(A)$	ith eigenvalue of the matrix $A \in \mathbb{R}^{n\times n}$
int($\mathcal{D}$)	Interior of the set $\mathcal{D}$
$\partial\mathcal{D}$	Boundary of the set $\mathcal{D}$
$\mathcal{A}$	Set of Hurwitz matrices $A \in \mathbb{R}^{n\times n}$
$\bar{A}$	$A \oplus A, \qquad A \in \mathbb{R}^{n\times n}$
$\tilde{A}$	$A \star I_n + I_n \star A = 2A \star I_n, \qquad A \in \mathbb{R}^{n\times n}$
mspec(A)	Multispectrum of matrix $A \in \mathbb{R}^{n\times n}$, i.e. the set consisting of all the eigenvalues of A, including repeated eigenvalues
$\mathcal{I}_n$	Index set $\{1, 2, \dots, n\}$

$\overline{\cup}$	Ordered union of two sets, taking only one occurrence of repeated members
$\mathcal{D}^{\#}$	Cardinality of set $\mathcal{D}$
$M \in \mathbb{R}^{n\times n}$	$\tilde{\lambda}_i(M), i = 1,2,\dots,p$ represents the real non-zero eigenvalues of M when the vector is nonrepeating.

3.1.2 Guardian Map

The basic results of this work rely on the understanding of the guardian map for Hurwitz matrices [62, 63, 64, 65] .

A guardian map is used to transform a matrix stability problem to a non-singularity problem of an associate matrix. A common guardian map involves using the Kronecker sum of a matrix with itself. The Kronecker sum induces the guardian map υ_1: $\mathbb{R}^{nxn} \to \mathbb{R}$ where $\upsilon_1(A) \coloneqq \det(A \oplus A)$.

Definition directly from [62]:

Let $S \subseteq \mathbb{R}^{nxn}$ be an open set. The map υ: $\mathbb{R}^{nxn} \to \mathbb{R}$ is said to guard the set S if $\upsilon(A) \neq 0$ for all $A \in S$ and $\upsilon(A) = 0$ for all $A \in \partial S$. The map υ is called the guardian map for S.

$$(\rho_1, \rho_2)^T \in \{\rho = r\, v(\theta); r \in (-\infty, \dots), \tag{3.4}$$

The Kronecker sum is defined in Equation (3.5).

$$A \oplus B = \begin{pmatrix} a_{11}+b_{11} & b_{12} & a_{1n} & 0 \\ b_{21} & a_{11}+b_{22} & 0 & a_{12} \\ a_{21} & 0 & a_{22}+b_{11} & b_{12} \\ 0 & a_{21} & b_{21} & a_{22}+b_{22} \end{pmatrix} \tag{3.5}$$

The Kronecker product is defined in Equation (3.6).

$$A \otimes B = \begin{pmatrix} a_{11}B & \cdots & a_{1n}B \\ \vdots & \ddots & \vdots \\ a_{n1}B & \cdots & a_{nn}B \end{pmatrix} \tag{3.6}$$

A particularly useful property of the Kronecker sum and product is shown in Equation (3.7).

$$A \oplus B = A \otimes I + I \otimes B \tag{3.7}$$

3.1.3 Bialternate Sum

For matrices $A, B \in \mathbb{R}^{n\times n}$ with elements a_{ij} and b_{ij}, the index function $\widetilde{m}$ will be defined by:

$$\widetilde{m}(n,i,j) \coloneqq (j-1)n + 1 - \frac{1}{2}j(j+1) \tag{3.8}$$

The bialternate product of A and B is the matrix of $F = A \star B$. It has the dimension $\frac{1}{2}n(n-1) \times \frac{1}{2}n(n-1)$ and is composed of the following elements [66, 67, 68] :

$$f_{\widetilde{m}(n,p,q),\widetilde{m}(n,r,s)} \coloneqq \frac{1}{2}\left(\begin{vmatrix} a_{pr} & a_{ps} \\ b_{qr} & b_{qs} \end{vmatrix} + \begin{vmatrix} b_{pr} & b_{ps} \\ a_{qr} & a_{qs} \end{vmatrix}\right) \tag{3.9}$$

where $p, r = 2, 3, \dots, n$; $q = 1,2, \dots, p-1$ and $s = 1,2, \dots, r-1$. Thus, it can be inferred that $A \star B = B \star A$. For clarity, an example is laid out in Equations (3.10) and (3.11).

$$A = \begin{bmatrix} a_{11} & a_{12} & a_{13} \\ a_{21} & a_{22} & a_{23} \\ a_{31} & a_{32} & a_{33} \end{bmatrix} \; and \; B = \begin{bmatrix} b_{11} & b_{12} & b_{13} \\ b_{21} & b_{22} & b_{23} \\ b_{31} & b_{32} & b_{33} \end{bmatrix} \tag{3.10}$$

$$A \star B = \frac{1}{2}\begin{bmatrix} \begin{pmatrix} a_{22}b_{11} + a_{11}b_{22} \\ -a_{12}b_{21} - a_{21}b_{12} \end{pmatrix} & \begin{pmatrix} a_{11}b_{23} + a_{23}b_{11} \\ -a_{21}b_{13} - a_{13}b_{21} \end{pmatrix} & \begin{pmatrix} a_{12}b_{23} + a_{23}b_{12} \\ -a_{22}b_{13} - a_{13}b_{22} \end{pmatrix} \\ \begin{pmatrix} a_{11}b_{32} + a_{32}b_{11} \\ -a_{12}b_{31} - a_{31}b_{12} \end{pmatrix} & \begin{pmatrix} a_{11}b_{33} + a_{33}b_{11} \\ -a_{13}b_{31} - a_{31}b_{13} \end{pmatrix} & \begin{pmatrix} a_{12}b_{33} + a_{33}b_{12} \\ -a_{13}b_{32} - a_{32}b_{13} \end{pmatrix} \\ \begin{pmatrix} a_{21}b_{32} + a_{32}b_{21} \\ -a_{22}b_{31} - a_{31}b_{22} \end{pmatrix} & \begin{pmatrix} a_{21}b_{33} + a_{33}b_{21} \\ -a_{23}b_{31} - a_{31}b_{23} \end{pmatrix} & \begin{pmatrix} a_{22}b_{33} + a_{33}b_{22} \\ -a_{23}b_{32} - a_{32}b_{23} \end{pmatrix} \end{bmatrix} \tag{3.11}$$

The bialternate sum of $\tilde{A}$ of matrix A with itself is defined in (3.12) as is published in [69], [66], and [67].

$$\tilde{A} = A \star I_n + I_n \star A = 2A \star I_n. \tag{3.12}$$

If $\tilde{a}_{ij}$ denotes the ijth element of $\widetilde{A}$, then it follows that,

$$\tilde{a}_{\widetilde{m}(n,p,q),\widetilde{m}(n,r,s)} = \begin{vmatrix} a_{pr} & a_{ps} \\ \delta_{qr} & \delta_{qs} \end{vmatrix} + \begin{vmatrix} \delta_{pr} & \delta_{ps} \\ a_{qr} & a_{qs} \end{vmatrix} \tag{3.13}$$

The variable δ_{ij} is the Kronecker delta such that $\begin{cases}\delta_{ij}=1\ if\ i=j\\ \delta_{ij}=0\ \ if\ i\neq j\end{cases}$. The other variables range from $p,r=2,3,\dots,n; q=1,2,\dots,p-1$ and $s=1,2,\dots,r-1$. Thus, it can be said that $\tilde{A}\in\mathbb{R}^{\frac{1}{2}n(n-1)\times\frac{1}{2}n(n-1)}$ if $A\in\mathbb{R}^{n\times n}$. An example using Equation (3.13) is shown in (3.14) and (3.15).

$$A_1=\begin{bmatrix}a_{11} & a_{12}\\ a_{21} & a_{22}\end{bmatrix}$$
$$\tilde{A}_1=a_{11}+a_{22} \tag{3.14}$$

$$A_2=\begin{bmatrix}a_{11} & a_{12} & a_{13}\\ a_{21} & a_{22} & a_{23}\\ a_{31} & a_{32} & a_{33}\end{bmatrix},$$
$$\tilde{A}_2=\begin{bmatrix}a_{11}+a_{22} & a_{23} & -a_{13}\\ a_{32} & a_{11}+a_{33} & a_{12}\\ -a_{31} & a_{21} & a_{22}+a_{33}\end{bmatrix}, \tag{3.15}$$

This definition of the bialternate sum with itself provides the foundation to show that (3.16) is also true when $A_0, A_g\in\mathbb{R}^{nxn}$ and $\rho\in\mathbb{R}$.

$$\widetilde{\square_0+\square\square_{\square}}=\widetilde{\square_0}+\square\widetilde{\square_{\square}} \tag{3.16}$$

3.1.4 Definition 3 from [61]

$\square\in\mathbb{R}^{\square\times\square}$, where $\widetilde{\square}_{\square}(\square),\square=1,2,\dots,\square$ represents the real non-zero eigenvalues of $\square$ when the vector is nonrepeating. Let $\square_0=-\infty$, $\square_{\square}=-\frac{1}{\widetilde{\square}_{\square}(\square)}$. $\square_{\square+1}=+\infty$ such that the ordered set can be labeled as follows in Equation (3.17), assuming that $\square_{\square}<\square_{\square+1}$.

$$\mathcal{B}(\square):=\{\square_0,\square_1,\square_2,\dots\square_{\square},\square_{\square+1}\} \tag{3.17}$$

The significance of this definition comes from the fact that for any $\square\in\mathbb{R}$, the $\det(\square+\square\square)=0$ if and only if $\square\in\mathcal{B}(\square)$. This basically provides intervals on which the eigenvalues of the system can be evaluated for determinations of the entire stability domain.

3.1.5 Theorem 2 from [61]

Given an open interval Ω in $\mathbb{R}$, and $\square_0,\square_{\square}\in\mathbb{R}^{\square\times\square}$,define $\widetilde{\square}_0:=2\square_0*\square$ and $\widetilde{\square}_{\square}:=2\square_{\square}*\square$. Then, the following two statements are equivalent:

- $0\in\Omega$ and $\square(\square):=\square_0+\square\square_{\square}$ is Hurwitz for all $\square\in\Omega$

- $\square_0$ is Hurwitz and $0 \in \Omega \subseteq \square(\square_0^{-1}\mathrm{A_g}) \cap \square(\widetilde{\square}_0^{-1}\widetilde{\square}_\square)$

This theorem uses the guardian map of the determinate of a bialternate sum to determine the maximal continuous robsut stability interval including the origin.

3.1.6 Theorem 8 from [61]

The theorem is presented as follows:

Given $\square_0, \square_\square \in \mathbb{R}^{\square\times\square}$ where $\det(\square_0 \oplus \square_0) \neq 0$, let

$$\widetilde{\square_0} = 2\square_0 \star \square_\square \tag{3.18}$$

$$\widetilde{\square_\square} = 2\square_\square \star \square_\square \tag{3.19}$$

$$\square = \left(\mathcal{B}\left(\square_0^{-1}\square_\square\right) \cup \mathcal{B}\left(\widetilde{\square}_0^{-1}\widetilde{\square}_\square\right)\right)^{\#} - 2 \tag{3.20}$$

Define the open set

$$\Omega_\epsilon := \bigcup_{\square\in\mathcal{I}} (\square_\square, \square_{\square+1}) \tag{3.21}$$

Where $\square_\square, \square_{\square+1}$ are consecutive members of $\left(\mathcal{B}\left(\square_0^{-1}\square_\square\right) \cup \mathcal{B}\left(\widetilde{\square}_0^{-1}\widetilde{\square}_\square\right)\right)$ and the index set $\mathcal{I}$ is given by $\mathcal{I} := \left\{\square \in \mathcal{I}_\square^0 : \square_0 + \square_\square\square_\square\right\}$ and is Hurwitz for some $\square_\square \in (\square_\square, \square_{\square+1})$, $\square_\square, \square_{\square+1}$consecutive members of $\left(\mathcal{B}\left(\square_0^{-1}\square_\square\right) \cup \mathcal{B}\left(\widetilde{\square}_0^{-1}\widetilde{\square}_\square\right)\right)$.

Then, $\square_0 + \square\square_\square$ is Hurwitz if and only if $\square \in \Omega_\square$.

In more practical language, this theorem states a methodology for finding the bounds on the parameter to maintain system stability. It is saying that if for some given $\square_\square$ in set $\left(\mathcal{B}\left(\square_0^{-1}\square_\square\right) \cup \mathcal{B}\left(\widetilde{\square}_0^{-1}\widetilde{\square}_\square\right)\right)$, there is a value for which $\square_0 + \square_\square\square_\square$is Hurwitz. This can be extended to all values of $\square$ if it is contained in the open set defined as Ω_ϵ.

To utilize the outlined principles, it is now necessary to calculate the maximum real eigenvalue of $\square_0 + \square\square_\square$. This set of eigenvalues will be compared with the elements of the set given

$\left(\mathcal{B}\left(\square_0^{-1}\square_{\square}\right) \cup \mathcal{B}\left(\widetilde{\square}_0^{-1}\widetilde{\square}_{\square}\right)\right)$. The stable eigenvalues will determine where $\square$ is defined for the Hurwitz $\square_0 + \square\square_{\square}$.

3.1.7 Convex Combination

From the previous section, the bounds of the stability domain in parameter space $\square$ for the system $\square(\square)$ can be determined. To ensure that there is a continuous path that the parameter can travel on in between $\square_0$ and $\square_{\square}$, it is necessary to see if $\square$ forms a convex combination between $\square_0$ and $\square_{\square}$. Regardless of the dimensionality of the system, this technique will always provide a line between the two systems in the parameter (or scheduling variable) space. This space is defined by the set of $\square$ for the eigenvalues on the $\square\square$ axis. A convex set which is defined in [70, 71] states that for a given linear space $\square$, a subset $\square$ is defined such that $\square \subset \square$ is convex if any two points in $\square$ can be connected with a line segment using (3.22).

$$\begin{gathered}\square\square_0 + (1-\square)\square_{\square} \in \square \\ 0 \le \square \le 1\end{gathered} \tag{3.22}$$

For the problem formulation of this paper, this means that the set of parameters determined from [61] must be contained in the convex subset $\square$ to find the convex combination of $\square_0$ and $\square_{\square}$. Finding this combination shows that with the variation of one parameter, the current system condition defined at $\square_0$ has a smooth path to the equilibrium point $\square_{\square}$ for which a controller has been designed. Regardless of how many scheduling variables are needed to properly control a system, the distance between the two points, *i.e.*, $\square_0$ and $\square_{\square}$ will always be a line in one parameter. This allows for the scaling of this technique to larger systems.

In order to determine if there is actually a path between the two systems by which one parameter can be varied to move the current system to the equilibrium point, it is necessary to ensure that the parameter, $\square$, for which $\square_0 + \square\square_{\square}$ is Hurwitz, meets the constraints of a convex combination. Since it is already known that the value $\square$ is the set for $\square_0 + \square\square_{\square}$ is in the stability domain; it is just necessary to ensure that those values include $0 \le \square \le 1$. This will guarantee that when the gain of the equilibrium is applied to the current system, there is a stable path of operating points between them.

3.2 **Gain Scheduling Controller Application**

The goal of this research is to apply gain scheduling techniques to power systems controls. The control or the gain can be switched as the system operating conditions change. Doing this requires a basic knowledge of what gain scheduling is and how it is applied to nonlinear systems. A linear controller for the power system is created based on a linearized system, but the actual implementation occurs on the real nonlinear system.

Designing a gain-scheduled controller for a nonlinear plant can be summarized with a four-step procedure [56].

1. Linear parameter varying (LPV) plant models must be determined from the nonlinear plant through one of two procedures

    a. Jacobian linearization of the nonlinear plant about a family operating or equilibrium points

    b. Quasi-LPV scheduling by rewriting the plant dynamics to hide nonlinearities as time varying parameters to be used as scheduling variables

2. Design linear controllers for the LPV plant model derived through either method. Provide a family of linear controllers corresponding to the LPV plant or require an interpolation process to find a family of linear controllers from a set of controllers designed for isolated values of the scheduling variables

3. Schedule gains such that the controller coefficients (gains) of the family of linear controllers can be varied (scheduled) based on the current values of the scheduling variables

4. Assess performance by evaluating the local stability and performance properties of the gain scheduled controller. Non-local evaluation is done through simulation studies.

Because the first step in gain scheduling design is deriving a linear parameter-dependent description for the nonlinear plant, the background information will start there.

3.2.1 Linear Parameter Varying Systems

An LPV system is one in which the linear system dynamics depend on time-varying exogenous parameters. Although the trajectories of these parameters do not need to be known *a priori*, it should be possible to measure them online. Because they cannot be known previously, time-varying control methods based on previous and future values cannot be utilized [34]. A continuous time LPV system has the form seen in Equation (3.23).

$$\begin{aligned} \dot{x}(t) &= A\big(\rho(t)\big)x(t) + B\big(\rho(t)\big)u \\ y(t) &= C\big(\rho(t)\big)x(t) + D\big(\rho(t)\big)u \end{aligned} \tag{3.23}$$

□(□) is a measurable, bounded time-varying parameter vector, and □(·), □(·), □(·), □(·) are the state matrices that are fixed functions of □ [20, 34, 56]. This LPV system can be obtained through either the Jacobian linearization or quasi-LPV method. For this paper, the LPV was obtained through a classical linearization.

3.2.2 Linear Controller Families

The linear gain scheduled controller uses the plant linearization family to design a linear controller family [56]. During the design, the scheduling variable □ is used as a parameter. However, during the implementation □ is used as a time-varying input signal to the gain scheduling controller. It can be dependent on an exogenous input and/or a state or output measurement [56]. The current values of the scheduling variables are used to determine the controller coefficients continuously [51, 58, 59, 60] .

3.2.3 Gain Scheduling

As discussed in the previous section, the technique utilized here is linearization scheduling. In this case, the fixed scheduling variable values are functions of the internal plant variables and/or exogenous signals corresponding to the parameterization.

Because of this, there are several restrictions placed on the control design. First, it is necessary for the system to be changing slowly [51, 56] because, typically, only local stability can be assured. This requires running many more simulations in order to ensure that the results meet the performance criteria. However, it is beneficial to note that the traditional linearization technique is not as computationally intensive as other nonlinear design approaches [56]. Some research has been conducted in the field of adaptive controls as seen in [57].

The local behavior about each equilibrium of the nonlinear plant is described by the corresponding fixed □. These are local deviation signals from near the equilibrium parameterized by □ for the linearized plant [56]. Furthermore, when linearization-scheduling it is necessary to have the equilibrium family of the controller match the plant equilibrium family. This will ensure that the closed loop system is within a boundary of error, and that the family of controllers is actually the designed family of controllers [56].

3.2.4 Determining the Stability Domain

Because the traditional linearization technique is used, there is no assurance of performance. Though there is no guarantee, this method generally yields positive results in practice [56]. In this paper, the "domain of attraction" concept is used to ensure that the system will respond properly to an applied control (i.e. move to an equilibrium point). The concept originally developed in [61] is applied here to determine the parameter bounds that guarantee the stability of a system with slow moving parameters.

The set of parameter values that place the eigenvalues on the □□ axis can be determined, by evaluating the LPV model developed as part of the gain scheduling control procedure [61]. This is useful because the □□ axis provides the boundary between system stability and instability. The question answered in [61] is, "Do the intervals between the parameters which cause eigenvalues to be on □□ axis correspond to stable or unstable eigenvalues of □(□)?" The parameter values containing the stable eigenvalues create the bounds of the domain of attraction of the system □(□). Many methods proposed in [61] suffer from their inability to determine all of the stability domains if they are disjoint. However, the theory used in this paper can provide all of the domains of attraction. Again, this application is only valid for slow linear parameter varying systems. The need for this constraint is proven in [61].

3.3 **Example**

In order to better illustrate the interesting results of these computations, a small example is provided. This is a 2-dimensional example which will begin with three different □ matrices shown in Equations (3.24), (3.25), and (3.26).

$$\square_0 = \begin{bmatrix} -10 & 0 & -1 \\ 0 & -5 & 0 \\ -1 & -1 & -8 \end{bmatrix} \tag{3.24}$$

$$\square_1 = \begin{bmatrix} 1.6 & -1.0 & -0.1 \\ -0.7 & -1.1 & -0.6 \\ -0.2 & 5.0 & -0.3 \end{bmatrix} \tag{3.25}$$

$$A_2 = \begin{bmatrix} 1.2 & 2.0 & -2.2 \\ 1.0 & -1.2 & 0.2 \\ 1.2 & 0.6 & -0.5 \end{bmatrix} \tag{3.26}$$

For which

$$\square(\square) = \square_0 + \square_1\square_1 + \square_2\square_2 \tag{3.27}$$

$$\square_\square = \cos(\square)\,\square_1 + \sin(\square)\,\square_2 \quad \forall \quad \square \in [0, \square) \tag{3.28}$$

$$\square_0 \oplus \square_\square = \begin{bmatrix} -10 & 0 & -1 \\ 0 & -5 & 0 \\ -1 & -1 & -8 \end{bmatrix} \oplus \cos(\square) \begin{bmatrix} 1.6 & -1.0 & -0.1 \\ -0.7 & -1.1 & -0.6 \\ -0.2 & 5.0 & -0.3 \end{bmatrix} + \sin(\square) \begin{bmatrix} 1.2 & 2.0 & -2.2 \\ 1.0 & -1.2 & 0.2 \\ 1.2 & 0.6 & -0.5 \end{bmatrix} \tag{3.29}$$

To study the stability of this example, take the maximal one-dimensional stability region along any particular trajectory

$(\rho_1, \rho_2)^T \in \{\rho = r\, v(\theta); r \in (-\infty, \ldots.),\quad v(\theta) = (\cos\theta \sin\theta)^T\}$ and repeating over all directions $\theta \in [0{,}360)$. The results of this analysis are shown in Figure 3.1.

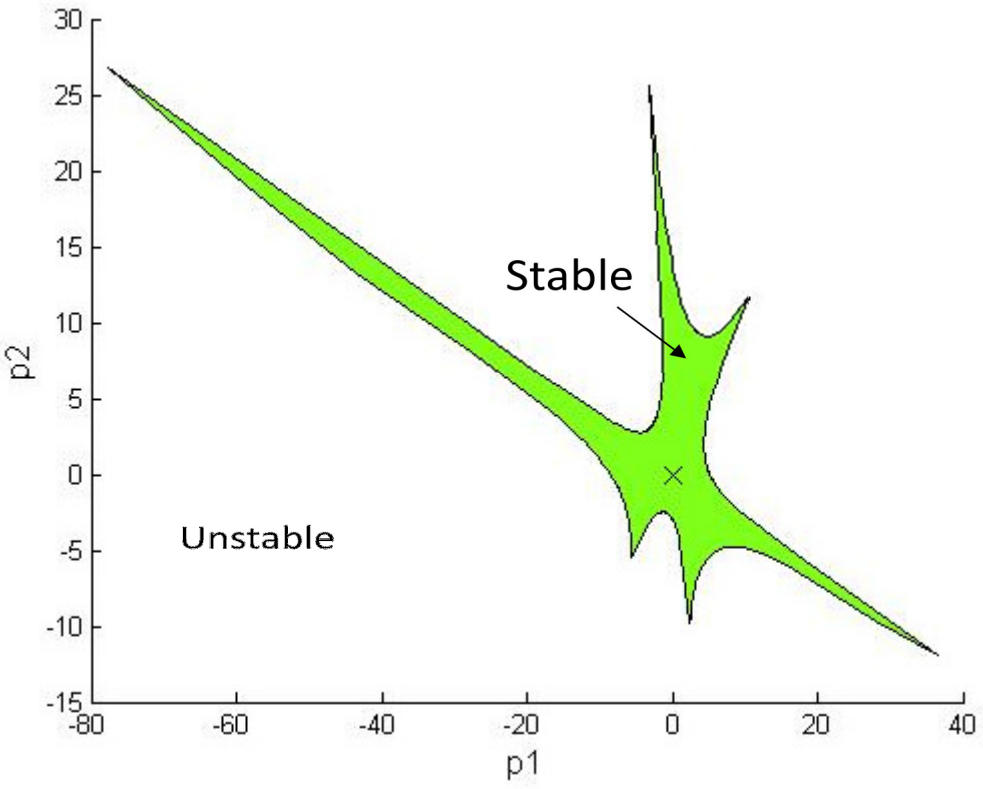

Figure 3.1– Graph of stability region created through varying multiple parameters

3.4 **Proposed Methodology for a Power System Application**

The methodology proposed in this paper follows the basic outline for finding a gain scheduling controller. After the linearization of the systems and the corresponding controllers are found, the stability domain will be calculated using the method proposed in [61] and evaluated to see if it forms a convex combination with □$_0$ and □$_□$.

3.4.1 Traditional Linearization

The non-linear system which is being studied in this paper is the two-area, four machine system [30] with classically modeled generators. An HVDC line has been added for control between buses 5-15. Figure 3.2 shows the one line diagram of the test system. The MATLAB suite created in [41] was used to model this system. The program computes for the load flow solution, and uses small perturbations to develop an LTI representation of the non-linear system. This program is run for several contingency cases to form equilibrium points about which controllers can be designed. The two parameters being varied were the outage of a tie-line and an increase of a load. A summary of these cases is shown in Table 3.2.

As mentioned previously, tie line flows found with PMU measurements are an intuitive and useful scheduling variable. The flows can indicate when lines are out, when variations in generation and load occur, or when other system parameters change. At this point, it is also important to note that in a real power system, PMUs measure the power flowing in an uncontrolled system. Therefore, it is desirable to map the load and the reactance parameters as they vary in an uncontrolled system to schedule parameters of the uncontrolled system. For the given system, the variables are the power flowing in the tie-line. However, for the purposes of such a small system, they are being considered separately as TL1 and TL2.

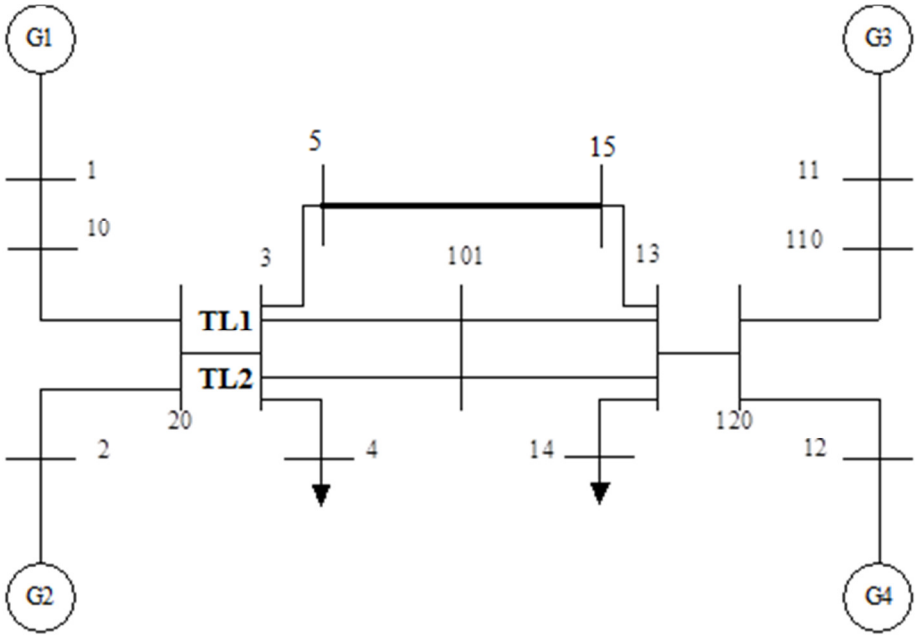

Figure 3.2 - Four Machine System with HVDC Lines

Table 3.2. Contingency Information

Case	Contingency Details
1	Base Case
2	Remove TL2

3	Increase load at Bus 4 by 10%
4	Remove Tie Line between 3-101, Increase load at Bus 4 by 10%
5	Test Point – Tie line reactance at step 7, load increased 2%

The linearized state space representation is presented to further help the understanding of the problem formulation. Figure 3.3 shows, in state space, four different equilibrium points about which the system was linearized. The original equilibrium point (denoted by the triangle) at which the system had been operating was disturbed and began to move along the trajectory shown by the line and is now at the current point denoted by the solid circle. At this point, the scheduling variable will need to determine which equilibrium point contains it within its domain of attraction. The trajectory of the disturbance determines which domain of attraction contains the point. The numbered arrows are denoting the clockwise spiraling trajectory of the current point as it spirals into one of the equilibriums to reach stability [72]. It is to be noted here that the more properly damped the system is, once the control has been applied, the faster it will reach an equilibrium point.

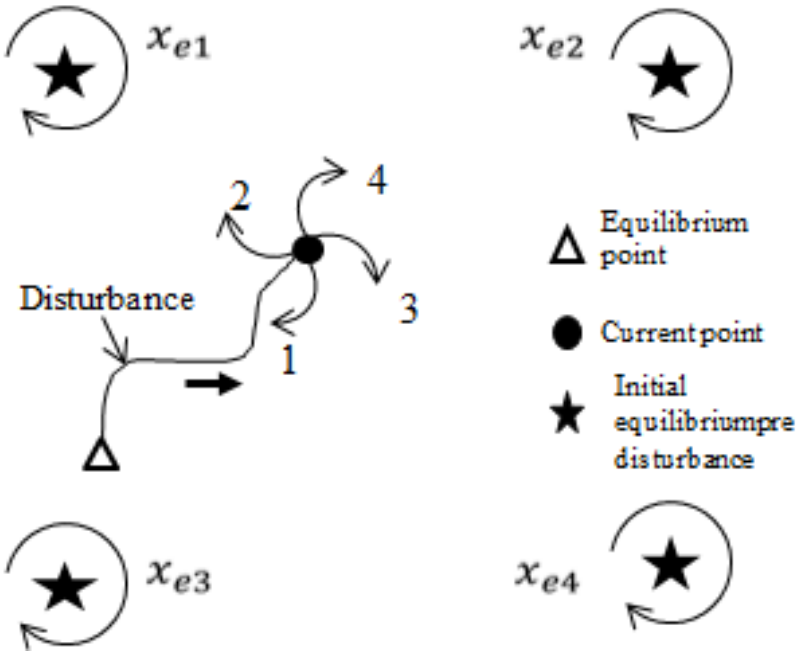

Figure 3.3 - System Movement Towards Equilibria

3.4.2 Control Development

The controllers developed at each of the equilibriums were formulated with a multi-objective control problem using the Robust Control Toolbox in MATLAB. During this study, state feedback was used which meant that we solve for a $\square_2/\square_\infty$ controller given a set defined damping ratio. The $\square_\infty$ control is responsible for disturbance rejection whereas the control effort is optimized through the $\square_2$ control. The poles are placed within the region defined by the desired damping ratio to ensure a desirable time response. The designs of these multi-objective controllers ensure that the closed loop plants for each of the equilibriums will provide robust stability [71] [73]. For the present instance, the controllers are designed for each point. However, if there were thousands of cases, the multi-objective formulation could create one control for several similar contingencies that have been grouped together.

3.4.3 Parameter Mapping

In order to see how the parameters were mapped, two sets of simulations were run to create a grid in parameter space. The first set was described by setting the load to a 5% increase while varying the reactance of the line from the base value to an outage in 11 steps. The reactance values were found by changing the admittance in steps of 10%. The second set was found by

setting the reactance to the fifth step as it increased to an outage. This was performed by decreasing the admittance by 50% and varying the load from the base value to a 10% in 11 steps as shown in Figure 3.4.

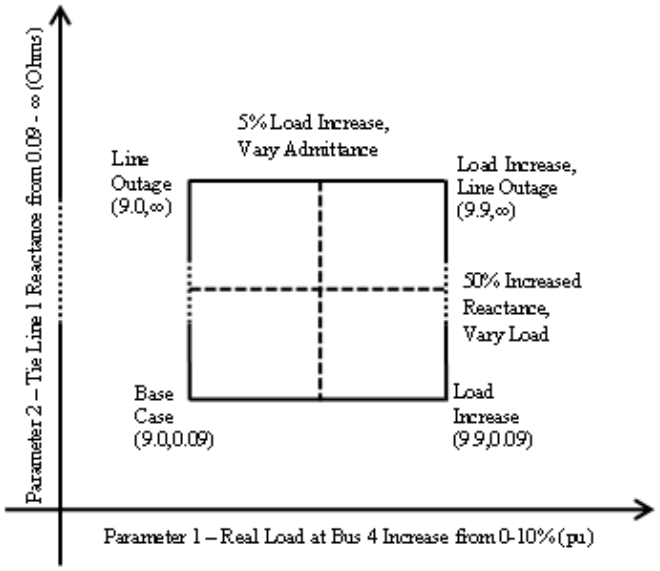

Figure 3.4 - Parameter Space Mapping

For each simulation where the parameters varied, the power flows in the tie-lines were saved and plotted in scheduling parameter space as seen in Figure 3.5. The point of mapping them is to ensure that the parameter variations correspond to the power flows. This is a further way to guarantee that using power flows is actually a good measure for a scheduling variable based on the parameter variations.

The correlation between the parameters and the scheduling variables is evident from Figure 3.5. This proves that the power flows are indeed a good indicator of parameters varying in the system. Figure 3.5 also points to the convex combination between the values for the test point and those for the line outage, load increase case. The way in which this line was found will be discussed in the next section

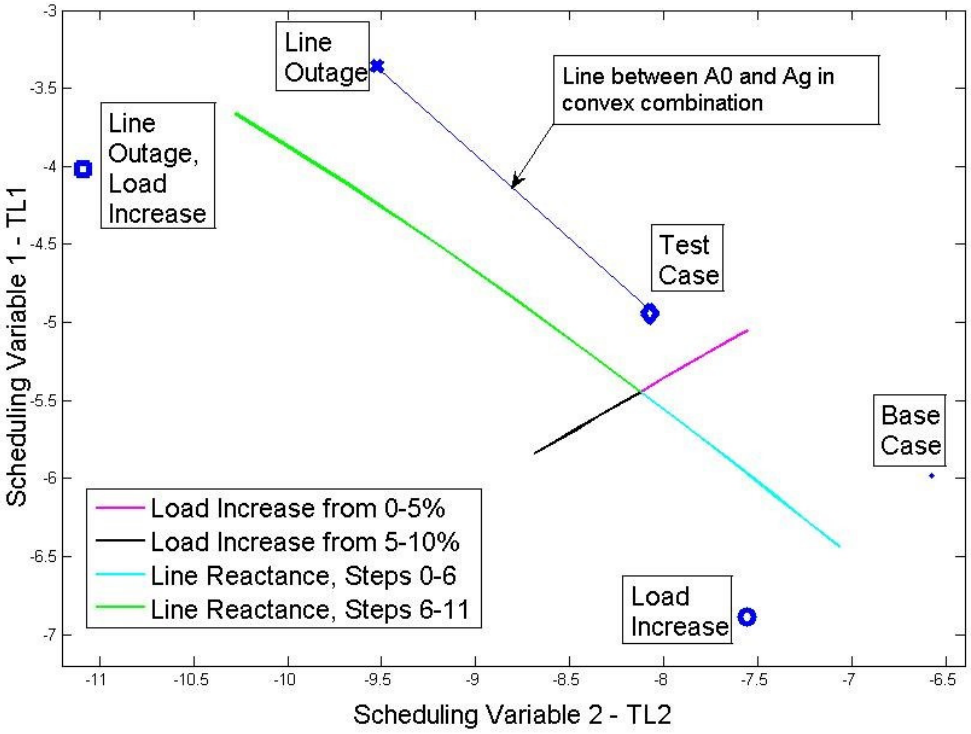

Figure 3.5 - Parameter Mapping Plot

3.4.4 Results of Power Systems Application

The results of the linearization performed by the MATLAB suite from [41] were as expected. The set of parameterized values for the test case and the equilibrium point in the corresponding quadrant in scheduling variable space yielded good results. Figure 3.6 shows the stable eigenvalue as bold and underlined. Also, it shows that the stable eigenvalue, $\square_{\square\square\square\square} = -0.13$, of $\square(\square)$ is defined in the interval between $\square \in (-1.583, 4.151)$. The arrow is meant to indicate that the eigenvalue occurs between the two parameter values to which it points. Additionally, the set for which $\square$ gives a stable $\square(\square)$ also includes $0 \leq \square \leq 1$. Therefore, a convex combination can be formed between the equilibrium point $\square_{\square}$ and the current system point $\square_0$. This result indicates that there is a line connecting the two points where the system is less likely to become unstable when the designed linear controller is applied to the uncontrolled system. This is stated as "less likely" because it is still the application of a linear control to a non-linear system. This is not a guaranteed way to ensure that the test system is contained within the domain of attraction of the equilibrium point

Part of parameter set for which eigenvalues lie on the jω axis	-86.342	-1.5828	4.151	8.356
Eigenvalues of A(ρ)	14.45	0.23	**-0.13**	0.09

Figure 3.6 - Parameter Set Eigenvalues

To show the effect of the control created by Case 3 on Case 5, the eigenvalues were plotted. The uncontrolled values are circled in red, and then end past the required 5%.

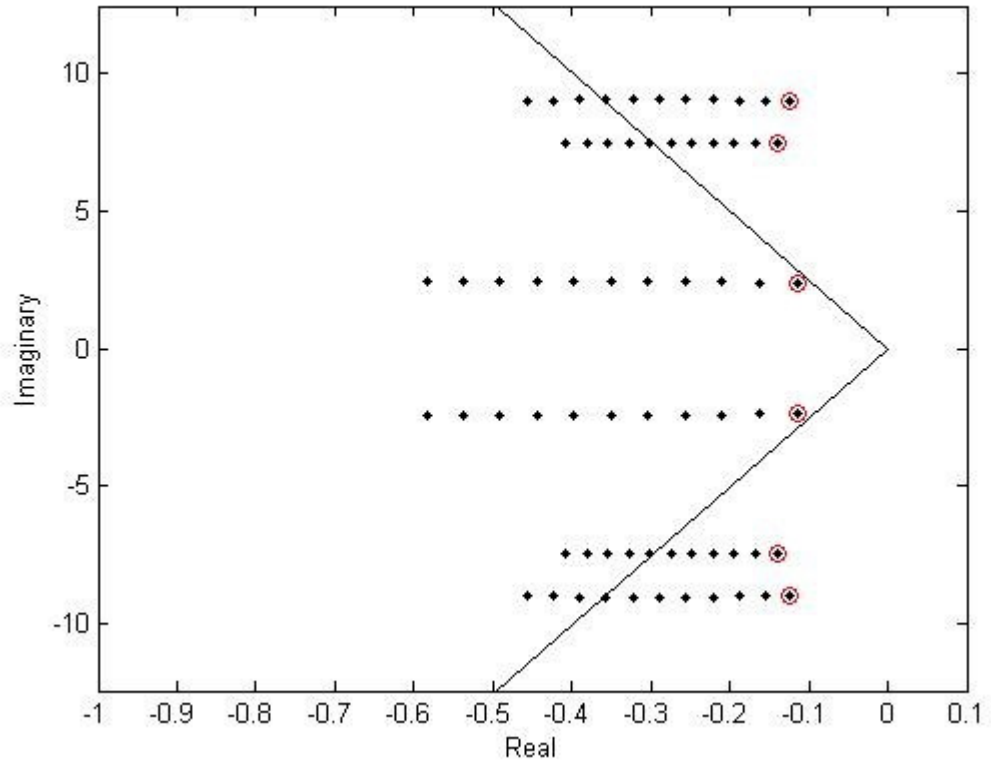

Figure 3.7 - Damped Eigenvalues

The methodology developed provides a unique and simple way of determining whether the linearization technique provides suitable gain scheduling control. Although it does not prove sufficiency, it is a considerable improvement to the notion of assuming that it works because the

linearization is similar to the non-linear system. Additionally, it is extremely easy to scale to large power systems where there are many power flows because two points in scheduling variable space can always be connected with a line. However, for further work and to actually provide sufficiency, the quadratic Lyapunov function would need to be calculated numerically to find the exact stability domain of the non-linear system.

Chapter 4. System Theory Introduction

In an effort to predict the world around us, it is useful to model and define systems. There are two main classifications of systems: non-linear and linear. The following sections will explore more thoroughly the mathematical differences between these system types and the varying benefits and limitations of them in real-world applications.

4.1 **Preliminary Mathematics**

Because the system theory that forms the basis for this work is very theory intensive, this review begins with a few mathematical preliminaries for terms which will be used throughout.

4.1.1 Definite and Semi-Definite Functions

A function, $\mathrm{V}(\mathbf{x})$, is said to be **positive definite** in $D \subset \mathbb{R}^n$ if

$$\mathrm{V}(\square) = 0 \tag{4.1}$$

$$\mathrm{V}(\square) > 0 \quad \forall \quad \square \in \square - \{\square\}$$

A function, $\mathrm{V}(\mathbf{x})$, is said to be **positive semi-definite** in $D \subset \mathbb{R}^n$ if

$$\mathrm{V}(\square) = 0 \tag{4.2}$$

$$\mathrm{V}(\square) \geq 0 \quad \forall \quad \square \in \square - \{\square\}$$

The function, $V(\mathbf{x})$, is negative definite if $-V$ is positive definite; and it follows that $V(\mathbf{x})$ is negative semi-definite is $-V$ is positive semi-definite.

4.1.2 Continuous Functions

The function, f, which maps f: $\mathbb{R}^n \to \mathbb{R}^m$ is continuous at a point x if $f(x_k) \to f(x)$ whenever $x_k \to x$. It is equivalent to say that $\boldsymbol{f}$ is continuous at $\boldsymbol{x}$ if, for a given $\epsilon > 0$ there exists a $\delta > 0$ so that Equation (4.3) holds true.

$$\|\square - \square\| < \square \quad \Rightarrow \quad \|\square(\square) - \square(\square)\| < \square \tag{4.3}$$

If the function f is continuous at every point of S, then f is continuous on the set S. The secondary conditions of the inequalities above for ϵ *and* δ ($only\ dependent\ on\ \epsilon$) must be held true for all $x, y \in S$ for the function f to be uniformly continuous on S. Thus, continuity is defined at a point, and uniform continuity is defined on a set.

4.1.3 Convergence of Sequences & Boundedness

The sequence of vectors $x_0, x_1, \ldots, x_k \in \mathbb{R}^n$is denoted by $\{x_k\}$ and will converge to the limit vector x if the condition in Equation (4.4) is met.

$$\|\square_{\square} - \square\| \to 0 \text{ as } \square \to \infty \tag{4.4}$$

It is equivalent to say that given any $\epsilon > 0\ \exists\ N\ such\ that$ the condition in Equation (4.5) is met as well. The bounded sequence, $\{x_k\}$ in $\mathbb{R}^n$ will have at least one accumulation point in $\mathbb{R}^n$.

$$\|x_k - x\| < \square, \forall\ \square \geq \square \tag{4.5}$$

4.1.4 Monotonic Norm Convergence

The sequence of real numbers, $\{r_k\}$, is said to be monotonically increasing or nondecreasing if $r_k \leq r_{k+1}\ \forall\ k$. If $r_k < r_{k+1}$, the sequence is said to be strictly increasing. The oppositie is true for monotonically decreasing or nonincreasing sequences where $r_k \geq r_{k+1}$. The sequence is strictly decreasing if $r_k > r_{k+1}$. Also note that an upward bounded increasing sequence of real numbers converges to a real number. The same is true for a decreasing sequence of real numbers bounded from below.

4.1.5 Existence and Uniqueness of Solutions

In a deterministic system, for which the equations of motions are properly defined, the mathematical model will always be able to predict the future state of the system given a defined initial state. For this to be possible, the initial value problem described in Equation (4.6) must have a unique solution.

$$\dot{□} = □(□, □); □(□_0) = □_0 \tag{4.6}$$

By enforcing the Lipschitz condition as a constraint on the right-hand side of the function $f(x, t)$, the *existence* and *uniqueness* of a solution can be ensured. The Lipschitz condition requires that $f(x, t)$ satisfy Equation (4.7) in the neighborhood of (x_0, t_0).

$$\begin{aligned} &\|□(□, □) - □(□, □)\| \leq □\|□ - □\| \qquad □ \geq 0 \\ &\forall \ □, □ \in □ = \{□ \in □^{□} | \ \|□ - □_0\| \leq □\} \\ &\forall \ □ \in [□_0, □_1] \end{aligned} \tag{4.7}$$

Thus, there exists some $T > 0$ such that the state equation in Equation (4.6) has a unique solution over the time period $[t_0, t_0 + T]$. A function which satisfies Equation (4.7) is Lipschitz in x with the positive Lipschitz constant, $\mathcal{L}$. Less formally, the Lipschitz condition is a way of bounding how much a function can increase or decrease. It is a condition which holds in $\boldsymbol{x}$ of $f(\boldsymbol{x}, t)$, not over t. Additionally, the value of $\mathcal{L}$ does not need to be uniform in $\boldsymbol{x}$.

For a formal proof, see [46]. The significance of a locally Lipschitz result is that the δ value could be extremely small and of little use. Additionally, the Lipschitz property is stronger than continuity. The classification of a function as continuous differentiable is a stronger than the local Lipschitz condition.

For a scalar function of just a single variable, the condition shown in Equation (4.8) is required. This means that the magnitude of the derivative of f must be limited to the neighborhood of x_0.

$$\frac{|□(□) - □(□)|}{|□ - □|} \leq □ \tag{4.8}$$

4.1.6 Invariant subspaces

First, let us define the subspace, S, as an invariant subspace of the square matrix, A. This means that for each vector x in S, the vector Ax will also be in S. This is shown graphically in Figure

4.1. The range, null space, and eigenspaces are all types of invariant subspaces of A. This is significant because if the state of an LTI system begins in an invariant subspace of the system matrix, it will never leave that subspace [74].

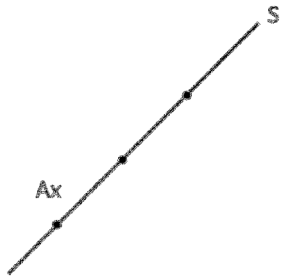

Figure 4.1 - Invariant Subspace

A set M is an invariant set if the condition in Equation (4.9) is met.

$$\square(0) \in \square \quad \Rightarrow \quad \square(\square) \in \square \quad \forall \quad \square \in \square \tag{4.9}$$

The set M is a positive invariant set if

$$\square(0) \in \square \quad \Rightarrow \quad \square(t) \in \square \quad \forall \quad \square \geq 0 \tag{4.10}$$

The distance between point $\boldsymbol{p}$ and the set M is defined as

$$\square\square\square\square(\square, \square) = \inf_{\square \in \square} \|\square - \square\| \tag{4.11}$$

The trajectory $\boldsymbol{x}(t)$ converges to the set M as $t \to \infty$ if for every $\epsilon > 0$ there esists a time $T > 0$ such that

$$\square\square\square\square(\square(\square), \square) < \square \quad \forall \quad \square > \square \tag{4.12}$$

When an equilibrium is asymptomatically stable at $\boldsymbol{x} = 0$, it implies that the set $\{\mathbf{0}\}$ is invariant. The significance of this is that once a function which is decreasing monotonically enters a level set, it will never leave that set. When the trajectory enters a level set given arbitrarily by $V(x) = c$, it is not possible to leave the set $\Omega_c \coloneqq \{x \in \mathbb{R}^n | V(x) \leq c\}$. This is known as the invariance of sub-level sets shown in Figure 4.2 and helps visualize stability in the Lyapunov sense as defined in the subsequent sections.

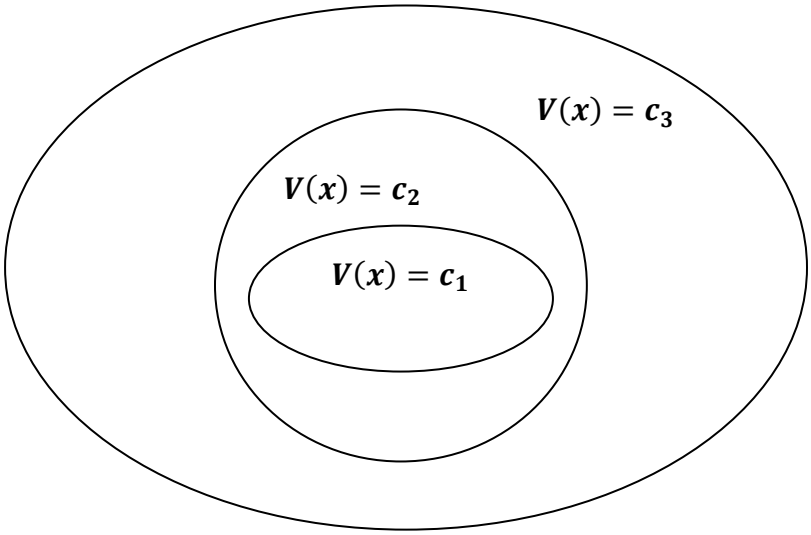

Figure 4.2 – Sublevel Set Diagram

Despite the simple ellipses shown above, determining the level sets of a perfectly defined Lyapunov function can be a nearly impossible task. The most important component of the analysis is to ensure that the system state will move towards a stable equilibrium over time. However, as the system moves towards that equilibrium, but is possible that the trajectory may increase temporarily even though it is stable.

4.2 **Non-Linear Systems**

With these preliminaries covered, the next step is to evaluate non-linear systems.

4.2.1 Set of Non-Linear Equations

First, we begin with the general form of a finite dimensional nonlinear control system which is described through Equations (4.13) and (4.14).

$$\dot{\square} = \square(\square, \square, \square), \qquad \square(\square_0) = \square_0 \tag{4.13}$$

$$\square = \square(\square, \square, \square) \tag{4.14}$$

In this representation,

- $x(t) \in \mathbb{R}^n$ is the state history – the memory the dynamical system has of its past

- $u(t) \in \mathbb{R}^m$ is the input or control history
- $y(t) \in \mathbb{R}^p$ is the output history

The solution or trajectory will include any pair $(x(t), u(t))$ which satisifies the state equations over the time internal that includes $t = t_0$. Another way of saying this is that the transient response of the system is provided by the solution of $x(t)$ for $t \geq t_0$ given that the initial condition describes the initial stored energy, $x(t_0^-)$, and $u(t) = 0$. Even though many physical systems do not present themselves as a state model, one can be created by carefully choosing the state variables.

A special case of non-linear systems includes an unforced state equation:

$$\dot{\square} = \square(\square, \square) \tag{4.15}$$

It should be noted that working with an unforced state equation does not necessarily mean that the system input is zero. An input could be specified as any given function of time, state feedback, or both. It is just considered unforced because the substitution of $u = \gamma$ in equation (4.13) eliminates u and yields an unforced state equation.

Additionally, a special case of the state model arises when the function, f, is not a function of time, t. This just means that the right hand side of the state equation in (4.13) will not change when the time origin shifts to $t_0 = t_0 + a$. These are called autonomous or time invariant systems and can be represented as shown in (4.16)

$$\dot{x} = f(x) \tag{4.16}$$

The special case of a non-linear system is the linear system:

$$\dot{\square} = \square(\square)\square + \square(\square)\square \tag{4.17}$$

$$\square = \square(\square)\square + \square(\square)\square \tag{4.18}$$

Much of this discussion will focus on linear time-invariant systems which take the form:

$$\dot{\square} = \square\square + \square\square \tag{4.19}$$

□ = □□ + □□ (4.20)

The value of the function $x(t)$ is the amount of energy left in the system at any time such that the zero energy state occurs when $x = x_{eq} = 0$. The implication of a zero energy state is that the energy provided through the initial conditions or a disturbance will dissipate as time progresses. Further details of this scenario are discussed in Section 4.3.

4.2.2 A Second Order System Example

Many references [46, 75] use a second order system to clarify some of the system representation described above. Following their lead, Equation (4.21) represents a second order autonomous system through two scalar differential equations.

$$\dot{□}_1 = □_1(□_1, □_2) = □_1(□) \quad (4.21)$$

$$\dot{□}_2 = □_2(□_1, □_2) = □_2(□)$$

For which, $x(t) = \big(x_1(t), x_2(t)\big)$ is the solution. Note this assumes that there is a unique solution. The initial state is $x(0) = x_0 = (x_{01}, x_{02})$. Thus, the locus in the $x_1 - x_2$ plane for the solution $x(t) \ \ \forall \ t \geq 0$ is a curve which passes through the point x_0. As described above, the curve is the trajectory, or orbit, of Equation (4.21 beginning at x_0. The $x_1 - x_2$ plane is generally described as the state or phase plane. The family of all the trajectories is the phase portrait. The vector field on the state plane, $f(x) = (f_1(x), f_2(x))$, is tangent to the trajectory at the point x since $\frac{dx_2}{dx_1} = \frac{f_2(x)}{f_1(x)}$. Basically, the phase portrait is the removal of the time axis such that one would look down at all of the curves as though they are on top of each other. Because the time axis has been removed, it is impossible to recover the solution $\big(x_1(t), x_2(t)\big)$ associated with any particular trajectory. However, it does provide a qualitative understanding of the system behavior. A closed trajectory indicates a period solution exists because the system will have a sustained oscillation. A spiral which is shrinking indicates that the oscillation is decreasing.

For each point, x, in the plane has an assigned vector $f(x)$. Figure 4.3 is used to visually represent this by basing $f(x)$ at x – which can also be described as assigning x as the directed line segment from $x \to x + f(x)$. Thus, if $f(x) = (3x_1^2, x_2)$, at $x = (1,1)$ meaning that $x +$

$f(x) = (1,1) + (3,1) = (4,2)$. An arrow pointing in the direction of $(4,2)$ will connect these two points as seen in Figure 4.3.

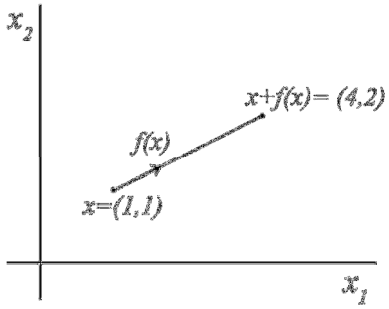

Figure 4.3 - Vector Field Representation

Basic geometry indicates that the length of this arrow will be proportional to $\sqrt{f_1^2(x) + f_2^2(x)}$. The vector field at a particular point is tangent to the trajectory through that point. Thus, it is possible to construct the trajectory starting at a point, x_0, from the vector field diagram. The second-order autonomous system has a phase portrait which consists of the family of all of the solution curves or trajectories. Computer simulations are commonly used for phase portrait creation, but to know more about how to do it by hand, see reference [46]. There will be significantly more examples of phase planes in the Pendulum Example in Section 4.6.

4.3 **An Equilibrium**

The equilibrium point is one of the foundational concepts for understanding state space. An equilibrium is defined as any constant state vector where $\boldsymbol{x} = \boldsymbol{x}_{eq}$ for which, whenever the system begins at $\boldsymbol{x}(t_0) = \boldsymbol{x}_{eq}$, it will stay at $\boldsymbol{x}_{eq}$ for all future time. This is equivalent to satisfying the constraint that $\boldsymbol{f}(\boldsymbol{x}_{eq}) = \boldsymbol{0}$. The equilibrium points of the autonomous system in (4.13) are the real roots of $\boldsymbol{f}(\boldsymbol{x}) = \boldsymbol{0}$ [46]. This simply means that when a system is at an equilibrium point, and there is no external input, it will remain in that state for infinity. Similarly, inertia decrees that an object at rest will stay at rest. On occasion, it can be referred to as a singular point.

Although non-linear and linear systems can have equilibrium, there are different implications for what those equilibriums mean for each type of system.

4.3.1 Non – Linear Equilibrium

A non-linear system can have many different, isolated equilibria to which the system can converge. The equilibrium the state converges to is dependent on the initial condition. It is common for a nonlinear system to exhibit two or more modes of behavior. Additionally, unlike linear system states which will approach infinity as time goes towards infinity, nonlinear systems can have unstable modes which go to infinity in a finite escape time [46].

4.3.2 Linear Equilibrium

A linear system can only have one isolated equilibrium point or a continuum of equilibrium points in the null space of the state matrix, A. The singular isolated point is equivalent to saying it has only one steady-state operating point that attracts the system regardless of the initial condition. In the event that the state matrix is singular, the equilibrium will be spanned by a convex combination of the equilibria because it cannot have multiple isolated equilibria. If x_{eq1} and x_{eq2} are both equilibria, by linearity, any point on the line $\alpha x_{eq1} + (1-\alpha)x_{eq2}$ will also be an equilibrium point [46]. Generally speaking, it is possible to determine the qualitative behavior of a nonlinear system near the equilibrium point through a linearization with respect to that point. Linear systems will be further discussed in Section 0.

The matrix A will have a nontrivial null space when one or more eigenvalues are zero. This is because any vector in the null space of A is an equilibrium point for the system, thus forming an equilibrium subspace rather than an equilibrium point [46].

To be able to understand the behavior of system trajectories near the equilibrium points, the formal notion of stability must be defined and understood.

4.4 **Stability**

In the event of a disturbance, a stable system will move from the original equilibrium, but eventually transition to a new equilibrium point and will stay there even when the disturbance is removed [46]. An unstable system state will head towards infinity as time passes.

At this point, it must be noted that stability in the non-linear sense is only a function of the equilibrium point – not the system as a whole. A system could have multiple stable and unstable equilibrium points dependent on current conditions.

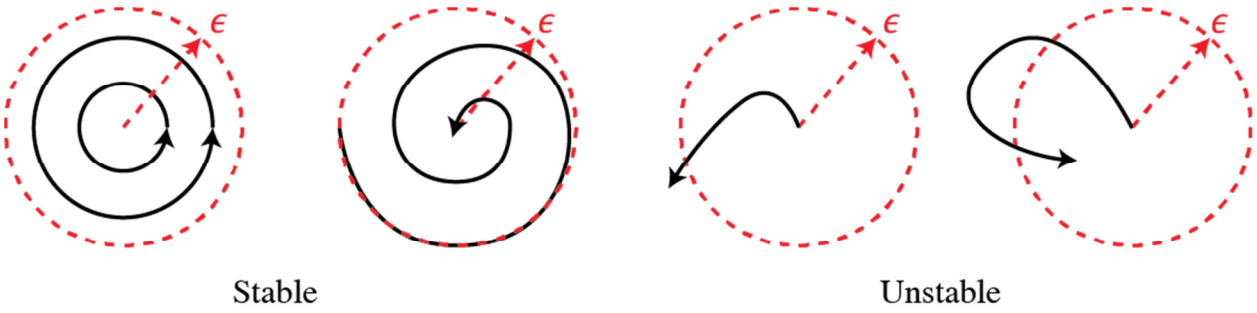

Figure 4.4 - Stability Definition Graphical Explanations

Three commonly used methods to determine stability are:

1. Solve the differential equation
2. Lyapunov's Lyapunov's Indirect Method: Linearize the system dynamics, examine eigenvalues
3. Lyapunov's Lyapunov's Direct Method: Construct and analyze an energy-like function

4.4.1 Stability Definitions

This is a small introduction to the very basic definitions of stable equilibrium points.

Definition:

The equilibrium $\boldsymbol{x}_{eq} = \mathbf{0}$ is considered stable if for all $\epsilon > 0$, there exists a $\delta = \delta(\epsilon) > 0$ such that

$$\|\square(0)\| < \square \quad \Rightarrow \quad \|\square(\square)\| < \square \quad \forall \quad \square \geq 0. \tag{4.22}$$

The equilibrium $\boldsymbol{x}_{eq} = \mathbf{0}$ is unstable if it is not stable. Even though it seems redundant, it means that the equilibrium is unstable if there exists any $\epsilon > 0$ when there is no value of δ to satisfy the stability condition.

Uniform stability requires that for each $\epsilon > 0$, there is a $\delta(\epsilon) > 0$ that is independent of t_0 and also satisfies the original stability equation, Equation (4.22).

4.4.2 Lyapunov

The work of Aleksandr Lyapunov forms the basis for much of modern day controls. It is actually the only universal method for investigating the stability of a generally configured nonlinear dynamical system [76]. A Lyapunov function is used to prove the stability of a system's equilibrium. The following sections explore the properties and implications of these functions.

The definition for Lyapunov stability [76] is defined below with both equations and graphics. It begins with the autonomous system defined by Equation (4.23).

$$\dot{□} = □(□) \tag{4.23}$$

The function $f\colon D \to \mathbb{R}^n$ is a locally Lipschitz map from the domain, $D \subset \mathbb{R}^n$ into $\mathbb{R}^n$.

The equilibrium point is defined as $x_{eq} \in D$ such that $f(x_{eq}) = 0$ is true.

Thus, $x(t) = x_{eq} \forall\, t \geq 0$ is a solution for the ODE.

This equilibrium point is considered Lyapunov stable if for all

$$□ > 0 \;\exists\; □ > 0 \; □□□□ \; □□□□ \; (\|□(□_0) - □_{□□}\|) \leq □ \tag{4.24}$$

$$\|□(□) - □_{□□}\| \leq □ \tag{4.25}$$
$$□ \geq □_0 \geq 0$$

This translates very well into Figure 4.5. It is also easy to see from the graphical representation that by choosing a sufficiently small δ, the value ϵ can be made arbitrarily small as well. In very plain terms, Lyapunov stability shows that if the solution begins near x_{eq} it will remain near it for all time.

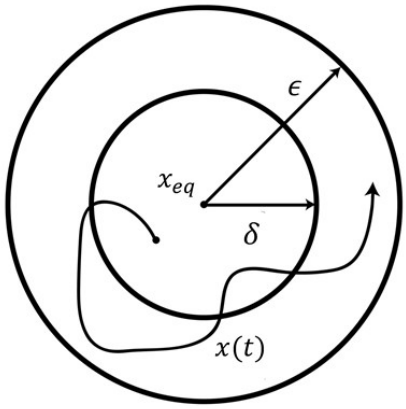

Figure 4.5 - Lyapunov Stability Illustration

4.4.3 Lyapunov Proof

The proof of this is as follows:

Given any $\epsilon > 0$, choose $r \in (0, \epsilon]$ small enough that

$\square_{\square} = \{\square \in \square^{\square} \mid \|\square\| \leq \square\} \subset \square$

Let $\alpha = \min_{\|x\|=r} V(x)$ --- *Note:* $\alpha > 0$ because $V(x) > 0$.

Let $\beta \in (0, \alpha)$ and define a set:

$\square_{\square} = \{\square \in \square_{\square} | \ \square(\square) \leq \square\}$

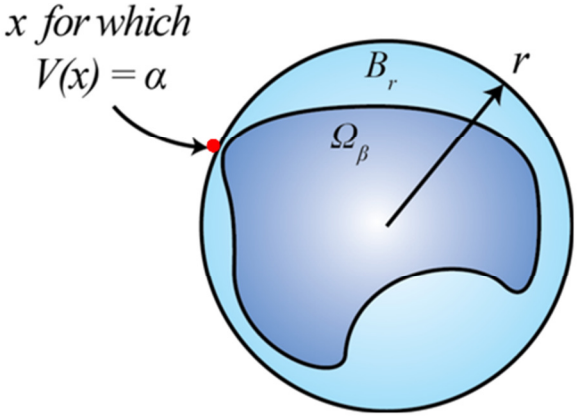

Figure 4.6 - Lyapunov Alpha Ball

Note that

$\dot{V}(x(t)) \leq 0 \quad \Rightarrow \quad V(x(t)) \leq V(x(0)) \leq \alpha \quad \forall \quad t \leq 0$

This means that any trajectory starting in

$\Omega_\beta = \{x \in B_r \mid V(x) \leq \beta\}$

at time $t = 0$ will remain in Ω_β for all time $t \geq 0$.

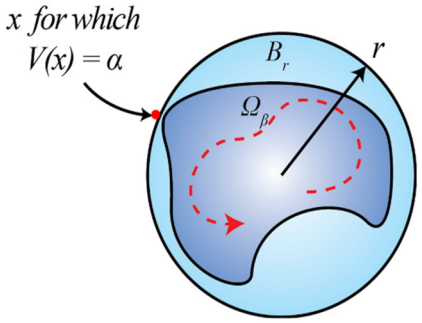

Figure 4.7 - Lyapunov Ball with Trajectory

Any initial state in Ω_β yields a unique solution that exists $\forall\, t \geq 0$.

Continuity of V requires that there exists some $\delta > 0$ such that

$\|\boldsymbol{x} - \{\mathbf{0}\}\| < \delta \;\Rightarrow \|V(\boldsymbol{x}) - V(\mathbf{0})\| < \beta, \quad$ that is $\|\boldsymbol{x}\| < \delta \;\Rightarrow\; V(\boldsymbol{x}) < \beta.$

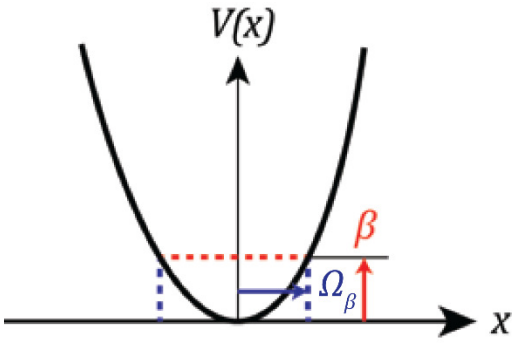

Figure 4.8 - Parabola Description of Ball

Next, use δ to define a ball B_δ of radius δ. We see that for all $t \geq 0$,

$\boldsymbol{x}(0) \in B_\delta \quad \Rightarrow \quad \boldsymbol{x}(0) \in \Omega_\beta \quad \Rightarrow \quad \boldsymbol{x}(t) \in \Omega_\beta \quad \Rightarrow \quad \boldsymbol{x}(t) \in B_r \quad \Rightarrow \quad \|\boldsymbol{x}(t)\| < r \leq \epsilon$

This is shown in Figure 4.9, and proves the first claim that $V > 0$ & $\dot{V} \leq 0 \quad \Rightarrow \quad$ Stability

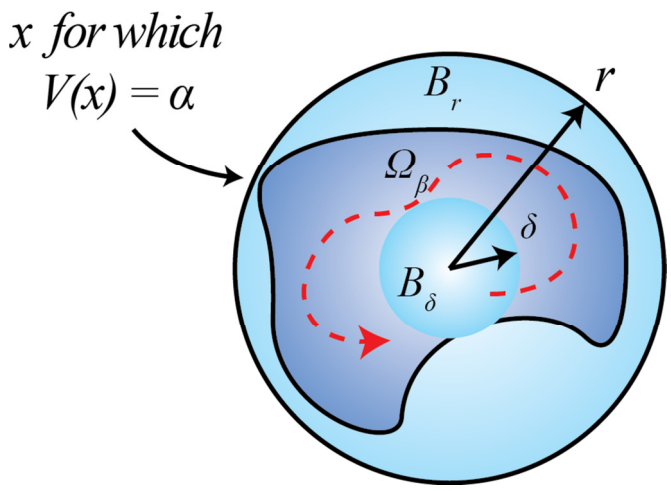

Figure 4.9 - Lyapunov Ball Definition

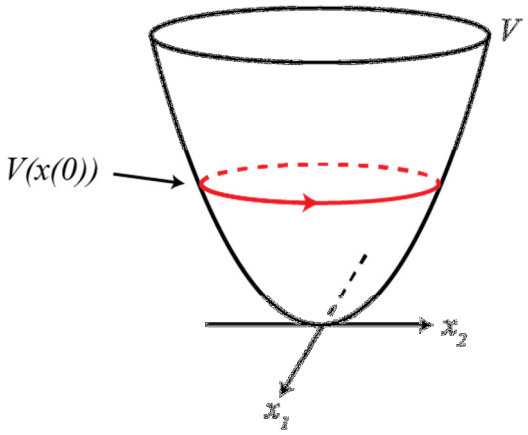

Figure 4.10 - Geometric Interpretation of Lyapunov Theorem when $V(\boldsymbol{x}) > 0$ and $\dot{V}(\boldsymbol{x}) \leq 0$ in D showing that $\boldsymbol{x} = \mathbf{0}$ is only stable.

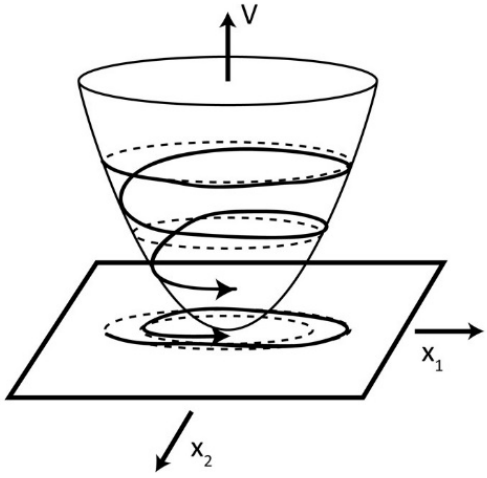

Figure 4.11 - Geometric Interpretation of Lyapunov Theorem where $V(\boldsymbol{x}) > 0$and $\dot{V}(\boldsymbol{x}) < 0$ in D showing that $\boldsymbol{x} = \mathbf{0}$ asymptotic stability.

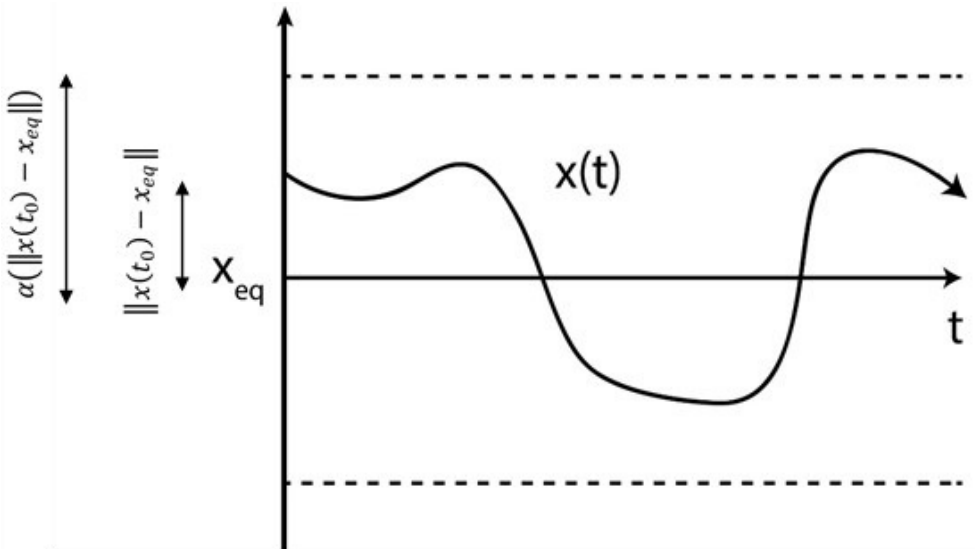

Figure 4.12 - Lyapunov Stable System as a Function of Time

4.4.4 Lyapunov's Direct Method

Obviously, there are benefits and drawbacks to the different methods. The direct method does not require that the differential equation be solved. It does only provide sufficient conditions for stability – meaning that if a Lyapunov function is not found, the system could still be stable. The trickiest part of this method is that there is no general technique for finding a Lyapunov function.

4.4.5 Asymptotic Stability

For asymptotic stability, not all solutions must converge to the equilibrium state. However, all solutions which begin in the neighborhood of the equilibrium converge to the equilibrium state. Basically, an equilibrium is asymptotically stable if it attracts nearby trajectories.

The definition states that an equilibrium state, $\boldsymbol{x_{eq}}$, is asymptotically stable (AS) if the following conditions are met.

1. It is stable
2. There exists $R > 0$ which can be chosen such that the conditions in Equation (4.26).

$$\|\square(\square_0) - \square_{\square\square}\| < \square \;\Rightarrow\; \lim_{\square\to\infty} \square(\square) = \square_{\square\square} \tag{4.26}$$

The set of initial values which are attracted to the equilibrium state $\square_{\square\square}$ is called the *region of attraction*. Thus, when a function is globally asymptotically stable, the region of attraction is the entire state space.

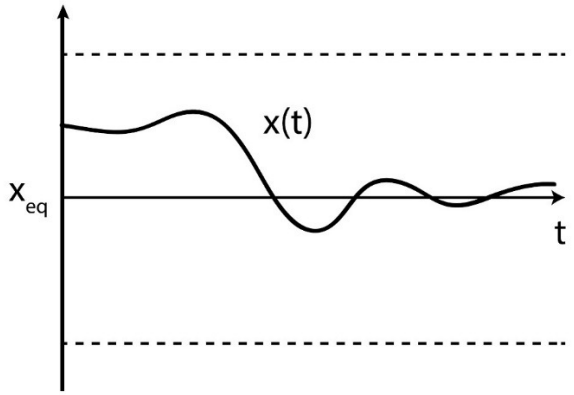

Figure 4.13 - Asymptotic Function

4.4.6 Global Asymptotic Stability

Global asymptotic stability (GAS) of an equilibrium state is described in plain words by saying that the point is Lyapunov stable and that *every* solution $x(\cdot)$ converges to x_{eq} as time increases. If the equilibrium point is GAS, there are no other equilibrium states, and all solutions are bounded. When these conditions are met, a system is called globally asymptotically stable. The requirements of these conditions are described below.

1. The system is stable
2. Every solution $x(\cdot)$ converges to x_{eq} as time increases such that Equation (4.27) holds true.

$$\lim_{t\to\infty} x(t) = x_{eq} \tag{4.27}$$

To conclude that the origin is globally asymptotically stable requires more than just for $V(\boldsymbol{x}) > 0$ and $\dot{V}(\boldsymbol{x}) < 0 \in \mathbb{R}^n$. If there exists a continuously differentiable function $V(\boldsymbol{x})$, defined on all of $\mathbb{R}^n$, that will satisfy the conditions defined in Equations (4.28) and (4.29) which require all trajectories to converge to the equilibrium, then $\boldsymbol{x} = \mathbf{0}$ is globally asymptotically stable.

$$\begin{aligned} &V(0) = 0 \\ &V(x) > 0 \ \ \forall \ x \neq 0 \\ &\dot{V}(\boldsymbol{x}) < 0 \ \ \forall \ x \neq 0 \end{aligned} \tag{4.28}$$

$$\square(\square) \to \infty \quad \forall \quad \|\square\| \to \infty \tag{4.29}$$

These requirements are satisfied by a function which is considered *radially bounded* [46].

4.4.7 Lyapunov's Indirect Method

Lyapunov stability theory can be utilized to demonstrate the following results:

***Stability*:** When all of the eigenvalues of the linearized A matrix have negative real parts, the nonlinear system is exponentially stable about the equilibrium, $\boldsymbol{x}_{eq}$. This is the equivalent of saying that if the linearized system is exponentially stable, the nonlinear system is exponentially stable about $\boldsymbol{x}_{eq}$.

***Instability*:** If at least one eigenvalue of the linearized system A matrix contains a positive real part, the nonlinear system is unstable about x_{eq}.

The Indirect Method linearizes the system dynamics and examines their eigenvalues. System linearization and eigenvalues analysis was described in Section 0.

4.5 **Basin of Attraction**

The *region of attraction* of an asymptotically stable equilibrium is the set of all states which, if taken as initial conditions, give rise to trajectories that converge to the equilibrium. This is very useful information about a system, but computing regions of attraction can be difficult.

From the proof of Lyapunov's stability theorem, every trajectory starting in the set remains there as shown in Equation (4.30).

$$\square_{\square} = \{\square \in \square_{\square} \mid \square(\square) \leq \square\} \tag{4.30}$$

Choose β as large as possible and take Ω_β as a *conservative estimate* of the region of attraction. A point on a stable manifold will attract to an equilibrium which provides insight as to whether the operating condition is in a stable or unstable operating condition.

4.6 **Pendulum Example**

One of the most common examples in non-linear system theory is that of the pendulum. This example should help provide an understanding of the principles described above.

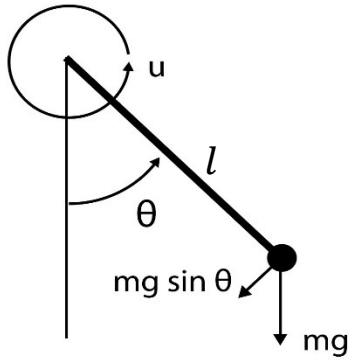

Figure 4.14 - Pendulum Diagram

In this diagram, θ is the angle subtended to the rod. l is the length of the rod which we are assuming has no mass and is rigid. m is the mass of the ball, and g is obviously the acceleration due to gravity. The value u defined in the diagram indicates the ways in which the pivot point can be altered through an input. For the purposes of this example, the frictional coefficient k, which would be proportional to the speed of the ball, is included. A frictionless pendulum is basically a pendulum without any damping added to the system. In a pendulum without damping, given an initial push from equilibrium, the system will oscillate with a nondisspasitive energy exchange between kinetic and potential energy. Using Newton's second law of motion, it is possible to write the pendulum equation in the tangential direction as Equation (4.31). By writing the equation of motion in the tangential direction, it is possible to ignore the rod tension in the normal direction.

□□□̈ = −□□□□□□ − □□□̇ (4.31)

In order to obtain the state space model, choose the state variables of the equation of motion to be those shown in Equations (4.32) and (4.33).

$$□_1 = □ \tag{4.32}$$

$$□_2 = \dot{□} \tag{4.33}$$

Thus, the state equations become Equations (4.34) and (4.35).

$$\dot{□}_1 = □_2 \tag{4.34}$$

$$\dot{\square}_2 = -\frac{\square}{\square}\square\square\square\ \square_1 - \frac{\square}{\square}\square_2 \tag{4.35}$$

To find the equilibrium points of the system, first set $\begin{Bmatrix}\dot{x}_1\\ \dot{x}_2\end{Bmatrix} = \begin{Bmatrix}0\\0\end{Bmatrix}$ *or* $\dot{x}_1 = \dot{x}_2 = 0$ and solve for the state variables.

$$0 = \square_2 \tag{4.36}$$

$$0 = -\frac{\square}{\square}\square\square\square\ \square_1 - \frac{\square}{\square}\square_2 \tag{4.37}$$

Thus, it is clear that in solving for the variables that Equation (4.38) is the equilibrium solution.

$$\square_{\square\square} = \begin{Bmatrix}\square_1\\ \square_2\end{Bmatrix} = \begin{Bmatrix}\pm\square\square\\ 0\end{Bmatrix} \quad \square\square\square\ \square = 0, \pm 1, \pm 2\ldots. \tag{4.38}$$

However, it should be noted that even though that is the mathematical solution, a pendulum can only have two points corresponding to $n = 0$ and $n = 1$.

The first step in evaluating the stability is to choose a Lyapunov function. A logical first option would be the total energy of the pendulum shown in Equation (4.39). The first component is the potential energy and the second is the kinetic energy.

$$\begin{aligned}\square(\square) &:= \int_0^{x_1} \frac{\square}{\square}\sin y\, dy + \frac{x_2^2}{2} \\ &= \frac{\square}{\square}(1 - \square\square\square\square_1) + \frac{\square_2^2}{2} \quad \geq 0\end{aligned} \tag{4.39}$$

Which must be able to meet the criteria defined in Equations (4.40) and (4.41).

$$\square(\square) = \frac{\square}{\square}(1 - \square\square\square\square_1) + \frac{\square_2^2}{2} > 0 \quad \square\square\square\square\ -2\square < \square_1 < 2\square \tag{4.40}$$

$$\square(0) = 0 \tag{4.41}$$

The derivative of the trajectories is provided by Equation (4.39) **Error! Reference source not found.** for point $\boldsymbol{x_{eq}} = \begin{Bmatrix}\mathbf{0}\\ \mathbf{0}\end{Bmatrix}$.

$$\frac{\partial}{\partial x}(f - f_{eq})f(x) = \left[\frac{g}{l}\cos x_1 \quad x_2\right]\left[-\frac{g}{l}\cos x_1 - \frac{c}{m}x_2\right]$$

$$= \frac{g}{l}x_2\cos x_1 + x_2\left(-\frac{g}{l}\cos x_1 - \frac{c}{m}x_2\right) \tag{4.42}$$

$$= -\frac{c}{m}x_2^2 \leq 0 \quad \forall \quad x \in \mathbb{R}^n$$

Thus, the origin is Lyapunov stable, but $\dot{V}(x)$ is not negative definite, only negative semi-definite. It cannot be negative definite because $\dot{V}(x) = 0$ for $x_2 = 0$ regardless of the value of x_1. However, the phase portrait of a pendulum indicates that the origin is actually asymptotically stable as seen in Figure 4.15. Thus, when the Lyapunov function fails to provide a solution for asymptotic stability, La Salle's Invariance principle can be utilized to find a more thorough conclusion [46].

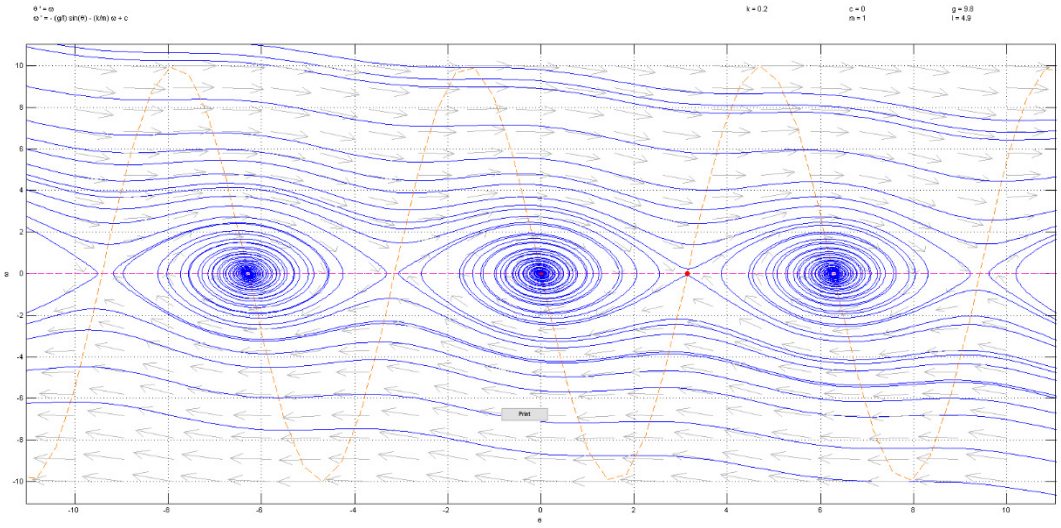

Figure 4.15 - Phase Portrait of Damped Pendulum

In order to show that the origin is actually asymptotically stable, it is necessary to use LaSalle's Invariance Principle. Further information on it this can be utilized can be found in [50].

The system linearization follows to show the changes in the system results. It begins by differentiation as seen in Equation (4.43).

$$\frac{\partial \dot{\mathbf{x}}}{\partial \mathbf{x}} = \begin{bmatrix} \frac{\partial \dot{x}_1}{\partial x_1} & \frac{\partial \dot{x}_1}{\partial x_2} \\ \frac{\partial \dot{x}_2}{\partial x_1} & \frac{\partial \dot{x}_2}{\partial x_2} \end{bmatrix} = \begin{bmatrix} 0 & 1 \\ -\frac{k}{m}\cos(x_1) & -\frac{c}{m} \end{bmatrix} \tag{4.43}$$

By inserting $(x_1^*, x_2^*) = (0,0)$ into Equation (4.43), the matrix A follows in Equation (4.44)

$$A = \begin{bmatrix} 0 & 1 \\ -\frac{k}{m} & -\frac{c}{m} \end{bmatrix} \tag{4.44}$$

Figure 4.16 shows the linearization of the damped pendulum about the origin.

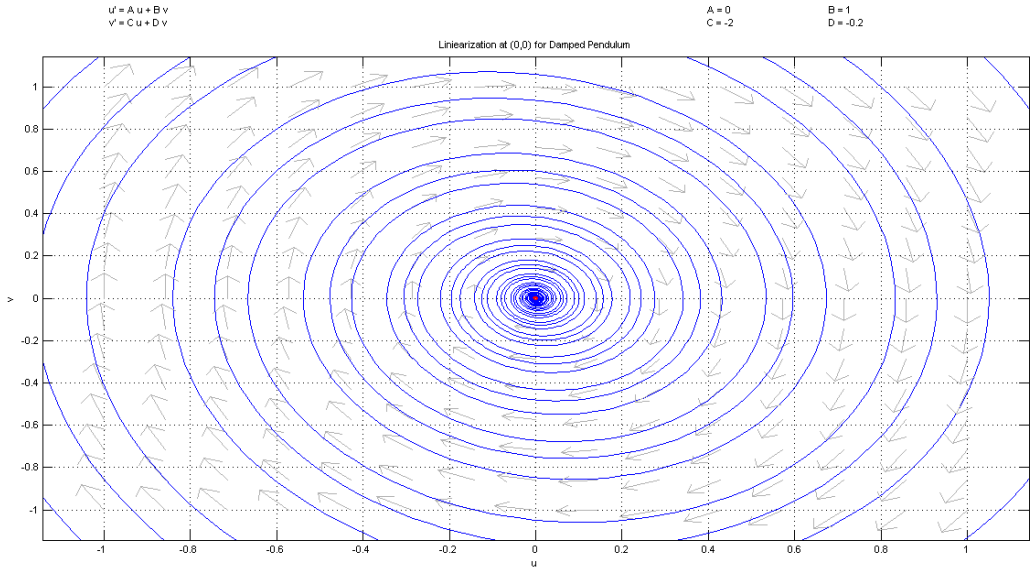

Figure 4.16 - Linearized Pendulum about the Origin

4.6.1.1 Point $x_{eq} = \begin{Bmatrix} \pi \\ 0 \end{Bmatrix}$

This equilibrium point is called a saddle point since the Lyapunov $\epsilon - \delta$ requirements cannot be met for even the tiniest values of ϵ. Using the previous Lyapunov function in Equation (4.39) and inserting $\boldsymbol{x_{eq}} = \begin{Bmatrix} \boldsymbol{\pi} \\ \mathbf{0} \end{Bmatrix}$ provides Equation (4.44).

$$\frac{\partial \dot{x}}{\partial x}(x - x_{eq})\dot{x}(x)$$

$$= \begin{bmatrix} \frac{k}{m} \cos(x_1 - \pi) & x_2 \end{bmatrix} \begin{bmatrix} -\frac{k}{m} \sin x_1 - \frac{c}{m} x_2 \end{bmatrix} \tag{4.45}$$

$$= -\frac{2k}{m} x_2 \sin x_1 - \frac{c}{m} x_2^2 \gtreqless 0$$

Thus, it is not possible to conclude that $x_{eq} = (\pi, 0)$ is a Lyapunov stable. The phase portrait in Figure 4.15 actually shows that it is not.

By inserting $(x_1^*, x_2^*) = (\pi, 0)$ into Equation (4.43), the matrix A follows in Equation (4.45)

$$A = \begin{bmatrix} 0 & 1 \\ \frac{k}{m} & -\frac{c}{m} \end{bmatrix} \tag{4.46}$$

The linearization about this point is shown in Figure 4.17. This makes sense as even if the system moves the slightest bit from $x_{eq} = (\pi, 0)$, it will never return to equilibrium at that point.

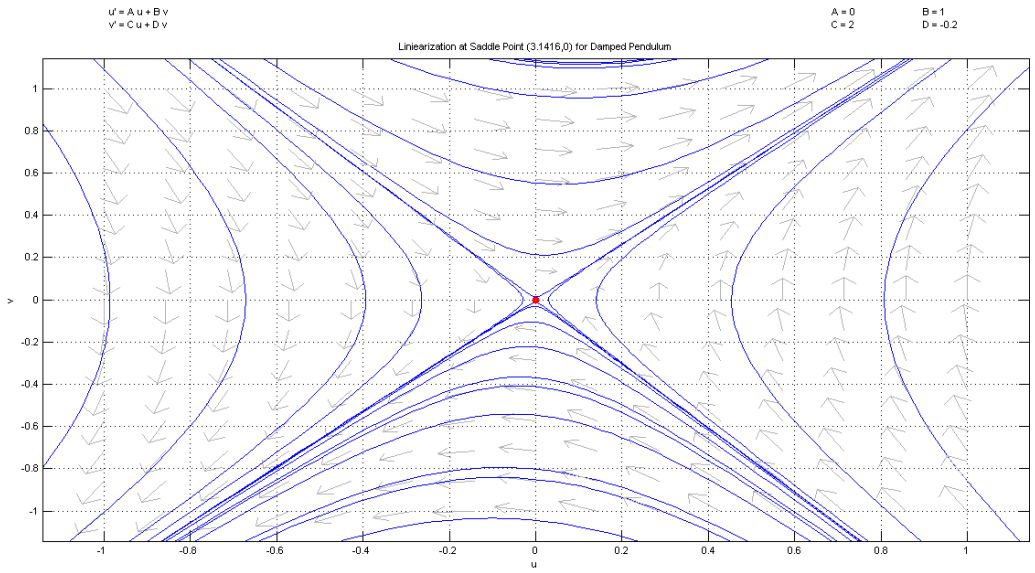

Figure 4.17 - Unstable Equilibrium of Damped Pendulum System

The review of non linear system theory demonstrates some of the concepts and background that lay the foundation for how difficult it is to analyze even a simple nonlinear system. Additionally, it looks to show the insights gained through taking on this challenge.

Chapter 5. Results

5.1 **Introduction to Power Systems Applications**

The methodology and algorithm explained in this chapter aim to address the shortfalls of the strictly linear analysis of power systems. As discussed in the previous chapters, the accurate understanding of a power system requires including all of the present nonlinearities. However, for a power system that has many machines, this is not a feasible requirement. In order to address this constraint while still attempting to model the nonlinearities, an approach is taken that utilizes a few linear system techniques mixed with an application of Lyapunov's direct method.

5.2 **Modeling requirements**

The modeling requirements for this system were based in assuring that the simulation would have sufficient detail and information to perform a slow moving transient analysis with meaningful control feedback applied. This application focuses on interarea oscillations which are not associated with first swing stability traditionally analyzed with transient analysis of faults. The primary source of control for both example systems required analysis and modeling of an LCC-HVDC line. The dynamics of an HVDC line can greatly affect fast varying system dynamics; however, since this thesis is devoted to slower moving phenomena, only the appropriately timed converter dynamics have been taken into account.

The simulations were completed using Powertech's DSATools suite including PSAT, SSAT, and TSAT for powerflow, small signal, and transient analysis [35].

5.3 **Case Creation**

For each system studied, there was a methodology used in case creation. Given an initial study case, a set of contingencies has to be selected. An N-1 analysis was conducted as well as variations in the loads and generators across the system. All of the contingencies were evaluated using a small signal analysis using SSAT [35]. The purpose of this was to find a contingency set with the most varied system modes. Once the set was selected, the state space matrices created in SSAT were loaded into Matlab [36] for further system analysis and control derivation. This will be discussed in a bit more detail in Section 5.4.

Once the contingency set was defined and the controls developed, many small variations to the powerflow cases were made. These variations were defined to be incremental changes of the contingency definition. For example, if the contingency was an increase in load at a bus by 10%, each powerflow created would have a 0.5% change in load at that bus. These small variations would continue to increase so that loads or line flows are impacted. The variations of this powerflow case would have a different contingency applied to it. For each set of powerflows, a particular contingency is applied. This methodology was applied to ensure that there was a large range of contingencies and powerflow variations that would properly identify the control needed for the contingency applied rather than just the topological change. For both the 4 Machine and 127 Bus systems, a table is provided to clarify the contingencies and their associated powerflow changes.

All of the powerflow cases created have contingencies applied to them in a time domain simulation run by TSAT [35].

5.4 **Control Design**

While there are numerous ways to design state feedback control, multi-objective feedback was used for the purposes of this work. The benefits of multiple objectives are that formation ensures a desirable disturbance rejection, the control effort is optimized, and desired damping is specified. A controller which meets these criteria is designed through a linear matrix inequality (LMI) approach where a H_2/H_∞ controller with pole placement was created. The system diagram for this formulation is shown in Figure 5.1.

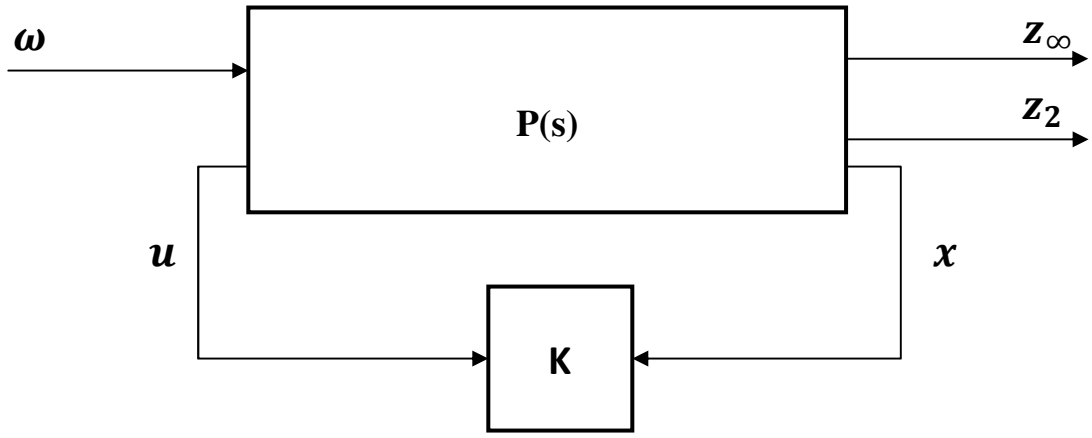

Figure 5.1- Multi-Objective State Feedback Control Diagram

The state equations for this system are shown in Equation (5.1).

$$\begin{aligned} \dot{\square} &= \square\square + \square_1\square + \square_2\square \\ \square_\infty &= \square_1\square + \square_{11}\square + \square_{12}\square \\ \square_2 &= \square_2\square + \square_{22}\square \\ \square &= \square_\square\square + \square_{\square 1}\square + \square_{\square 2}\square \end{aligned} \tag{5.1}$$

where

- **x** is the system state
- **u** is the control
- ω is a disturbance
- $\boldsymbol{z_\infty}$ and $\boldsymbol{z_2}$are for the $\mathbf{H_2/H_\infty}$ problems
- **y** is the output

It necessary to assume the ω values are the same in each equation in order to find a convex approximation [58]. The end result of this design is to create closed loop transfer functions from ω to z_∞ and $z_2$with a state-feedback law of $u = Kx$ such that [41]:

- The RMS gain of the of H_∞ problem is bounded by a positive value
- The control cost associated with the H_2 problem is bounded by a positive value
- A combination of the sum of the squared norms with weighting factors is minimized

- The closed loop poles lie in the left-half plane defined by D

The closed loop state equations are shown in Equation (5.2):

$$\begin{aligned} \dot{\square} &= (\square + \square_2\square)\square + \square_1\square \\ \square_\infty &= (\square_1 + \square_{12}\square)\square + \square_{11}\square \\ \square_2 &= (\square_2 + \square_{22}\square)\square \\ \square &= \square_\square\square + \square_{\square 1}\square + \square_{\square 2}\square \end{aligned} \tag{5.2}$$

The following papers are good resources for further understanding and analysis of these control design techniques [53, 71, 77].

5.5 **Numerical Requirements**

When thinking of the power system, it is apparent that the equilibrium points of it are not in fact at zero. This is not intrinsically a problem, but much literature assumes that the state trajectory can be calculated as $\hat{x}(t) = x(t) - x_e$ where $\square_\square$ is a known quantity. However, this is definitely not the case with generator angles which will move from their pre-disturbance equilibrium to a new one that is required by changes in power flow across the system. See Figure 5.2 for an idea of the changes in generator angles pre and post disturbance.

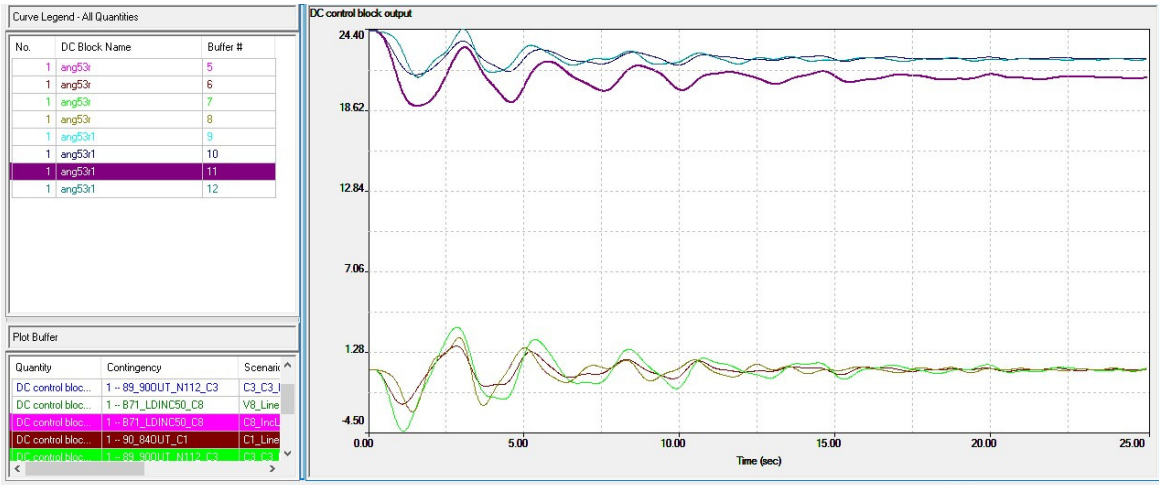

Figure 5.2 – The unfiltered and filtered angles of a generator in the 127 bus system.

Since the final equilibrium cannot be known at the beginning of the event, it is necessary for this analysis to filter the state inputs so that they will return to a zero equilibrium to ensure that the algorithms have worked properly. Without this, the time series values of the Lyapunov function will reach an unknown, nonzero value which does not sufficiently indicate the stability of the system. Basically, the Lyapunov function would include some unknown linear or constant terms

so that $\square(0) \neq 0$ and the derivative of the function would not vanish at zero. This was accomplished with a washout filter.

5.6 **Creating V, $\dot{V}$, $\ddot{V}$**

The relationship between the dynamics of a system, $\square$, to the Lyapunov function, $\square$, are not well understood except in the case of linear systems. A stable linear system will always permit a quadratic Lyapunov function. Stable and smooth homogenous linear systems will also always have homogenous Lyapunov functions [78]. The homogenous function $\square$ satisfies $f(\lambda x) = \lambda^d x$ for some constant $\square$.

The importance of Lyapunov's theorem is that it allows for the system stability to be determined without explicitly solving the differential equations. Thus, the question of stability can be answered by finding a positive definite function of the state which will decrease monotonically along all trajectories.

The following section describes the calculation of the Lyapunov functions and associated derivatives for the dynamical system $\dot{x} = f(x)$, where $f : \mathbb{R}^n \to \mathbb{R}^n$ is continuously differentiable with a unique equilibrium at the origin. . The function $V(x)$ is continuously differentiable and defined in $\square \subset \mathbb{R}^n, 0 \in \square$. The derivative along the trajectories of $\dot{x} = f(x)$ is defined below in Equation (5.3):

$$\dot{\square}(\square) = \sum_{\square=1}^{\square} \frac{\square\square}{\square\square_{\square}} \dot{\square}_{\square} = \sum_{\square=1}^{\square} \frac{\square\square}{\square\square_{\square}} \square_{\square}(\square)$$

$$= \begin{bmatrix} \frac{\partial V}{\partial x_1} & \frac{\partial V}{\partial x_2} & \cdots & \frac{\partial V}{\partial x_n} \end{bmatrix} \begin{bmatrix} f_1(x) \\ f_2(x) \\ \vdots \\ f_n(x) \end{bmatrix} = \frac{\partial V}{\partial x} f(x) = \begin{bmatrix} \frac{\partial V}{\partial x_1} & \frac{\partial V}{\partial x_2} & \cdots & \frac{\partial V}{\partial x_n} \end{bmatrix} \begin{bmatrix} f_1(x) \\ f_2(x) \\ \vdots \\ f_n(x) \end{bmatrix} = \frac{\partial V}{\partial x} f(x) \tag{5.3}$$

$$= \frac{\square\square}{\square\square_1}(\square)\square_1(\square) + \frac{\square\square}{\square\square_2}(\square)\square\square_2(\square) + \cdots + \frac{\square\square}{\square\square_{\square}}(\square)\square_{\square}(\square)$$

If the solution is linear quadratic, the equations are simplified into Equations (5.4) and (5.5) below.

$$\frac{\partial V}{\partial x}\big(x(t)\big) = 2x^T P \tag{5.4}$$

$$\frac{\partial}{\partial t}\left(V(x)\right)\dot{x}(x) = \nabla^T\left(\nabla^T P + P\nabla\right)\dot{x} = -\nabla^T Q\dot{x} < 0 \quad \forall x \neq 0 \tag{5.5}$$

Thus, according to [79, 80], the first three derivatives of the Lyapunov function $V: \mathbb{R}^n \to \mathbb{R}$ are as follows in Equations (5.9) - (5.6):

$$V(x) > 0 \quad \forall \quad x \neq 0, \quad V(x) = 0 \tag{5.6}$$

$$\dot{V}(x) = < \frac{\partial V(x)}{\partial x}, \dot{x}(x) > \tag{5.7}$$

$$\ddot{V}(x) = < \frac{\partial \dot{V}(x)}{\partial x}, \dot{x}(x) > \tag{5.8}$$

$$\dddot{V}(x) = < \frac{\partial \ddot{V}(x)}{\partial x}, \dot{x}(x) > \tag{5.9}$$

Where $<\cdot,\cdot>$ denotes a standard inner product in $\mathbb{R}^n$ and $\frac{\partial V(x)}{\partial x} \in \mathbb{R}^n$ is the gradient of $V(x)$.

When f is linear such that $\dot{x} = Ax$ and V is quadratic the Lyapunov function and associated derivatives are defined as follows in Equations (5.10) - (5.13).

$$V(x) = x^T P x \tag{5.10}$$

$$\dot{V}(x) = x^T\left(\dot{x}P + x^T\dot{x}\right)x \tag{5.11}$$

$$\ddot{V}(x) = x^T\left(\dot{x}^2 + 2x^T\dot{x}\dot{x} + x^{T^2}\ddot{x}\right)x \tag{5.12}$$

$$\dddot{V}(x) = x^T\left(\dot{x}^3 + 3x^T\ddot{x}\dot{x}^2 + 3x^{T^2}\dot{x}\ddot{x} + x^{T^3}\dddot{x}\right)x \tag{5.13}$$

In the event that $V(x(t))$ is decreasing at a point in time, the only way it can start to increase is if both $\dot{V}(x(t))$ and $\ddot{V}(x(t))$ are positive for a period of time. When $V(x(t))$ starts to increase, it is obvious that $\dot{V}(x(t)) > 0$. Additionally, because $V(x(t))$ was decreasing before starting to increase, the value of $\dot{V}(x(t))$ must change signs from negative to positive. Thus, $\ddot{V}(x(t))$ must be positive while this transition occurs and for a short time afterwards since these are continuous functions.

To show some of the advantages of the higher level derivatives, [82] is examined for reference. For the continuous time dynamical system in (5.1), if there exists scalars $\tau_1 \geq 0$ and $\tau_2 \geq 0$, and a Lyapunov function that is three times differentiable where the first three derivatives are given as in (5.7)-(5.9), then ((5.14) follows

$$\tau_2 \dddot{V}(x) + \tau_1 \ddot{V}(x) + \dot{V}(x) < 0 \tag{5.14}$$

For all $x \neq 0$. In this case, for any $x(0)$, $V\big(x(t)\big) \to 0$ as $t \to \infty$ and the origin of $\dot{x} = f(x)$ is globally asymptotically stable.

It's simple to see that if $\tau_1 = \tau_2 = 0$, the original Lyapunov theorem is provided. It is important to note that for all conditions of this theorem, it is necessary for Lyapunov function to be lower bounded and thus, $V(0) = 0$ and $V(x) > 0 \quad \forall \quad x \neq 0$. The formal proof of this can be found in [82] with supplemental work from [50]. Basically, it is just evaluating multiple different time steps of the Lyapunov function and searching for scalar coefficient weights.

5.6.1 Pendulum

To show the efficacy of these relaxations, it is easy to refer back to the pendulum example. The main observation here is that despite the fact that □̇(x(t)) > 0 at several points in time, it does continue to the equilibrium. In addition to the traditional formulation, a scalar offset has been added to the equations which helps demonstrate some of the oddities that can arise in the numerical calculations.

Figure 5.3 shows a time series plot of the Lyapunov function and its first and second derivative calculated in different ways. This plot shows interesting insight into the ability of the Lyapunov criteria to be relaxed for problems. In Figure 5.3, the value of the Lyapunov function is given by $V = □'□□$. The Lyapunov derivative was determined from Equation (5.7) such that $\dot{V} = 2 * f(x)'Px$. The linear calculation of the Lyapunov derivative is shown by $\dot{V} = -x'Qx$ or Equation (5.11). The calculation of second Lyapunov derivatives is given by Equation (5.8). There stars on the Lyapunov function to indicate locations where $\dot{V} > 0$. The vertical lines are at a few different points to highlight these locations as well. As expected, the values and signs of the function and derivatives follow the calculus basics.

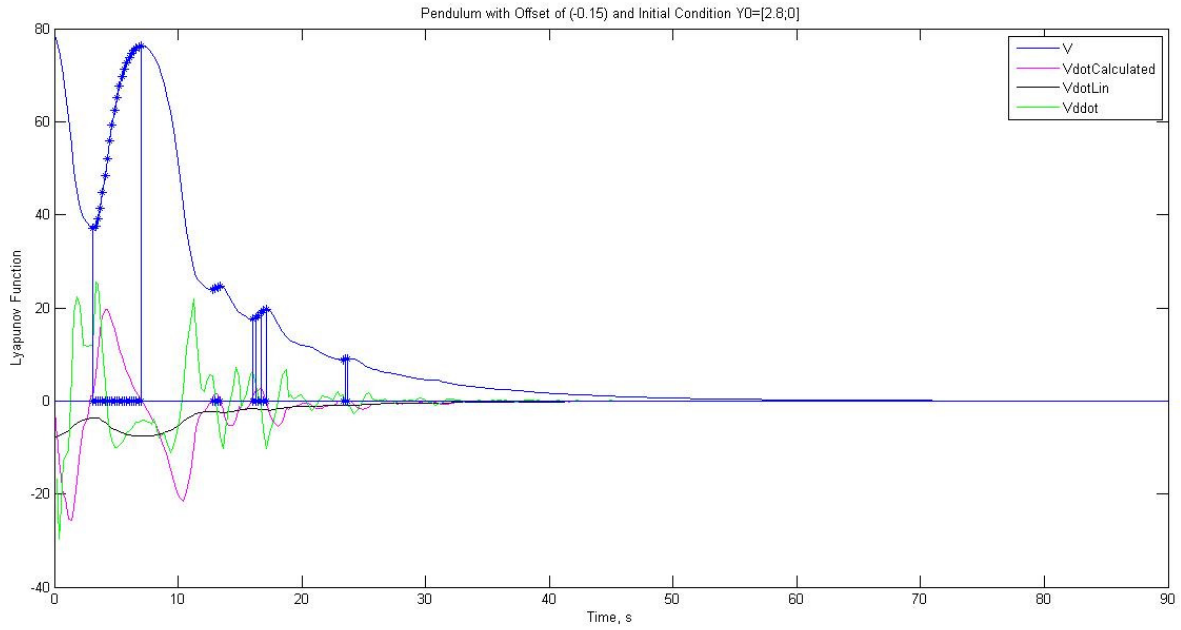

Figure 5.3 - Time series for Lyapunov function and first and second derivatives.

The graph below in Figure 5.4 – Phase portrait and Level Curves of pendulum – Dots show where Vexceeds the level curve because $\dot{V} > 0$Figure 5.4 with decreasing ellipsoids around the origin is the level curves of the Lyapunov function. The blue curve shows the trajectory of the system assuming that the states initial starting point is $x = [2.8,0]'$. The invariance of sublevel sets which should be demonstrated by the Lyapunov function never leaving these curves after entering is not quite shown here. The point that is labeled the last place that $\dot{} > 0$ is on the boundary of that curve because there are moments in the time series graph where $\dot{} > 0$, as seen in Figure 5.4. Thus, it would make sense that there would be a violation of these level sets. Additionally, the states of the pendulum are plotted in Figure 5.5. Due to very light system damping, the states will continue to trend down to zero over time.

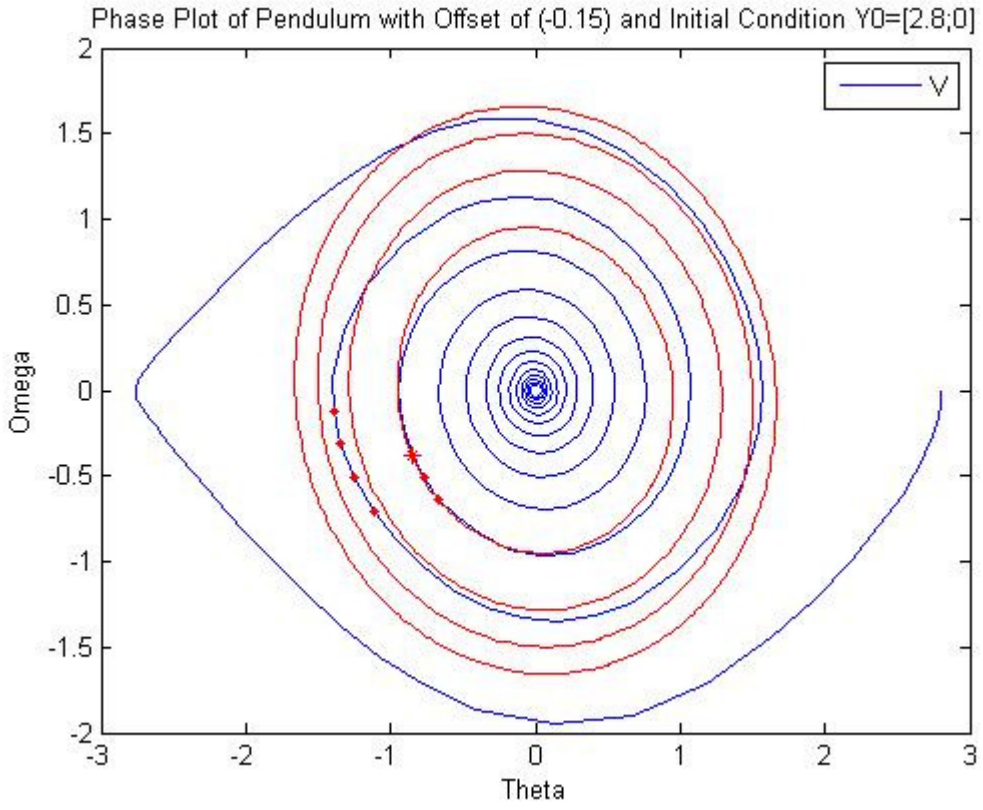

Figure 5.4 – Phase portrait and Level Curves of pendulum – Dots show where Vexceeds the level curve because $\dot{V} > 0$

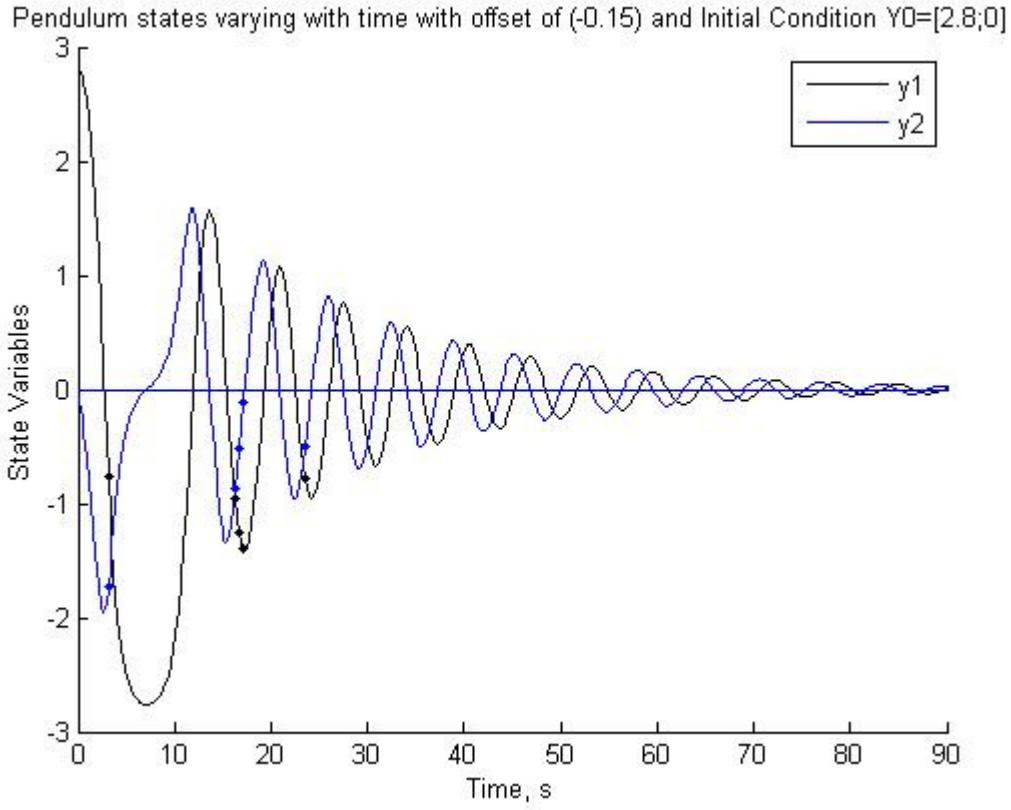

Figure 5.5 – Time Series of State Variables with Markers of Times when $\dot{V} > 0$

5.7 **Using the Lyapunov Function Values**

Once all of the values of the Lyapunov function have been created, it is necessary to apply some sort of pattern recognition algorithm in order to appropriately categorize the data. This objective was completed using a decision tree algorithm based on the Classification and Regression Tree (CART) application [81, 82]. Obviously, there are many different types of data mining techniques which could be applicable for power system data. Those methods include utilizing artificial neural networks and fuzzy logic [83]. However, there are several reasons that CART was chosen for this particular analysis including the computing efficiency and straight forward approach to mining data and building offline trees.

5.8 **CART requirements**

The main purpose of the CART tree is to mine the provided data and build a tree with a series of "if-then" statements to follow to classify incoming data. It is a binary decision tree created by

splitting a parent node (using the "if-then" statements) into two child nodes until there are enough differentiations to properly characterize the input data. The tree will stop growing when the terminal node class is determined to be sufficiently pure based on the threshold set. It also stops growing when the data categorization accuracy no longer improves when further partitions are made.

The decision trees function well in power systems applications because it is simple to create many different cases offline that could have lines, generation, or load profiles varying. Then, these cases are provided to CART in their pre-classified states and attributes which relate to the particular state of operation.

Decision trees have become a popular way of analyzing power system data over the past few decades [38, 84, 85].

According to [86] this algorithm accounts for approximately 88% of all prediction methods in studying transient stability. Predominantly, power systems research has focused on using voltage angles or current magnitudes for decision making [85, 87, 88, 89, 90, 91, 92, 93, 94, 95]. Sources [85, 87, 89] suggest ways to monitor or predict the real-time transient or voltage stability of a system using voltage angles. Decision trees which split on a single attribute are utilized in [92, 93, 94] .

Additionally, there have been great improvements with the application of the CART algorithm to data which has more than one attribute [40, 57, 96, 97].

5.8.1 Decision Tree Preliminary

Decision Trees (DT) consist of two types of nodes: decision nodes and terminal nodes. As previously mentioned, a decision node's function is to receive data and then separate that data into two distinct sets. These new sets of data become two children nodes to the decision nodes. If these children nodes contain sufficiently distinct classes of data then they become terminal nodes, which are merely class-specific nodes that indicate the end of a certain sequence of decisions. Otherwise, the children nodes become additional decision nodes. A sample DT configuration is shown in Figure 5.7.

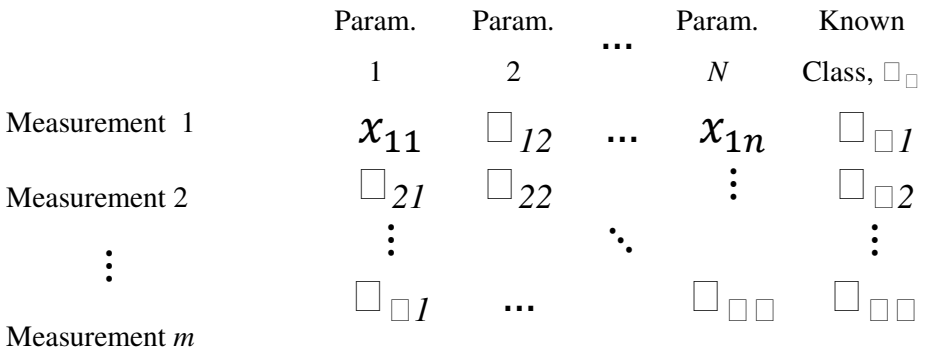

Figure 5.6 – Typical Learning Matrix layout for use with Decision Trees.

As a supervised learning technique, DT's are typically configured using what we will refer to as a learning matrix. This matrix contains m measurement samples with n attributes or parameters each. The data in this matrix must have the same set of parameters as the type of data that the DT will be used to classify. The learning matrix also includes the known classes of each measurement sample. A typical layout of the learning matrix is shown in Figure 5.6.

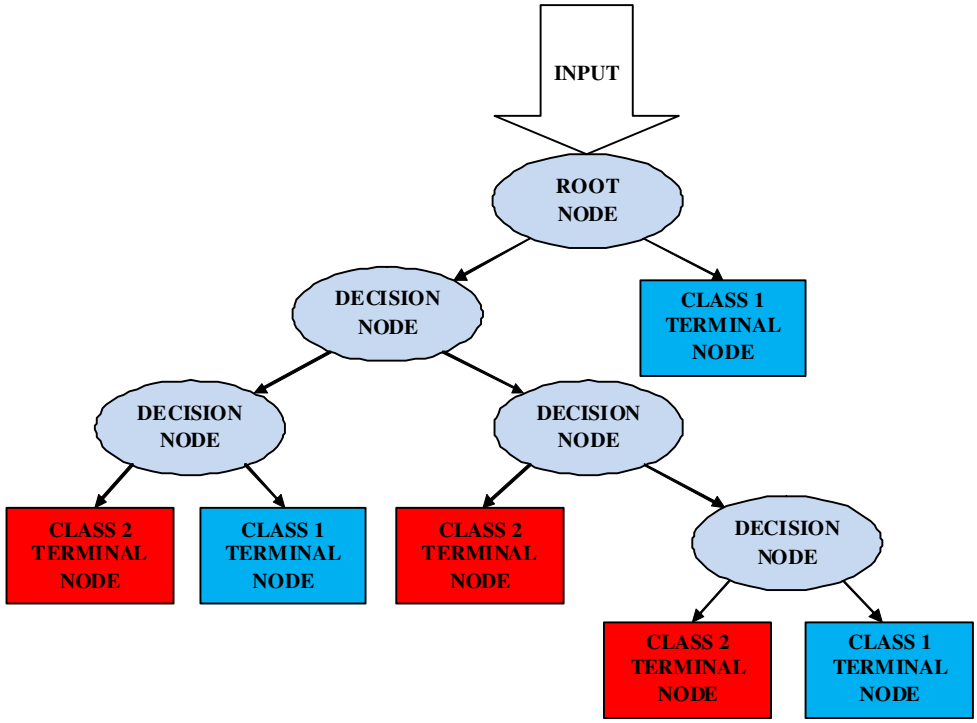

Figure 5.7 - Example Decision Tree Configuration

5.8.2 Growing Decision Trees

Determining the appropriate configuration for a DT is referred to as "growing" a DT, so named because the process begins with a single decision node, the root node, and additional decision nodes are added until classification is deemed sufficient. The primary tasks involved with DT growing are choosing decision parameters and their thresholds, designating nodes as terminal, and assigning classes to terminal nodes.

5.8.2.1 Impurity

The completion of these tasks requires a means of determining the effectiveness of decision nodes. Most often this is accomplished by calculating the "impurity" of the node's children nodes. Here, impurity refers to the homogeneity of the data at the node in terms of the data's classes; a node would be considered "pure" if it contained data with only a single class, and completely impure if it contained data with equal proportions of multiple classes.

One common index for assessing impurity is the Gina Impurity Index, defined in Equation (5.15) for every node, t [98].

$$□(□) = 1 - \sum_{□}^{□} □^2(□_□|□) \tag{5.15}$$

Here, $p(C_j|t)$ is the function used to estimate the probability of a measurement sample having class C_j given the fact that it is located at node t. This estimator itself is calculated using Equation (5.16).

$$□(□_□|□) = \frac{□(□_□, □)}{□(□)} \tag{5.16}$$

This defines the class probability estimator as the ratio of the joint probability of a sample having class C_j and existing at node t to the probability of a sample existing at node t. These two additional probabilities are defined in Equations (5.17) and (5.18).

$$□(□_□, □) = □(□_□)\frac{□_□(□_□)}{□(□_□)} \tag{5.17}$$

$$□(□_□) = \frac{□(□_□)}{□}$$

$$□(□) = \sum_{□}^{□} □(□_□, □) \tag{5.18}$$

Where □ refers to the total number of measurement samples, □(□_□) refers to the total number of samples with class □_□ , and □_□(□_□) refers to the number of measurement samples with class □_□ at node t.

5.8.2.2 Choosing decision parameters and thresholds

Decision nodes receive measurement samples consisting of multiple parameters and then decide to separate those samples into two groups for two separate children nodes. These decisions are made by comparing one of the samples' parameters to some separation threshold value.

Assume the algorithm is given a learning matrix □ with construction similar to the matrix in Figure 5.6 and with □ measurement samples and □ parameters per sample. It must then choose one parameter from the set of parameters $P = \{p_1, p_2, \ldots, p_n\}$ for our decision node □, along with a corresponding threshold value γ. If this decision parameter is numerical the decision to separate a sample is based on whether the sample's value is greater than or less than the

threshold. If the parameter is categorical, then the decision to separate is based on whether the sample's value is equal to the threshold value.

Given that each decision node creates a separation, $s = [p, \gamma]$, for the samples it receives, it is possible to evaluate the effectiveness of the node t as a function of its separation using the criterion defined in Equation (5.19) [98].

$$\Delta(\square, \square) = \square(\square) - [\square_{\square} * \square(\square_{\square}) + \square_{\square} * \square(\square_{\square})] \tag{5.19}$$

Let us additionally note each separation at each decision node as $s_t(p^*, \gamma)$.

This goodness-of-separation criterion approximates the effectiveness of the separation as the difference between the impurity of the decision node t and the impurities of its children, t_L and t_R. The proportions p_L and p_R are the ratios of samples that arrive at each child node as a result of the separation.

The optimal decision parameter, p^*, along with the optimal threshold value, γ^*, will maximize the goodness of separation criterion. To find these optimal parameters and thresholds, we simply evaluate Equation (5.19) for every $p \in P$ and every possible threshold according to the samples in $\square$. For each numerical parameter the midpoint between each pair of adjacent observations across the ordered samples is evaluated as a potential threshold. For each categorical parameter, every category observed for that parameter is evaluated as the threshold.

5.8.2.3 Terminating nodes

After finding p^* and γ^* for each existing decision node $\square$, we must then decide if the children nodes created from the resulting separations should be designated as terminal nodes. Two criteria inform this decision: the number of samples contained by the node, and the node's impurity.

If the change in impurity between generations of nodes is sufficiently low, the samples contained in the children nodes could be designated as separate classes. The precise impurity-change threshold used for this purpose is often left to experimentation. However, because gradual changes in this threshold might produce drastically different DT configurations, such a threshold could be difficult to optimize experimentally. A popular approach is simply to mandate total purity for a node's samples to be considered a class. This will result in a DT of maximum

size, but this DT can be pruned to a desired length if necessary (see [98] for further discussion of pruning procedures for DT's).

If the node contains too few samples, there is little motivation to continue growing that branch of nodes. There are few guidelines for selecting this minimum number of samples, and so this minimum is also often left to experimentation. Five or ten samples is a popular choice for the minimum number of samples [98].

5.8.2.4 Selecting a Class

Once a terminal node has been created, the class of that node's samples must be determined. This is accomplished by selecting the most likely class of those samples, using Equation (5.20) [98].

$$\square(\square_{\square}|\square) = \max_{i}(\square(\square_{\square}|\square)) \tag{5.20}$$

5.9 **The Overarching Process**

To help illustrate the steps that will be taken for each of the example systems, a flow chart is provided in Figure 5.8.

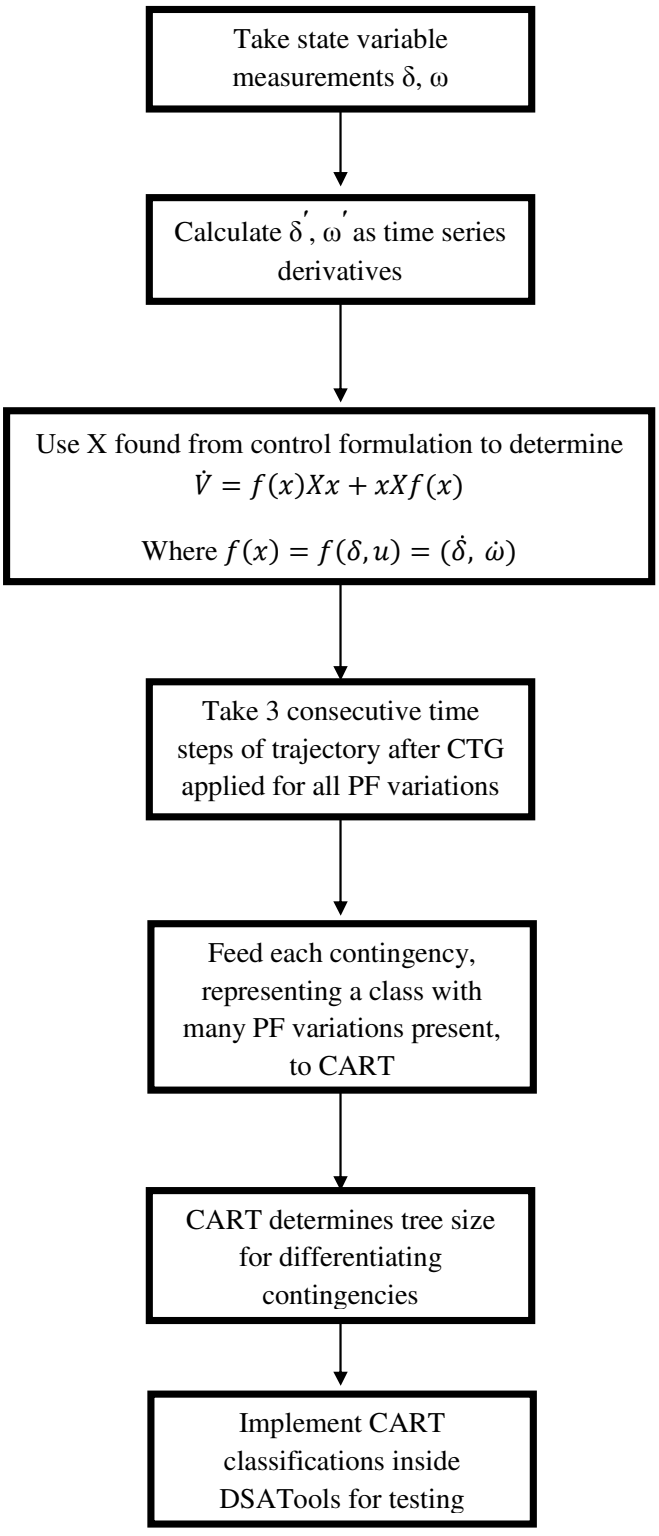

Figure 5.8 – Flow diagram indicating overall process

5.10 **29 Machine System Example**

An example of the process outlined in Figure 5.8 for the 29 machine reduced WECC system is laid out in this section. As shown in the work flow progression, the first step in the process is determining which contingencies to model and how to vary the powerflow for those sets.

5.10.1 Contingency and Powerflow Creation

Since this example provides a larger sample size, a traditional N-1 analysis was performed to determine how to find the largest number of uniquely varying modes. In addition to an N-1 analysis, varying changes to the load and generation profile were conducted. The following contingencies were chosen as the result of this analysis.

Table 5.1 Powerflow Variations and Contingencies for 4 Machine System

Contingency Event		**Powerflow Variations**
C0	Remove Line 77-84	Variations of loads at busses 7, 45, and 75
C1	Remove Line 90-84	Variation in admittances of lines 42, 45
C2	Remove Line 45-42	Variation of loads at busses 71, 26, and 124
C3	Remove Line 89-90	Variation in admittances of lines 64, 70
C4	Remove Line 7-9	Variation of loads in busses 90, 24, and 6
C5	Decrease Load 75 by 70%	Variation of admittances in lines 84, 90
C6	Increase Load 90 by 10%	Variation of admittances in lines 7, 9
C7	Remove Line 64-67	Variation of admittances in lines 77, 84
C8	Increase Load 71 by 10%	Variation of admittances in lines 89, 90

5.10.2 HVDC Feedback Control Design

As mentioned previously, the controller was designed using state feedback for control of an HVDC line in the system. Although HVDC controls can become very complicated, some of the extremely fast acting components do not need to be modeled for the purposes of small signal stability. The following figures capture the necessary dynamics for modeling non-transient behavior.

In Figure 5.9, the reduced version of the current order calculation is shown. The value of the current order is then used to calculate the firing angle for the rectifier in conjunction with the

measured DC current and control signal. Given that this analysis is not studying fault applications, it is not necessary to have some of the traditional voltage control limiters that would normally apply for HVDC line models because the voltage would not be dipping that low in a short period of time. The control signal here is the state feedback determined from the H_2/H_∞ problem.

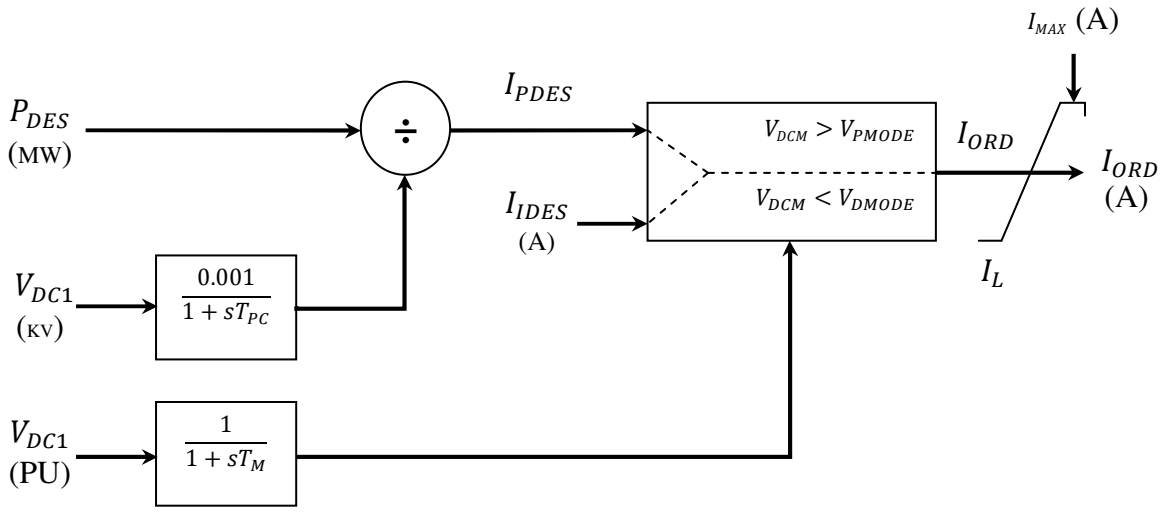

Figure 5.9 – The Current Order for the HVDC Line Control

The Figure 5.10 shows the calculation of the rectifier firing angle. The Figure 5.11 shows the calculation of the inverter firing angle.

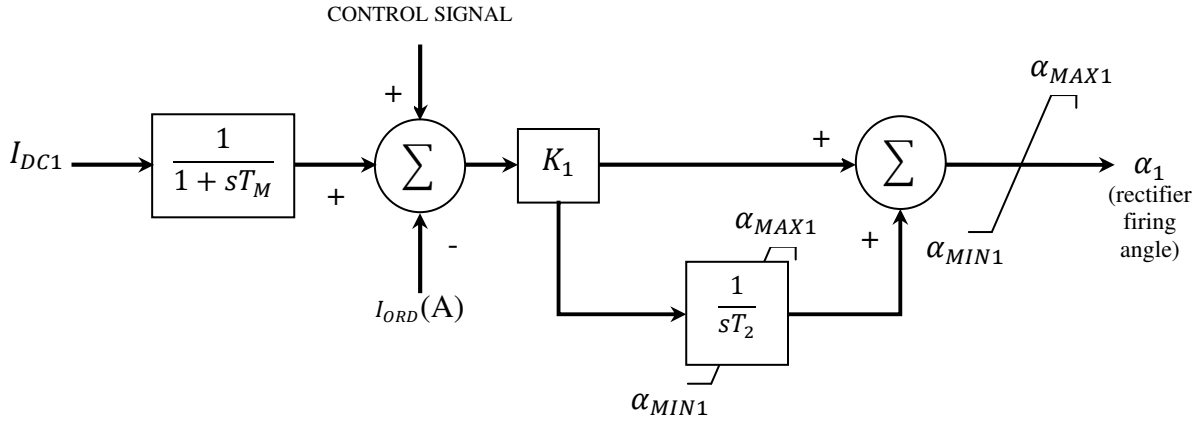

Figure 5.10 – The Rectifier Firing Angle Computation

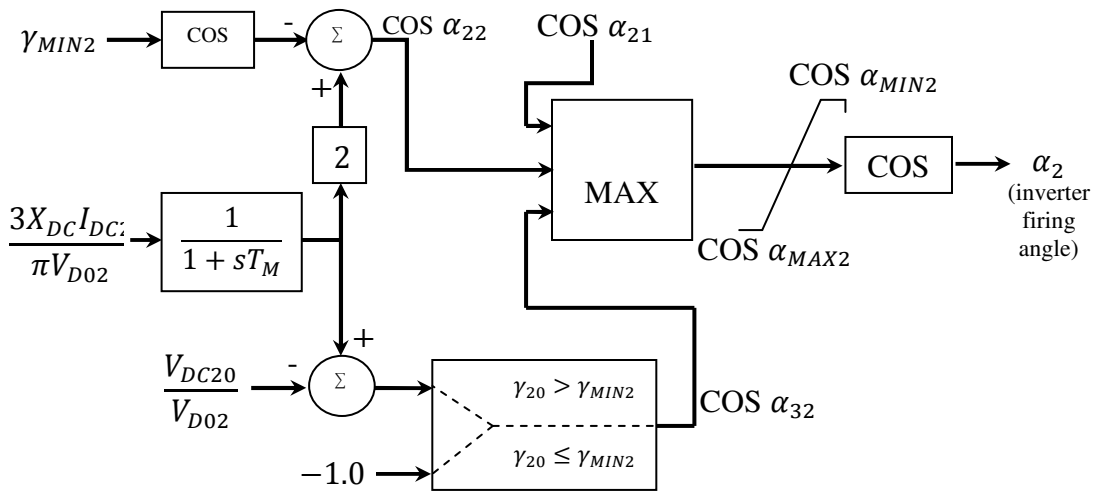

Figure 5.11 – The Inverter Firing Angle Computation

All of these are simplified versions of the HVDC line model since faster dynamics do not need to be modeled and this configuration design was found to be suitable for the application at hand.

5.10.3 Applying the Developed Control

The control developed through the multiobjective H_2/H_∞ problem with pole placement constraints shapes the input control to the HVDC system described above.

5.10.4 Applying the Developed Control

Given that in the 29 Machine System there are two HVDC lines which are modeled with the exact same dynamics as described in the Four Machine System, it did not really require a secondary section when reviewing the larger example system. Also similar to the Four Machine Example, a control was developed through the multiobjective H_2/H_∞ problem with pole placement constraints for each of the DC lines. As shown in Figure 5.12, the control developed using this algorithm worked successfully for the system on the whole as well as the interarea modes of interest.

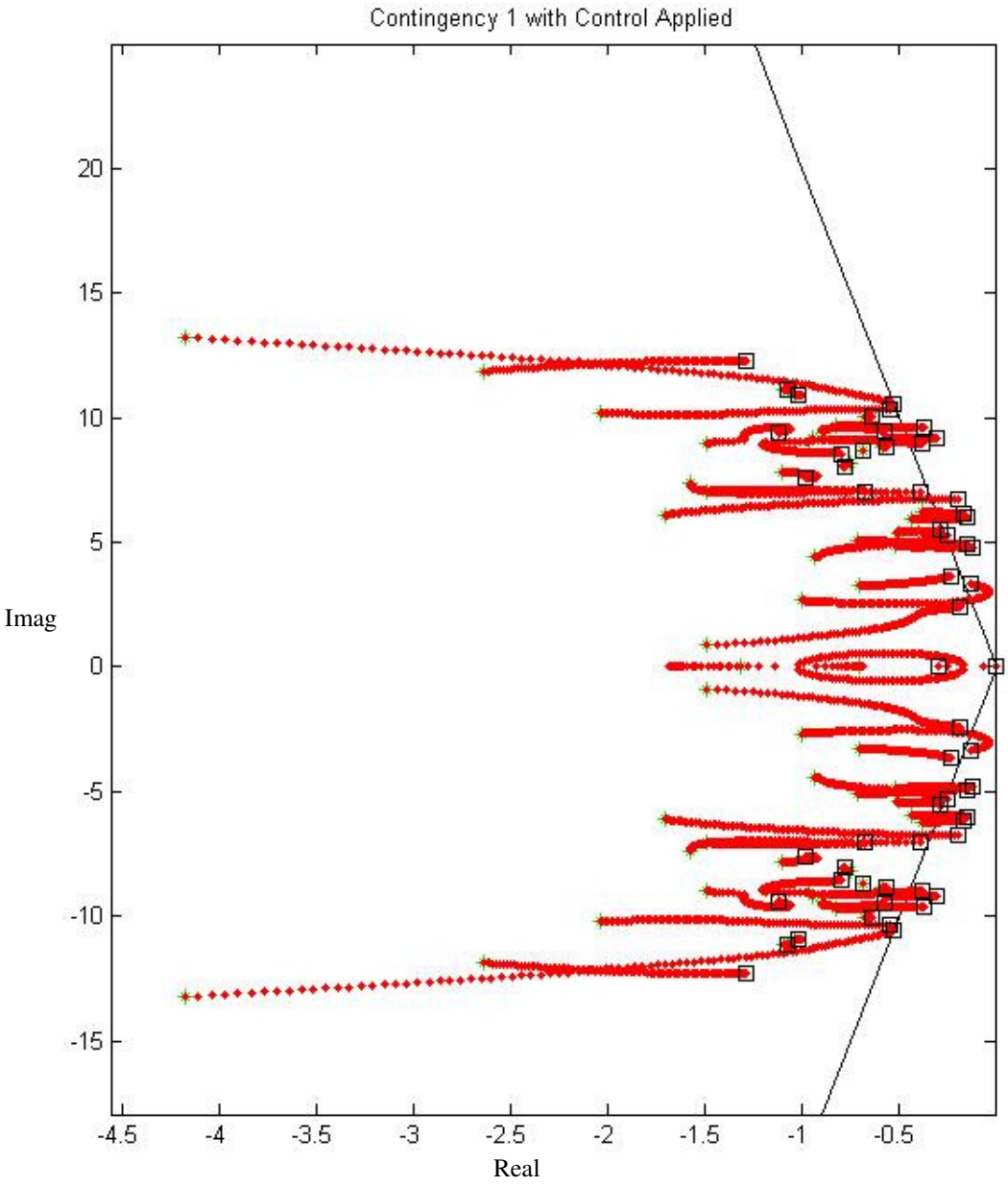

Figure 5.12 – Eigenvalue shift for 127 bus system under contingency 1 (C1)

5.10.5 System Manipulation for Reconciling Non Zero Equilibrium and Negative Definiteness Violations

In a power system evaluation, it becomes apparent that due to the numerical properties of the state inputs, there will be stable operating points even though the derivative of the Lyapunov function may be positive. In order to accurately understand these systems when their Lyapunov function indicates instability, it is necessary to evaluate the second derivative. This simple

mathematical concept normally used for graphing functions in high school provides useful insight. In addition to utilizing first and second derivatives, it is desirable to evaluate the boundedness of the system trajectory as it approaches equilibrium even if there are some small numerical inconsistencies between the actual model and what theory should provide.

5.10.6 Lyapunov Function Creation

For each contingency set, a large number of powerflow variations are created to provide a sort of regional state area around the contingency. All of these values were created in DSATools TSAT program, but exported into MATLAB for ease of displaying and graph manipulation. Figure 5.13 shows the DSATools output for the calculations of just one powerflow case for one contingency just for reference.

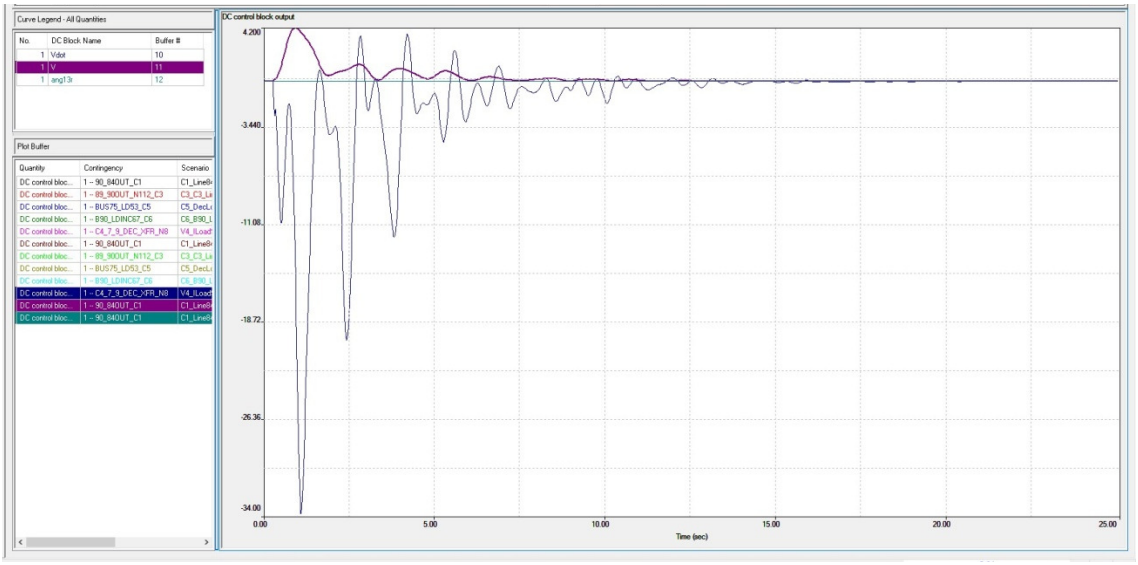

Figure 5.13 – Lyapunov functions and derivatives for one case in the set for Contingency 1 for 127 Bus System

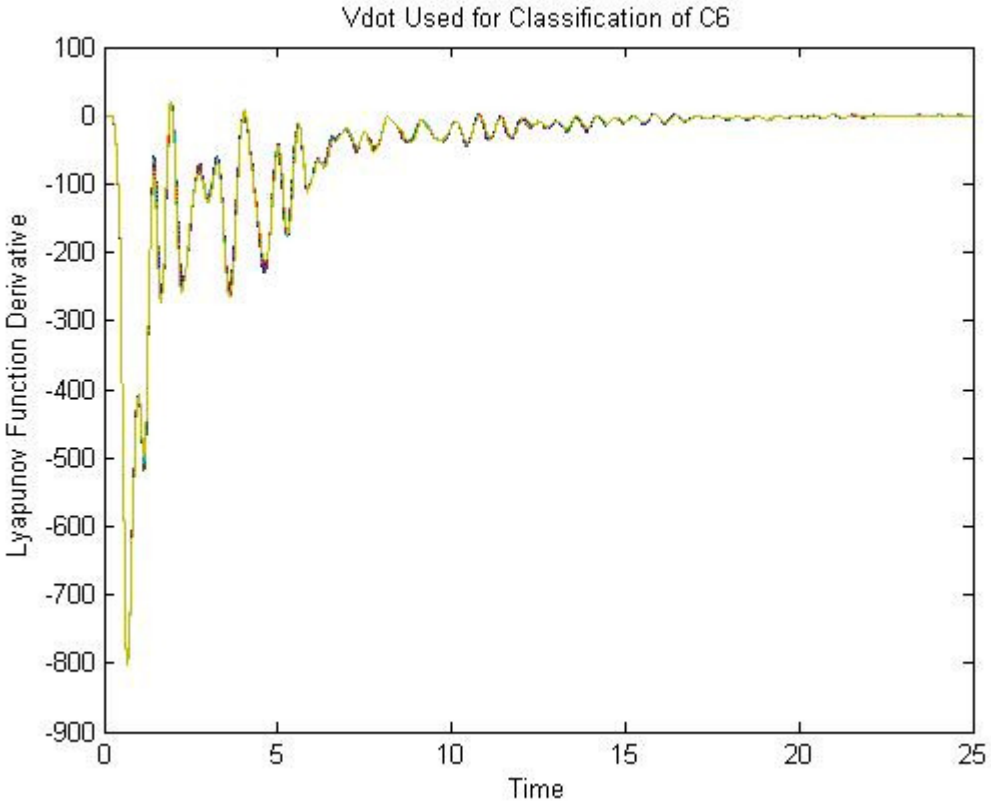

Figure 5.14 - $\dot{V}$ Values for all of the powerflow variations for Contingency 6

Figure 5.14 and the subsequent graphs in MATLAB are able to more easily show all of the plots for each powerflow variation. The following graphs provide information on what the values of all of the derivatives are for a few contingencies.

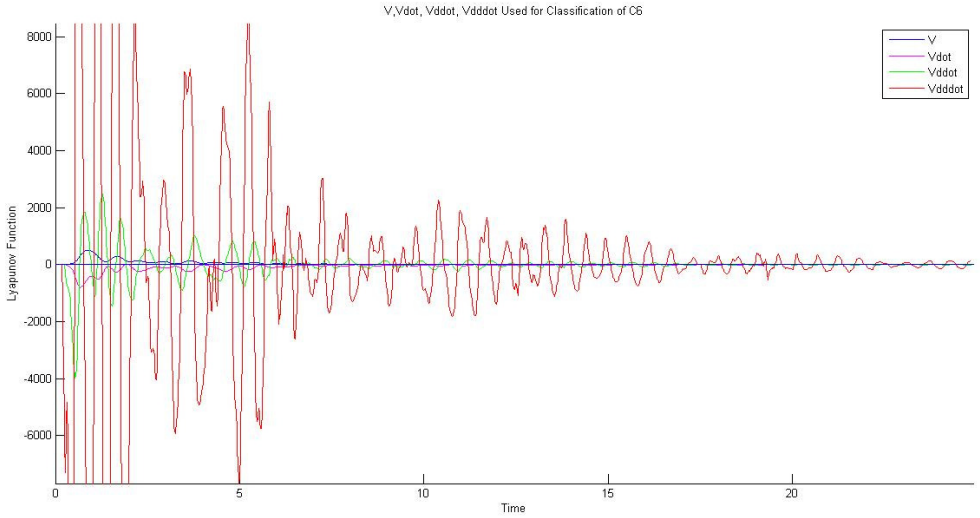

Figure 5.15 – Provides all of the derivatives necessary for evaluating the ability of the power system to return to a stable equilbrium

Most importantly, the information provided from Figure 5.16 – Multiple Derivative Summation for System StabilityFigure 5.16 shows that when solving (5.14) for the variations of τ, it is possible to show that the system will reach an equilibrium. A crude search was used to find the values of τ used. In future work, it would be desirable to set up a convex optimization program to look for these values to maximize the known stable operating space.

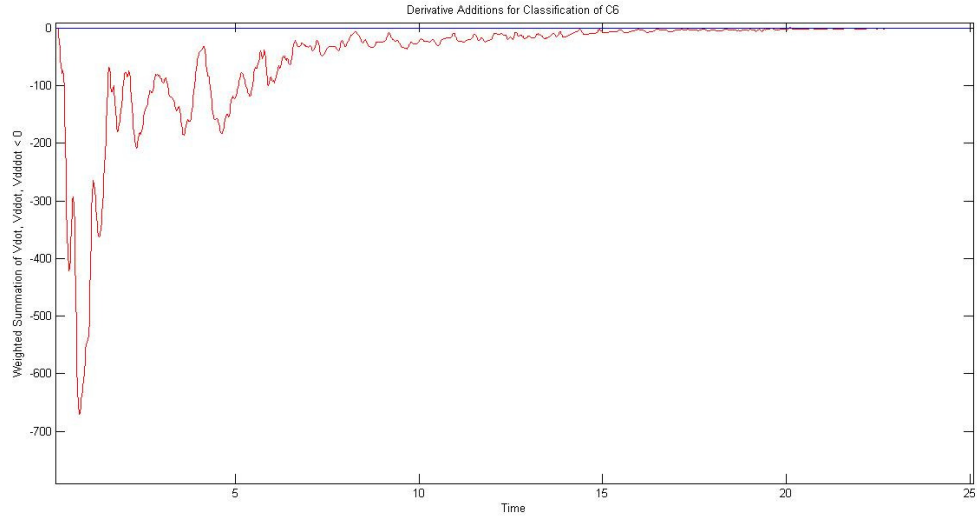

Figure 5.16 – Multiple Derivative Summation for System Stability

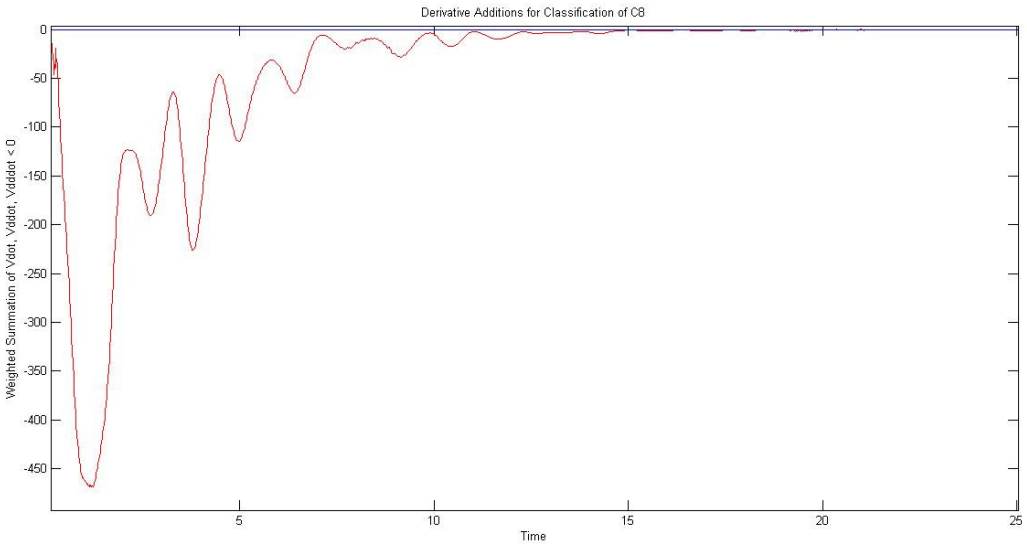

Figure 5.17 – Derivative Sums for one powerflow out of Contingency Set 6

5.10.7 CART Diagram

The following figures demonstrate how a classification analysis in CART was performed given the input data set. Furthermore, the decision tree generated by CART is shown and was calculated to have an accuracy of 99.7% according to the cross validation algorithm.

Figure 5.18 is used to show the snapshots in time when the sample values to feed into CART are taken. This figure in particular is looking at the values of $\dot{\boldsymbol{V}}$ for all of the powerflow cases created where Contingency 0 is applied. There is a cross section like this for each set of contingencies for all of their associated powerflow cases which are fed into the CART tree in Figure 5.19.

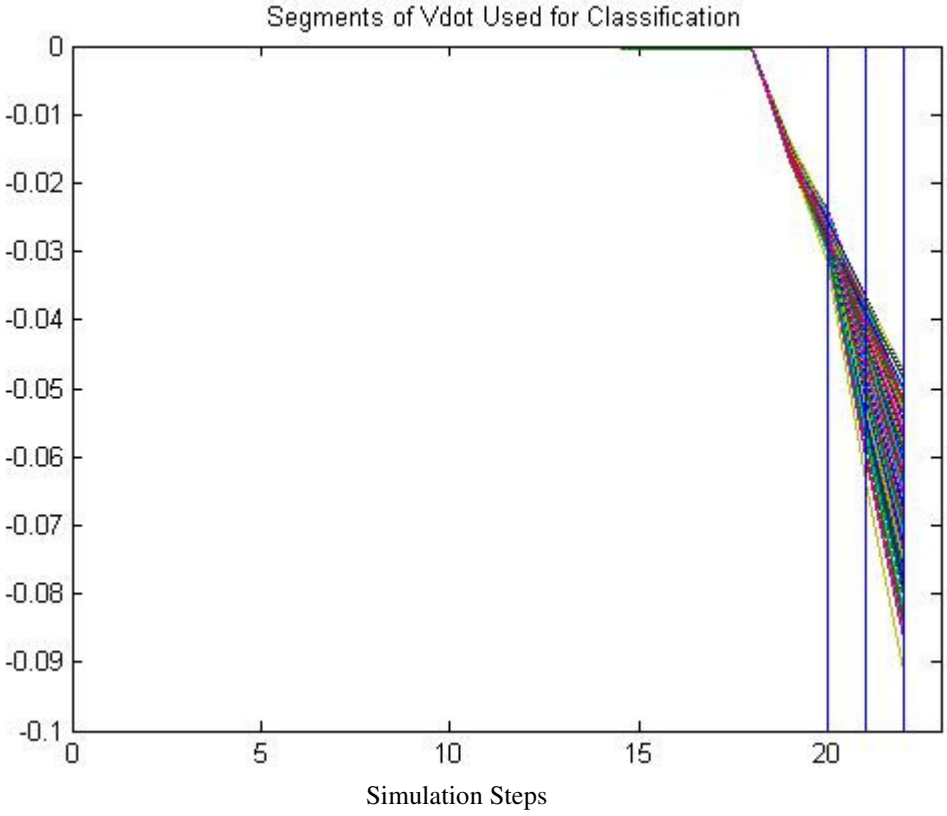

Figure 5.18 – The 20, 21, 22 Samples of $\dot{\boldsymbol{V}}$ taken for Contingency 0 Classification

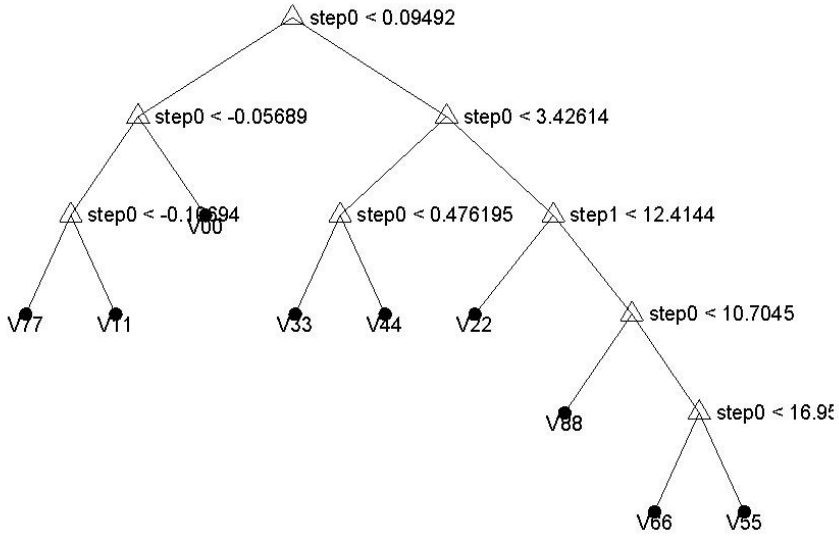

Figure 5.19 – CART diagram for 127 bus example

In Figure 5.20, the cost curve of the CART tree is shown to demonstrate the efficacy of the decision being made with each split level of the tree. This means that as the values continue to flow down the tree, the effectiveness of your decision is continually increasing.

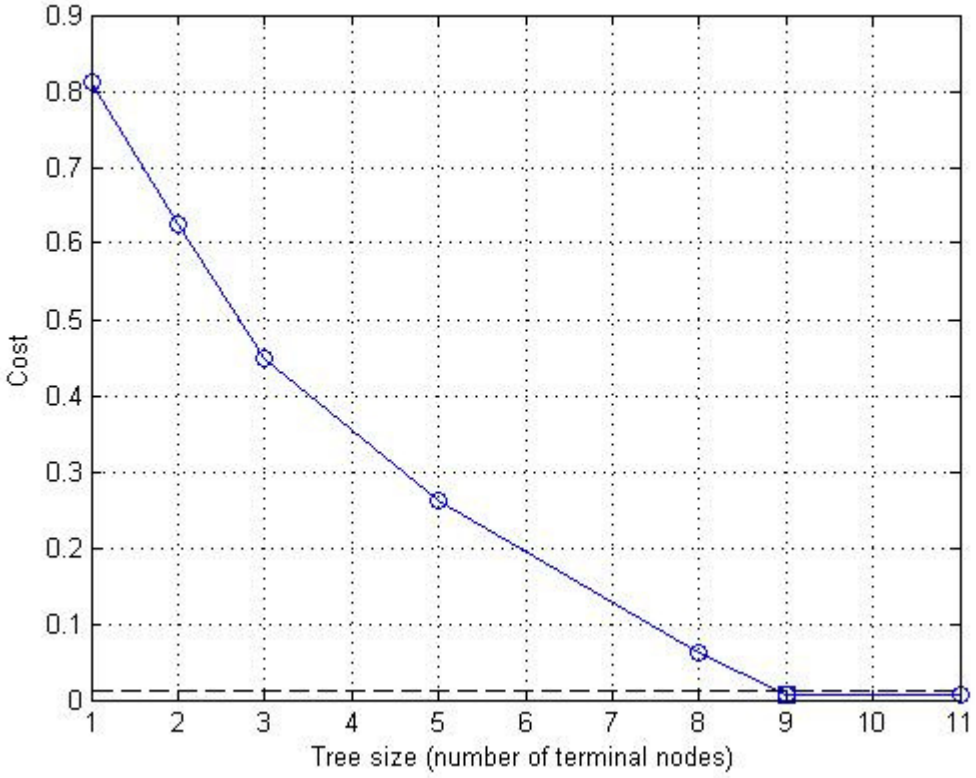

Figure 5.20 – Cost curve for number of terminal nodes in CART made for 127 bus example

5.10.8 Show changes in V with controls applied

To finish the testing of this work, it is necessary to embed all of the computations that the transient security assessment must perform during the simulation in TSAT. In order to do this, values must be provided for the steps on which they are supposed to split and then the particular control determined must be applied after that last time step. The change in the system states and of the Lyapunov functions can be seen when the control is applied as seen in Figure 5.21 and Figure 5.22.

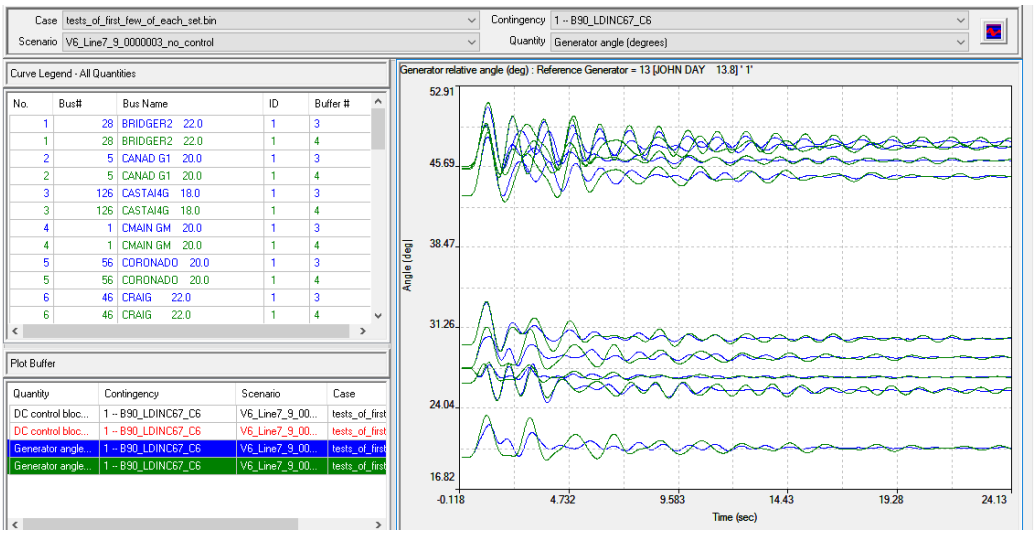

Figure 5.21 – Some Generator Angles with and without Control Applied

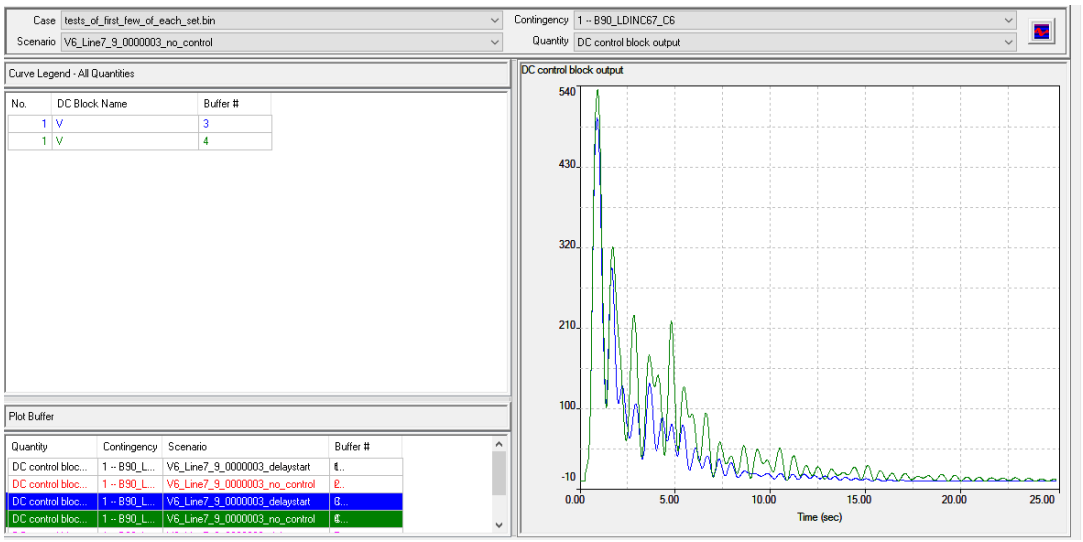

Figure 5.22 – Decrease in Lyapunov Function when Control Properly Applied

There had been efforts to determine whether changes in the control would be warranted after application of the initial choice. However, this was only feasible if the change in control efficiency was very small. The bandwidth of change set to decide to change controllers could be set more tightly, but may introduce chattering and noise from undesirable switches. If the weighting variables of the summed derivatives were to be better optimized, it could provide a

different metric for choosing the control and may provide more information on distinct variations later in the simulation.

The entire objective of this work has been to try define a loose region of attraction surrounding a particular equilibria of the power system. In doing so, many different mathematical concepts have had to work in unison to provide useful results. Additionally, the adaptations to a traditional nonlinear analysis prove practical for the study of any type of more complicated non linear system for which a specific solution may be impossible to determine. Furthermore, given the breadth of the systems which can be modeled for a power system, this technique can be beneficial in an actual operating scenario. Moreover, the bounds could be further enhance by taking system snapshots with varying degrees of topology that may be extremely uncommon (like a mobile device or temporary line for construction maintenance) to build a well populated system overview.

Chapter 6. Conclusions

The methodology, computational context, and analyses developed in this work provide insight into an area of power systems which has traditionally been unexplored. By relaxing some of the conditions surrounding the Lyapunov stability requirements in a way that provides practical assistance without rigorous proof, the applicability to power systems problems expands tremendously. This approach allows one to define a loose region of attraction surround an equilibria of the power system which is extremely useful since the power system is extremely nonlinear and always changing.

By further validating this algorithm on a reduced WECC 127 bus model, it helps explain how many variances in system state stem from the changes in system conditions. The methodology provides a solution for control application in a time frame which is acceptable for the types of oscillations and system changes that are interesting in a small signal analysis. However, it should be noted that the concept of wide area closed loop control in an actual utility is a distant reality. In many cases, the control operations in real time operations are determined and implemented by transmission or generation operators. As the complexity continues to increase, the burden on the operator will become heavy enough that more closed loop options will be necessary for a continually reliable and efficient power grid. Further efforts in this field could begin by evaluating other control options to help with oscillations in addition to the HVDC lines. As STATCOMs and SVCs are being installed more frequently throughout the US, they could be included for control options. Additionally, the influx of renewable energy will drastically change the types of operating conditions that are seen in real time. It would be extremely useful to have an understanding of the stability bounds of the system as these new technologies continue to

replace some of the previous coal units. Finally, there could be additional attention paid to group and extending of various stability boundaries to help alleviate the most stressed conditions.

The post-event system condition is dependent on the initial system operating condition as well as the nature of the disturbance. This means that power system stability is a property of the system motion around an equilibrium set.

Bibliography

[1] N. A. Armstrong, "The Engineered Century," *The Bridge,* pp. 14-18, Spring 2000.

[2] A. Pal and e. al., "Role of Power System Relays in a Large Scale Physical Attack," *6th Int. Conf. Liberalization & Modernization of Power Systems and CRIS Problems of Critical Infrastructures,* 2015.

[3] Western Electricity Coordinating Council, *Relationship Between the Western Interconnection and NERC,* 2005.

[4] Bouchecl, Artist, *North American Regional Reliability Councils and Interconnections.* [Art]. NERC, 2009.

[5] T. Group, "Energy - The Facts," 2013. [Online]. [Accessed 2013].

[6] I. Consulting, "www.solarstorms.org," 2003. [Online]. Available: http://www.solarstorms.org/ICFBlackout2003.pdf. [Accessed 2013].

[7] E. D. Sontag, Mathematical Control Theory, New York, NY: Springer-Verlay New York, 1998.

[8] O. Mayr, The Origins of Feedback Control, Cambridge, MA: MIT Press, 1970.

[9] A. Fuller, "The Early Development of Control Theory, Parts I and II," *Dynamic Systems, Measurement, and Control,* p. 98, 1976.

[10] W. J. P. III, System Dynamics, New York, NY: McGraw Hill, 2010.

[11] A. W. a. B. Wollenberg, Power Generation, Operation, and Control, New York: John Wiley & Sons, 1996.

[12] A. Abur and A. Exposito, Power System State Estimation Theory and Implementation: CRC, 2004.

[13] F. Schweppe and J. Wildes, "Power System Static - State Estimation, Part I: Exact Model," *IEEE Trans. Power Apparatus and Systems,* Vols. PAS-89, pp. 120-125, 1970.

[14] F. Schweppe and D. Rom, "Power System Static-State Estimation, Part II: Approximate Model," *IEEE Trans. on Power Apparatus and Systems,* Vols. PAS-89, pp. 125-130, 1970.

[15] A. Phadke and J. Thorp, in *Computer Relaying for Power Systems*, 2nd Edition ed., John Wiley, 1988, pp. 96-98, 144, 166-174.

[16] A. Phadke, J. Thorp and K. Karimi, "State Estimation with Phasor Measurements," *IEEE Trans. on Power Systems,* Vols. PWRS-1, no. 1, February 1986.

[17] A. Phadke and J. Thorp, Synchronized Phasor Measurements and Their Application, Springer Science + Business Media, 2008.

[18] B. Pal and B. Choudhuri, Robust Control in Power Systems, New York: Springer, 2005, pp. 1-55.

[19] K. Mekki, N. HadjSaid, R. Feuillet and D. Georges, "Design of Damping Controllers Using Linear Matrix Inequalities Techniques and Distant Signals to Reduce Control Interactions," in *IEEE 2001 Power Industry Computer Applications Conference*, 2001.

[20] Y. Zhang and A. Bose, "Design of Wide-Area Damping Controllers for Inter-area

Oscillations," *IEEE Trans. Power Syst.,* 2008.

[21] B. Chaudhuri and B. Pal, "Robust Damping of Multiple Swing Modes Employing Global Stabilizing Signals with a TCSC," *IEEE Trans. Power Syst.,* vol. 19, no. 1, pp. 499-506, February 2004.

[22] P. Chatterjee, A. Pal, J. Thorp and J. D. L. Ree, "Partitioned Linear State Estimation," *Proc. IEEE Power Eng. Soc. Conf. Innovative Smart Grid Technol.,* pp. 1-5, 18-20, February 2015.

[23] A. Pal, G. Sanchez-Ayala, J. Thorp and V. Centeno, "A Community-based Partitioning Approach for PMU Placement in Large Systems," *Electric Power Components & Systems.*

[24] K. Amare, V. Centeno and A. Pal, "Unified PMU Placement Algorithm for Power Systems".*2015 IEEE North American Power Symposium.*

[25] A. Pal, G. Sanchez, V. Centeno and J. Thorp, "A PMU Placement Scheme Ensuring Real-time Monitoring of Critical Busses of the Network," *IEEE Trans. Power Del.,* vol. 29, no. 2, April 2014.

[26] G. Sanchez, A. Pal, V. Centeno and W. Flores, "PMU Placement for the Central American Power Network and Its Possible Impacts," *Proc. IEEE Power Eng. Soc. Conf. Innovative Smart Grid Technol.,* pp. 1-7, October 2011.

[27] K. Jones, A. Pal and J. Thorp, "Methodology for Performing Synchrophasor Data Conditioning and Validation," *IEEE Trans. Power Syst.,* vol. 30, no. 3, pp. 1121-1130, May 2015.

[28] C. Mishra, A. Pal and V. Centeno, "Kalman-filter based Recursive Regression for Three-phase Line Parameter Estimation Using Phasor Measurements," *Proc. IEEE Eng. Soc. General Meeting,* pp. 1-5, 26-30, July 2015.

[29] K. Jones, J. Thorp and R. Gardner, "Three-phase Linear State Estimation Using Phasor Measurements," in *presented at the IEEE Power and Energy Society General Meeting*,

July 2013.

[30] P. Kundur, Power System Stability and Control, New York: McGraw-Hill, 1994.

[31] A. Pal, "Effect of Different Load Models on the Three-sample Based Quadratic Prediction Algorithm," *Proc. IEEE Power Eng. Soc. Conf. Innovative Smart Grid Technol.,* pp. 1-5, 18-20, February 2015.

[32] W. R. a. J. Shamma, "Research in Gain Scheduling," *Automatica,* vol. 36, 2000.

[33] H. N. a. J. Stoutstrup, "Gain Scheduling using the Youla Parameterization," in *Proceedings of the 38th Conference on Decision & Control*, Phoenix, 1999.

[34] K. Trangbaek, "Safe LPV Controller Switching," in *Proceedings of the 50th IEEE Conference on Decision and Control and European Control Conference*, Orlando, FL, USA, 2011.

[35] Inc., Powertech Labs, "DSA Tools," [Online]. Available: retrieved from http://www.dsatools.com.

[36] The MathWorks Inc., *MATLAB version 8.10.0 (computer software),* 2010.

[37] S. Systems. [Online]. Available: retrieved from http://www.salford-systems.com/cart.php.

[38] S. Kretsinger, S. Rovnyak, D. Brown and J. Thorp, "Parallel Decision Trees for Predicting Groups of Unstable Generators from Unsynchronized Phasor Measurements," *Proc. Precise Measurements in Power Systems Conference,* 25-29 October 1993.

[39] A. Swarnkar and K. Niazi, "CART for Online Security Evaluation and Preventive Control of Power Systems," in *Proc. of the 5th WSEAS/IASME Int. Conf. on Electric Power Systems, High Voltages, Electric Machines*, Tenerife, Spain, December 16-18, 2005.

[40] A. Pal, J. Thorp, T. Khan and S. Young, "Classification Trees for Complex Synchrophasor Data," *Elect. Power Compon. Syst.,* vol. 41, no. 14, pp. 1381-1396, Sep 2013.

[41] G. Rogers, Power System Oscillations, Norwell, MA: Kluwer, 2000.

[42] Electric Power Research Institute, "DC Multi-Infeed Study," EPRI, TR-TR-104586s, Projects 2675-04-05, 1994.

[43] H.-D. Chiang, Direct Methods for Stability Analysis of Electric Power Systems, Wiley, 2010.

[44] V. Di Dio, R. Miceli, C. Rando and G. Zizzo, "Dynamics photovoltaic generators: Technical aspects and economical valuation," in *SPEEDAM*, Pisa, 2010.

[45] "Wikipedia: The free encyclopedia.," Wikimedia Foundation, Inc., 25 06 2016. [Online]. Available: https://en.wikipedia.org/wiki/Inertia. [Accessed 01 07 2016].

[46] H. Khalil, Nonlinear Systems, 2nd ed., Englewood Cliffs, NJ: Prentice-Hall, 1996.

[47] G. Rogers, "The Application of Power System Stabilizers to a Multi-generator Plant," *IEEE Trans. Power Syst.,* vol. 15, no. 1, pp. 350-355, Feb 2000.

[48] H. Breulman, E. Grebe, M. Losing, W. Winter, R. Witzman, P. Dupuis, M. P. Houry, T. Margotin, J. Zerenyi, J. Duzik, J. Machowski, L. Martin, J. M. Rodrigues and E. Uretavizcaya, "Analysis and Damping of Inter-Area Oscllations in the UCTE/CENTREL Power System," *CIGRE,* vol. 38, no. 113, 2000.

[49] N. Martins, A. A. Barbosa, J. C. R. Ferraz, M. G. dos Santos, A. L. B. Bergamo, C. S. Yung, V. R. Oliveira and N. J. P. Macedo, "Returning Stabilizers for the north-south Brazilian interconnection," in *Power Engineering Society Summer Meeting*, Edmonton, 1999.

[50] I. Kamwa and L. Gerin-Lajoie, "State-Space System Identification- Toward MIMO Models for Modal Analysis and Optimization of Bulk Power Systems," *IEEE Transactions on Power Systems,* vol. 15, no. 1, pp. 326-335, 2000.

[51] S. Sayed Hassen, Robust and Gain-scheduled Control Using Linear Matrix Inequalities,

Melbourne, Australia: Monash Univ., 2001.

[52] A. Pal and J. Thorp, "Co-ordinated Control of Inter-Area Oscillations Using SMA and LMI," *Proc. IEEE Power Eng. Soc. Conf. Innovative Smart Grid Technology,* pp. 1-6, 16-20, January 2012.

[53] K. Vance, A. Pal and J. Thorp, "A Robust Control Technique for Damping Inter-area Oscillations," *Proc. IEEE Power and Energy Conference at Illinois (PECI),* pp. 1-8, 24-25, February 2012.

[54] A. Pal, J. Thorp and V. Centeno, "Applying a robust control technique to damp low frequency oscillation in the WECC," *International Journal of Electrical Power & Energy Systems,* vol. 44, no. 1, pp. 638-645, 2013.

[55] H. Niemann and J. Stoustrup, "Gain Scheduling Using the Youla Parametrization," in *Proc. of the 38th Conference on Decision & Control*, Phoenix, USA, 1999.

[56] W. Rugh and J. Shamma, "Research on Gain Scheduling," *Automatica 36,* 2000.

[57] T. Wang, A. Pal, J. Thorp, Z. Wang, J. Liu and Y. Yang, "Multi-polytyope Based Adaptive Robust Damping Control in Power Systems using CART," *IEEE Trans. Power Syst.,* vol. 30, no. 4, pp. 2063-2072, July 2015.

[58] P. Apkarian and P. Gahinet, "A Convex Characterization of Gain-scheduled H1 Controllers," *IEEE Trans. AUtom. Control 40,* no. 5, pp. 853-863, 1995.

[59] P. Apkarian, P. Gahinet and G. Becker, "Self-scheduled H1 Control of Linear Parameter-varying Systems: A Design Example," *Automatica 31,* no. 9, pp. 1251-1261, 1995.

[60] A. Packard, "Gain Scheduling via Linear Fractional Transformations," *Systems and Control Letters,* no. 22, pp. 79-92, 1994.

[61] X. Zhang, P. Tsiotras and A. Lanzon, "An Approach for Computing the Exact Stability Domain for a Class of LTI Parameter Dependent Systems," *International Journal of*

Control, vol. 79, no. 9, pp. 1046-1061, 9 September 2006.

[62] B. Barmish, New Tools for Robustness of Linear Systems., Macmillan Publishing Company, 1994.

[63] S. Rern, P. Kabamba and D. Bernstein, "Guardia map approach to robust stability of linear systems with constant real paramter uncertainty," *IEEE Transactions on Automatic Control,* vol. 39, pp. 162-164, 1994.

[64] L. Saydy, A. Tits and E. Abed, "Robust stability of linear systems relative to guarded domains," in *Proceedings of the 27th IEEE Conference of Decision and Control*, Austin, TX, 1988.

[65] L. Saydy, A. Tits and E. Abed, "Guardian maps and the generalized stability of parametrized families of matrices and polynomials," *Mathematics of Control, Signals, and Systems,* vol. 3, pp. 345-371, 1990.

[66] E. I. Jury, Inners and Stability of Dynamic Systems, Wiley, 1974.

[67] D. Mustafa and T. N. Davidson, "Block Bialternate Sum and Associated Stability Formulas," *Automatica,* vol. 31, no. 9, pp. 1263-1274, 1995.

[68] J. Magnus, Linear Structures, London: Charles Griffin, 1988.

[69] A. T. Fuller, "Conditions for a Matrix to Have Only Charactreristic Roots with NegativeReal Parts," *Journal of Mathematical Analysis and Applications,* vol. 23, no. 1, pp. 71-98, 1968.

[70] S. Boyd and L. Vandenberghe, Convex Optimization, Cambridge, UK: New York: Cambridge University Press, 2004.

[71] K. Vance and J. Thorp, "Robust Control for Inter-area Oscillations: A Polytopic Approach to Power Systems Control," 2012.

[72] G. Chen, Stability of Nonlinear Systems, New York, NY: Wiley, 2004.

[73] A. Bensenouci and A. Ghany, "Mixed H2/Hinf with Pole-placement Design of Robust LMI-based Output Feedback Controllers for Multi-area Load Frequency Control," in *EUROCON 2007: The International Conference on "Computer as a Tool"*, 2007.

[74] J. Rugh, Linear System Theory, 2nd Ed. ed., Princeton, NJ: Prentice-Hall, 1996.

[75] M. Corless, "Introduction to Dynamic Systems," West Lafayette, Indiana, 2011.

[76] A. Lyapunov, *The general problem of the stability of motion,* University of Kharkov, 1892.

[77] A. Pal, J. Thorp, S. Veda and V. Centeno, "Applying a Robust Control Technique to Damp Low Frequency Oscillations in the WECC," *Int. J. Elect. Power Energy Syst.,* vol. 44, no. 1, pp. 638-645, January 2013.

[78] L. Rosier, "Homogeneous Lyapunov function for homogeneous continuous vector fields.," *Systems Control Letters,* vol. 19, no. 6, pp. 467-473, 1992.

[79] A. A. Ahmadi and P. Parillo, "Non-monotonic Lyapunov functions for stability of discrete time nonlinear and switched systems," in *Proceedings of the 47th IEEE Conference onDecision and Control*, 2008.

[80] A. A. Ahmadi and P. A. Parillo, "Towards Scalable Algorithms with Formal Guarantees for Lyapunov Analysis of Control Systems via Algebraic Optimization," in *53rd IEEE Conference on Decision and Control*, Los Angeles, 2014.

[81] Salford Systems, [Online]. Available: retrieved from http://www.salford-systems.com/cart.php.

[82] in *CART: Tree-structured Non-parametric Data Analysis*, San Diego, CA, Salford Systems, 1995.

[83] A. Mishra and A. Saxena, "Data Mining Technology and its Applications to Power

Systems," *International Journal of Computer Applications,* vol. 137, no. 8, 2015.

[84] L. Breiman, J. Friedman, R. Olshen and C. Stone, in *Classification and Regression Tree*, Wadsworth & Brooks/Cole Advanced Books & Software, Pacific California, 1984.

[85] S. Rovnyak, S. Kretsinger, J. Thorp and D. Brown, "Decision Trees for Real-time Transient Stability Prediction," *IEEE Trans. Power Syst.,* vol. 9, no. 3, pp. 1417-1426, 1994.

[86] H. Mori, "State-of-the-art overview of data mining in power systems," in *Proc. IEEE Power Eng. Soc. General Meeting*, Montreal, 2006.

[87] S. Rovnyak and Y. Sheng, "Using measurement and decision tree processing for response-based discrete-event control," in *IEEE Power Engineering Society Summer Meeting*, 1999.

[88] R. Nuqui, A. Phadke, R. Schulz and N. Bhatt, "Fast On-line Voltage Security Monitoring Using Synchronized Phasor Measurements and Decision Trees," *IEEE Power Engineering Society Winter Meeting,* vol. 3, pp. 1347-1352, 2001.

[89] Y. Zhang and K. Tomsovic, "Real-time transient instability detection based on decision trees," in *International Conference on Intelligent System Applications to Power Systems*, 2009.

[90] L. Zhiyong and W. Weiling, "Phasor Measurements-aided Decision Trees for Power System Security Assessment," in *Second International Conference on Information and Computing Science, ICIC '09*, 2009.

[91] G. Qun and S. Rovnyak, "Decision Trees Using Synchronized Phasor Measurements for Wide-area Response-based Control," *IEEE Trans. Power Syst.,* vol. 24, no. 2, pp. 832-839, 2009.

[92] D. Ruisheng, K. Sun, V. Vittal, R. O. Keefe, M. Richardson, N. Bhatt, D. Stradford and S. Sarawgi, "Decision Tree-based Online Voltage Security Assessment using PMU measurements," *IEEE Trans. Power Syst.,* vol. 24, no. 2, pp. 832-839, 2009.

[93] F. Mahmoodianfard, M. Mohammadi, G. Gharepetian and H. Ayaneh, "Optimal PMU placement for voltage security assessment using decision tree," in *IEEE Bucharest PowerTech*, Bucharest, 2009.

[94] K. Sun, S. Likhate, V. VIttal, S. Kolluri and S. Mandal, "An Online Dynamic Security Assessment Scheme using Phasor Measurements and Decision Trees," *IEEE Trans. Power Syst.,* vol. 22, no. 4, pp. 1935-1943, 2007.

[95] D. Li and Y. Cao, "SOFM Based Support Vector Regression Model for Prediction and Its Application in Power System Transient Stability Forecasting," in *The 7th International Power Engineering Conference*, 2005.

[96] F. Gao, J. Thorp, S. Gao, A. Pal and K. Vance, "A Voltage Phasor Based Fault Classification Method for Phasor Measurement Unit Only State Estimator Output," *Elect. Power Compon. Syst.,* vol. 43, no. 1, pp. 22-31, January 2015.

[97] M. Li, A. Pal, A. Phadke and J. Thorp, "Transient Stability Prediction Based on Apparent Impedance Trajectory Recorde by PMUs," *Int. J. Elect. Power Energy Syst.,* vol. 54, pp. 498-504, January 2014.

[98] E. Bernabeu, J. Thorp and V. Centeno, " Methodology for a Security/Dependability Adaptive Protection Scheme Based on Data Mining," *IEEE Transactions on Power Delivery,* vol. 27, no. 1, pp. 104-111, 2012.

[100] F. Gao, J. Thorp, A. Pal and S. Gao, "Dynamic State Prediction Based on Auto-Regressive (AR) Model Using PMU Data," *Proc. IEEE Power and Energy Conference at Illinois (PECI),* pp. 1-5, 24-25 February 2012.

[101] A. Pal, P. Chatterjee, J. Thorp and V. Centeno, "On-line Calibration of Voltage Transformers Using Synchophasor Measurements," *IEEE Trans. Power Del.,* vol. 31, no. 1, pp. 370-380, February 2016.

[102] C. Barrett and e. al., "Impact of a Surface Nuclear Blast on the Transient Stability of the Power System," *Proc. 9th Int. Conf. Critical Information Infrastructures Security,* 1-10,

13-15 October 2014.

[103] A. Pal, I. Singh and B. Bhargava, "Stress Assessment in Power Systems and its Visualization Using Synchropasor Based Metrics," *Proc. IEEE 2014 North American Power Symposium (NAPS),* pp. 1-6, 7-9, September 2014.

[104] A. Kurdilla, *LaSalle's Invariance Priciple and Chetaev's Theorem,* Blacksburg: Virginia Tech, 2014.

[105] A. Pal and J. S. Thorp, "Co-ordinated control of inter-area oscillations using SMA and LMI," in *Innovative Smart Grid Technologies (ISGT), 2012 IEEE PES*, Washington D.C., 2012.